universität wien

DISSERTATION / DOCTORAL THESIS

Titel der Dissertation /Title of the Doctoral Thesis

Who's active in future soils? Unraveling the growth response of bacterial taxa under climate change

verfasst von / submitted by

Dennis André Metze

angestrebter akademischer Grad / in partial fulfilment of the requirements for the degree of

Doctor of Philosophy (PhD)

Wien, 2023/ Vienna 2023

Studienkennzahl lt. Studienblatt / degree programme code as it appears on the student record sheet:	UA 794 685 437
Dissertationsgebiet lt. Studienblatt / field of study as it appears on the student record sheet:	Biologie/Biology
Betreut von / Supervisor:	Univ.-Prof. Dr. Andreas Richter
Betreut von / Supervisor:	Assoc.-Prof. Dr. Christina Kaiser

Table of Contents

Acknowledgments

First and foremost, I want to thank my supervisors Andreas Richter and Christina Kaiser. I was sitting in a hostel in Pune with an unstable internet connection when you interviewed me for this position. It seems surreal how much has happened since then. I want to thank you for giving me the opportunity to embark on this journey with you. It has shaped me in many ways, and I learned a lot. This thesis wouldn't have been possible without your guidance and support. Thank you for your flexibility, your openness to new ideas, and for giving me the space that I needed to thrive.

I would also like to thank all my colleagues at TER. You have created a warm, tolerant, and healthy work environment. The value of such an environment cannot be stressed enough. A special shout-out goes to all the post-docs. You are not just great scientists but also great people and, therefore, have been role models to me since the beginning. A big thanks goes to Joana and Ye, too. They have been the pioneers of this generation of PhD students at TER and paved the way for the rest of us. I also want to thank all my fellow PhD and master's students at TER. Without you, these last years would have been significantly less fun. I have always enjoyed our conversations over lunch and coffee breaks. They play a big role in why I like going to work every day. I'm especially grateful for those of you who have become close friends.

I have been extremely lucky that my PhD was part of the European Project Future Arctic. I have a photo of all the ESRs in my room in Vienna which shows how important of a support group they were throughout this PhD. I'm especially grateful for Coline, Biplabi, and Virginia. Your friendship is a gift. I have learned so much from you and I'm grateful for all the time we spent together in Austria, Iceland, France, and Estonia. Virginia has heard the most about my PhD struggles and has become my family here in Vienna.

Finally, I want to thank my family and friends. It does not fit this page how much they mean to me and how much their love and support keep me going.

Abstract

Soil is arguably the most complex and diverse ecosystem on Earth, inhabited by a plethora of different microorganisms. While many of them are dormant or inactive at any given time, it is the fraction of active microbes that is driving all biogeochemical processes in soil. They control the fate of soil organic carbon and, therefore, play a crucial role in the climate system. Global surface temperatures are predicted to reach 2.2°C - 3.5 °C by the end of the century, and droughts are expected to become longer, more frequent, and intense. Understanding how active soil microbes respond to climate change is fundamental in predicting soil-climate feedbacks.

In this thesis, I investigated how three main global change factors (warming, drought, elevated atmospheric CO_2), alone or in combination, affected the active community of bacteria and archaea by measuring taxon-specific growth rates using quantitative stable isotope probing (qSIP). To avoid rewetting of dry soils via direct additions of liquid ^{18}O-water, I established vapor-qSIP, a novel technique that uses water vapor equilibration to enrich soil water in ^{18}O.

In montane grassland soils exposed to drought, potential future climate conditions (+ 3 °C warming and + 300 ppm atmospheric CO_2 over six years), and a combination of both, drought caused > 90 % of the bacterial and archaeal taxa active in control soils to stop growing. The percentage of active taxa in the total community shrunk from 35 % to 4 %. Bacterial growth in drought-affected soils was dominated by specialized members of the Actinobacteriota, particularly the genus *Streptomyces*. Six years of pre-exposure to future climate conditions alleviated drought effects on bacterial growth via more drought-tolerant taxa and a larger active community (9%).

In long-term warmed (> 50 years) (Sub)Arctic grassland soils, I found that elevated temperatures (+ 6° C) increased the number of growing bacterial taxa, including the size of the active community, but did not give rise to generally faster-growing populations. The composition of the active community shifted in long-term warmed soils and bacterial growth was dominated by distinct taxa. Hence, increased bacterial community growth in long-term warmed soils was not driven by faster-dividing populations of taxa also active at ambient temperatures but by the activated growth of new taxa. Furthermore, long-term warming

changed the direction of root-microbe interactions from positive to neutral based on data from in-situ installed root ingrowth and root exclusion cores. While roots promoted higher microbial growth rates at ambient conditions, this effect was lost with warming.

In this thesis, I opened the microbial black box behind community-aggregated measurements, providing new insights into which bacteria and archaea are still growing in climate change-affected soils. The presented taxon-resolved approach allowed us to capture environmental effects on the soil microbiome more reliably, helped to characterize microbial traits, and improved our understanding of the mechanisms underlying the microbial response to climate change which is crucial for more accurate soil carbon projections.

Zusammenfassung

Der Boden ist wohl das komplexeste und vielfältigste Ökosystem auf der Erde und wird von tausenden unterschiedlichen Mikroorganismen bevölkert. Die meisten von ihnen sind inaktiv, während nur ein kleiner Teil der mikrobiellen Gemeinschaft aktiv wächst und wichtige biogeochemische Prozesse im Boden vorantreibt. Bodenmikroorganismen beeinflussen, ob organischer Kohlenstoff im Boden verleibt oder als CO_2 in die Atmosphäre abgegeben wird. Dadurch spielen sie eine entscheidende Rolle für den Klimawandel. Die globalen Oberflächentemperaturen könnten bis zum Ende des Jahrhunderts um 2.2 °C bis 3.5 °C ansteigen, während Dürren voraussichtlich häufiger, länger und intensiver werden. Es ist weitestgehend unbekannt wie aktive Bodenmikroorganismen auf diese veränderten Bedingungen reagieren werden und unser bisheriges Verständnis begrenzt sich häufig auf Messungen der gesamten mikrobiellen Gemeinschaft, welche die vielfältigen Reaktionsmöglichkeiten einzelner Taxa außer Acht lassen. Dieses Wissen ist jedoch essenziell, um die Wechselwirkungen zwischen Boden und Klima besser voraussagen zu können

Im Rahmen dieser Dissertation habe ich den Einfluss von Erwärmung, Dürre, und erhöhten CO_2-Konzentrationen, sowie deren Zusammenspiel, auf die aktive Gemeinschaft von Bakterien und Archaeen untersucht. Hierfür habe ich das Wachstum individueller Taxa mittels quantitative stable isotope probing (qSIP) gemessen, einer Methode, die mikrobielles Wachstum über den Einbau isotopisch markierten Wassers (^{18}O-H_2O) in mikrobielle DNA bestimmt. Um die Bodenfeuchte unserer Proben konstant zu halten, habe ich eine neue qSIP-Methodik namens vapor-qSIP etabliert. Diese nutzt Wasserdampf aus einem externen Wasserreservoir, um Bodenwasser mit ^{18}O anzureichern (water vapor equilibration). So muss kein ^{18}O-Wasser direkt zugeben werden, was normalerweise die Aussagekraft der Messungen - besonders in trockenen Böden – verringert.

Die erste Studie dieser Dissertation dreht sich um den Effekt von Sommerdürre auf die aktive Gemeinschaft von Bakterien und Archaeen. Sommerdürre wurde im Rahmen eines multifaktoriellen Klimawandelexperimentes in einem Grünland in Steiermark unter aktuellen als auch zukünftigen klimatischen Bedingungen (sechs Jahre + 3 °C Erwärmung und + 300 ppm CO_2) simuliert. Dürre führte dazu, dass mehr als 90 % der Taxa, die im Normalboden aktiv waren, aufhörten zu wachsen. Der Anteil aktiver Taxa von der Gesamtgemeinschaft

verringerte sich von 35 % auf 4 %. Das bakterielle Wachstum in den trockenen Böden wurde von Mitgliedern des Phylums Actinobacteriota - besonders der Gattung Streptomyces - dominiert. Waren die Böden in den sechs vorherigen Jahren einem simulierten Zukunftsklima ausgesetzt, milderte das die Auswirkungen der Dürre. Mehr Taxa schienen dürretolerant and es waren noch 9 % der bakteriellen Gemeinschaft aktiv.

Für die zweite Studie habe ich subarktische Wiesenböden, die seit mehr als 50 Jahren natürlicher Erwärmung (+ 6 °C) ausgesetzt waren, untersucht. Langzeiterwärmung führte dazu, dass die Diversität wachsender Bakterien als auch deren Anteil an der Gesamtgemeinschaft größer wurde. Einzelne Bakterienpopulationen schienen hingegen im Durchschnitt nicht schneller zu wachsen. Die Zusammensetzung der aktiven Gemeinschaft veränderte sich in erwärmten Böden und das Wachstum wurde von anderen Bakterien als in den Kontrollböden dominiert. Insgesamt erhöhten steigende Temperaturen das Gesamtwachstum der bakteriellen Gemeinschaft. Jedoch konnte dieser Anstieg nicht darauf zurückgeführt werden, dass die gleichen Bakterien wie in den Kontrollböden schneller wuchsen, sondern dass viele zusätzliche Taxa aktiv wurden und somit die aktive Gemeinschaft an sich größer wurde. Darüber hinaus veränderten die mehr als 50 Jahre Erwärmung wie Pflanzenwurzeln Bodenmikroorganismen beeinflussten. Die dazugehörigen Daten basierten auf einem Experiment innerhalb dessen Wurzeln entweder daran gehindert oder nicht daran gehindert wurden in Bodenzylinder einzuwachsen, die im Feld eingesetzt wurden. Während Wurzeln unter Normalbedingungen den Bodenmikroorganismen halfen besser zu wachsen, ging dieser Effekt mit Erwärmung verloren.

Im Rahmen dieser Dissertation konnte ich zeigen, welche Bakterien und Archaeen in vom Klimawandel betroffenen Böden potenziell noch aktiv sind und wachsen. Dieser Ansatz kann dazu beitragen Umwelteinflüsse auf das Bodenmikrobiom zuverlässiger zu bestimmen, Eigenschaften einzelner Mikroorganismen leichter zu charakterisieren, und mikrobielle Reaktionsmechanismen besser zu verstehen.

Overview of Manuscripts

Chapter II

Manuscript title: Microbial growth under drought is confined to distinct taxa and modified by potential future climate conditions

Author names: Dennis Metze, Jörg Schnecker, Alberto Canarini, Lucia Fuchslueger, Benjamin J. Koch, Bram W. Stone, Bruce A. Hungate, Bela Hausmann, Hannes Schmidt, Andreas Schaumberger, Michael Bahn, Christina Kaiser, Andreas Richter.

Reference: Nature Communications | (2023)14:5895. https://doi.org/10.1038/s41467-023-41524-y

Author contributions: DM, AR, JS, LF, AC, and CK conceived the study, and AS, MB, and AR established the field site. AC, LF, and JS carried out fieldwork and incubations. DM performed the lab experiments and data analyses, with important inputs from BWS, BJK, HS, and BAH. BH processed the raw amplicon sequencing data. DM and AR drafted the manuscript. All co-authors contributed to the revision of the manuscript.

Chapter III

Manuscript title: Soil warming increases the number of growing bacterial taxa but not their growth rates

Author names: Dennis Metze, Jörg Schnecker, Coline Le Noir de Carlan, Biplabi Bhattarai, Erik Verbruggen, Ivika Ostonen, Ivan A. Janssens, Bjarni D. Sigurdsson, Bela Hausmann, Christina Kaiser, and Andreas Richter.

Reference: In revision

Author contributions: DM, AR, CK, EV, and IO conceived the study, and BDS, IJ, and AR established the field site. DM, CLNDC, and BB carried out fieldwork. DM, JS, and CLNDC performed the lab experiments. DM performed data analyses. BH processed the raw amplicon sequencing data. DM and AR drafted the manuscript. All co-authors contributed to the revision of the manuscript.

Chapter I

General introduction and thesis outline

Microbial life in soil and its role in climate change research

Microbial life in soil is abundant and diverse but remains a hidden world as it is invisible to the naked eye. While tropical forests reveal their opulence through a kaleidoscope of forms, colors, and sounds, we need molecular methods and advanced visualization tools to explore what is living belowground. Most soil microorganisms are bacteria and fungi but also archaea and protozoa, a diverse group of unicellular eukaryotes [1]. Together with plant roots, microorganisms constitute a large part of belowground biomass with approximately 21 billion tons of carbon (soil fungi = 12 Gt C, soil bacteria = 7 Gt C, soil archaea = 0.5 Gt C, soil protists = 1.5 Gt C) [2]. One teaspoon of soil can contain several billion microbial cells [3] and populations of tens of thousands of different species. Besides protozoa, there are other eukaryotes inhabiting the soil matrix, conventionally divided into soil macro- (e.g., earthworm, termites), meso- (e.g., collembola, mites), and microfauna (e.g., nematodes, rotifers) [4]. Soils also harbor a large amount and diversity of viruses [5]. Recent estimates suggest that soil is the most biodiverse habitat on Earth, being home to 59 % of all species including mammals, arthropods, and microorganisms (but excluding viruses) [6].

Microorganisms are the engines that drive biogeochemical cycles on Earth [7]. Their activities directly and indirectly contribute to soil and plant health. They are involved in a wide range of ecosystem services such as water purification, nutrient supply for plant growth, or prevention of soil erosion [8]. Due to their key role in carbon cycling, soil microorganisms act as microscopic climate regulators [9]. Globally, soils store more carbon than the atmosphere and vegetation combined [10, 11]. High-latitude soils of the boreal and arctic region harbor over half of these carbon stocks [12]. Soil microorganisms control the fate of soil organic carbon (SOC) and their activities regulate how much SOC remains stored in soils and how much is released into the atmosphere [10, 13, 14]. By degrading SOC, soil microbes produce CO_2 via heterotrophic respiration. Soil carbon sources can range from old materials preserved in permafrost soils to fresh carbon inputs from growing plants such as leaf litter or root exudates. The fluxes related to heterotrophic respiration of soil microbes equal ~60 billion tons of carbon per year and roughly match the respiration of autotrophic organisms [15]. At the same time, soil microbes form biomass and its remnants (necromass) become part of the stable soil carbon pool, for instance, via association with minerals [16, 17]. Whether soils act as future carbon sinks or carbon sources, will depend equally on how soil microorganisms

respond to climate change and how plants perform in a future climate. Rising temperatures may accelerate microbial activities including their greenhouse gas production, exacerbating the carbon cycle – climate feedback and amplifying climate change [18–20]. This underlines the pivotal role of soil microbes in climate change research. Over the past decade, researchers have repeatedly highlighted [1, 9, 10, 14, 21] that we need to improve our understanding of the soil microbiome under climate change to increase the accuracy of soil carbon projections and make better climate predictions [22–27]. However, much uncertainty remains due to the complex nature of soil ecosystems. Major gaps include quantitative information about shifts in microbial physiology or changes in plant-microbe interactions [1, 9, 14, 21]. Furthermore, we know little about the microbe-scale mechanisms that underly broad ecosystem changes [1] which requires a more 'microbe-centric' approach when investigating the impact of climate change [14]. For instance, most of our knowledge about shifts in microbial processes such as growth is based on community-aggregated measurements. This approach, however, neglects the taxon-specific response patterns from which these shifts emerge and, thus, limits our ability to predict them.

The impact of drought, warming, and elevated atmospheric CO_2 on the soil microbiome

Altered precipitation patterns (e.g., drought), warming, and elevated atmospheric CO_2 are among the top global change factors. The last 20 years were the driest in large areas of the world [28]. With climate change drought events are expected to increase in duration, frequency, and intensity [29]. Droughts not only pose a threat to human societies, for instance, by lowering agricultural yields and putting food security at risk but also affect natural ecosystems [30]. They reduce forest survival [31] and lower grassland productivity [32, 33]. The European Alps are no exception. Simulations assuming a 3°C rise in temperature predict a doubling of drought frequency in the Alps, from 1-2 months to 4 months per year, and an increase in the duration of the longest drought event [34]. In 2022, Europe experienced its second warmest year and hottest summer ever with broken temperature records from Spain to Sweden [35]. Furthermore, 2023 is on track to become the warmest year on record, predicted by the Copernicus Climate Change service of the European Commission. Globally, surface temperatures have increased by 1.1 °C compared to the years 1850 - 1900 and warming might reach + 3.2 °C (2.2 °C - 3.5 °C) by the end of the century without strengthening

policies [36]. Europe is one of the fastest warming regions and has already warmed by about 0.5 °C per decade since 1980 [37]. The Arctic, harboring immense carbon stocks [12], is even more climate-sensitive and has warmed four times faster than the global average since 1979 [38]. Atmospheric CO_2 concentrations have increased by 47 % since 1750 due to human activities (410 ppm in 2019), reaching their highest levels in 800,000 (very high confidence) or even 2 million years (high confidence) [36]. CO_2 concentrations rose by more than 2 ppm between 2021 and 2022 [37] and might reach up to 1000 ppm by 2100 depending on the simulated scenario [39].

Drought, warming, and elevated atmospheric CO_2 affect soil microbes and their complex habitat in many ways. As soils dry down, water is retained in corners, crevices, and a thinning film around soil particles [40]. The dry-down decreases pore connectivity, increases solute concentrations, and restricts diffusion [41]. This limits substrate availability for soil microbes and increases osmotic stress [42]. Water as an important solvent, transport medium, and resource for microbial growth is becoming scarce in drying soils and necessitates osmotic adjustments [42]. Drought declines microbial growth and respiration [43–45] and alters microbial community composition [46–49]. Microbial diversity and biomass show less clear responses, though, as they may decrease or remain constant [42, 49–52]. Life history strategies vary among soil microorganisms [53]. Some possess adaptive traits to endure drought events whereas others will become inactive, sporulate, or die. Relevant traits that infer drought tolerance include the accumulation of osmolytes (e.g., trehalose, ectoine, etc.) to balance the decreasing water potential and maintain turgor [41, 54], production of extracellular polymeric substances (EPS) to find protection in biofilms [42], or increased investments into resource acquisition [41, 54, 55]. All these strategies are, however, energetically expensive [41]. Alternatively, soil microbes may enter dormancy and persist until conditions become more favorable [42].

In contrast to drought, warming is expected to accelerate microbial activities because they rely on enzyme-catalyzed reactions that are inherently temperature-sensitive [56, 57]. However, complex microbial processes such as growth are rarely only temperature controlled, and the full temperature response of a system also depends on the availability of its resources. For example, warming may initially increase microbial respiration, driving large soil carbon losses, followed by a phase of acclimation when carbon losses subside [20, 58–

60]. The factors mediating this acclimation range from the depletion of labile carbon sources, over a subsequent reduction in microbial biomass, to a re-organization of the microbial community [58, 59]. The altered community composition may then favor the decomposition of remaining, more recalcitrant carbon sources, potentially causing additional carbon losses [58]. On a physiological level, higher temperatures inflate the costs of a soil microbe to maintain its metabolism [61]. However, some energy might be saved by downregulating its protein synthesis machinery [62]. Substrate depletion may also cause a soil microbe to invest more into resource acquisition as compared to growth [55]. Arctic soil microbes are particularly temperature-limited and show a pronounced warming response [12, 63]. Generalizing findings is difficult though, since warming effects on the soil microbiome are dependent on the local environment and may be shaped by biotic factors such as shifts in plant performance [21]. Regarding plants, warming can enhance plant productivity and increase belowground carbon allocation [64–66]. But depending on the environment, warming may also reduce plant productivity, for instance, by decreasing the production and biomass of roots [67, 68]. In a warmer climate, plant growth may also be hampered by nutrient limitation (e.g., nitrogen), resulting from enhanced competition between plants and soil microbes [65]. Factors like these may explain the variability of the microbial response to warming across different systems since warming has been reported to either increase [59, 69–71], decrease [72, 73], or not change microbial growth at all [70].

Elevated atmospheric CO_2 mainly acts on the soil microbiome indirectly via shifts in plant performance. Plants release 40 - 60 % of their assimilated carbon belowground [74, 75]. Some of this carbon goes to roots while another part can be utilized by soil microbes to grow and eventually become part of the stable SOC pool. Rising atmospheric CO_2 has been shown to increase plant productivity and belowground carbon allocation [76], fueling higher microbial growth [77] and, potentially, carbon storage. On the flip side, more root exudation may cause soil carbon losses via increased rhizosphere priming [78] or weakening bonds between minerals and stabilized SOC, making it available for microbial decomposition [79]. This underlines that indirect effects mediated by plants are an important factor in shaping the response of the soil microbiome to climate change with repercussions for the carbon cycle.

Future climate scenarios will be characterized by an interplay of drought, warming, and elevated CO_2. Nevertheless, our insights into possible nonlinear, interactive effects of climate

change factors remain limited, due to the low number of multifactorial climate change experiments [21, 80]. Our knowledge of plant-microbe interactions in such multifactorial climate change experiments is also limited. Higher CO_2 concentrations in the atmosphere, for instance, may conserve soil water due to reduced stomatal conductance and transpiration [21], potentially alleviating drought stress for soil microbes. Or suppose warming and elevated CO_2 stimulate plant productivity and increase root exudation rates, the extra carbon may counteract the additional respiratory demands of soil microbes at higher temperatures and allow them to grow faster. Higher temperatures will also act together with drought and may exacerbate drought stress for soil microbes. On the other hand, it may also prime them or affect their recovery after a drought event [81]. Investigating such potential interactive effects is crucial to making more realistic predictions but the multifactorial experiments needed to do so are still scarce.

Growing soil microbes drive biogeochemical transformations in soil

Soil microorganisms are key agents in almost all biogeochemical cycles. However, not all members of the community contribute equally to these processes. A large fraction of the soil microbial community is thought to be inactive or dormant at any given time [82]. However, recent evidence points to 25 – 70 % of active soil microbes [83], up from only 0.5 – 2 % in older studies [84]. Although inactive and dormant soil microbes maintain a minimal metabolism, their overall contribution to soil functions is negligible [85]. Active microbes are the main drivers of transformation processes in soil. Growth or reproduction is often used as a proxy for microbial activity and employed to differentiate dormant microbes from active ones [86–88]. I also use the terms ‘activity’ and ‘growth’ interchangeably. In the interest of completeness, this definition is not all-inclusive though since some active microbes may not replicate but increase in size, accumulate storage compounds, or grow too slowly to be detected as active. Current estimates suggest that one growing cell equals the activity of 1,000 starving cells and 1,000,000 dormant cells [89]. This highlights the ecological relevance of growing soil microbes [90] and their importance for soil carbon cycling [91]. Microbial growth has been reported to drive SOC decomposition [92] and to be directly related to ecosystem-level respiration rates [93]. Hence, investigating how climate change affects

microbial growth is crucial to better understanding the mechanisms behind shifts in soil carbon fluxes.

Whether a soil microbe is growing or inactive depends on a complex gene regulation network [1]. Fast-growing bacteria with more rRNA operons may be more competitive when resources are abundant [94]. Bacteria that have shifted their energy balance towards stress tolerance or resource acquisition, away from reproduction, may grow slower, even in favorable conditions [91]. In a sand microcosm, for instance, faster-growing *Bacillus weihenstephanensis* outcompetes slower-growing *Streptomyces atratus* which, in contrast, is more competitive under drought [95]. Growth is a central component of a microorganism's fitness and an important life history trait [96]. Traits impacting a microorganism's reproduction or survival are called life history traits [97]. If a soil microbe is growing in a certain environment, it must possess the adaptations to thrive under these conditions and be able to access scarce resources or withstand stress. Investigating the growth response of soil microbial taxa under different environmental conditions may enable us to infer the nature of some of their life history traits.

Although growing microbes are the main contributors to biogeochemical processes in soil, we still know little about their response to climate change. This is related to the way we study soil microbiomes. DNA-based methods such as 16S rRNA amplicon sequencing and metagenomics are currently the most popular tools to do so. However, they don't allow us to differentiate between active, inactive, and dead microorganisms since they rely on bulk DNA sequencing. This can confound how changes in the environment affect the soil microbiome [98]. Especially, considering that up to 40% of soil DNA can be relic DNA from dead microorganisms [99] and a large fraction of the soil microbial community is inactive or dormant [84]. This may explain why global change factors do not seem to alter microbial community composition in many cases, at least not in the short-term [100, 101]. A meta-analysis reported that global change factors did not significantly affect microbial community composition in more than 50% of the included studies (15 out of 26) [102]. RNA-based methods usually don't capture relic DNA but still don't allow for proper differentiation between active and dormant taxa because dormant taxa may also maintain high rRNA levels [42, 103]. Stable isotope probing (SIP) might be the most reliable tool to investigate how the soil microbiome responds to climate change [42] since it only considers organisms that have

incorporated a tracer, often ^{18}O-H_2O, into their DNA and are, thus, active and growing. This approach is especially insightful when only the active community responds to a shift in conditions while the total community does not change. Such patterns are usually overlooked using standard DNA-based methods and may lead to incomplete or even wrong conclusions.

A taxon-resolved approach to studying soil microbiome responses

When microbial activity or physiological parameters are reported, they are often based on community-aggregated measurements. These usually yield only one value that summarizes the response of thousands of different taxa and populations. Microbial growth estimates based on ^{18}O-H_2O incubations are a good example [59, 70]. They are calculated using the content and ^{18}O-enrichment of DNA [104], aggregating the growth of several groups of soil microorganisms including bacteria, fungi, and protists. While these measurements are useful for estimating the direction and magnitude of community responses, they do not reveal underlying population-level dynamics [105]. For instance, if warming does not change total community growth, its impact on microbial physiology may be interpreted as negligible. However, the microorganisms contributing to this response might be totally different ones. While some taxa could have stopped growing entirely with warming, others might have become more active. Soil microorganisms differ in their life history traits, therefore, who is growing will likely affect soil functioning with repercussions on SOC dynamics. Bacterial growth rates are taxonomically conserved [106] and appear to be directly linked to soil respiration [107, 108]. Growing taxa might also differ in their chemical composition, feeding back on necromass and, consequently, SOC chemistry [41]. Linking taxonomy and functional observations is also not possible by using only community-aggregated metrics [109]. In short, taxon-resolved measurements are key to better understanding the microbial mechanisms behind community-aggregated traits such as microbial growth or respiration [110].

Quantitative stable isotope probing (qSIP) [111] is currently one of the few methods [112] that allow estimating taxon-specific microbial growth in situ and within complex communities but without the need for cultivation. To determine substrate-independent growth, ^{18}O-H_2O is used as a tracer, and actively replicating taxa incorporate it into their DNA. Incorporating the heavy oxygen isotope increases the buoyant density of a growing microbe's DNA which can be separated into several density fractions using ultracentrifugation. Combined with 16S

rRNA amplicon sequencing and 16S rRNA gene quantification, we can then calculate density shifts between labeled and unlabeled samples and, subsequently, estimate taxon-specific growth rates [113]. Studies using qSIP have provided new insights into the contribution of single taxa to process rates and helped to characterize their phenotypes [107, 114]. Generally, bacterial growth rates under native soil conditions seem to substantially differ from their potential growth rates in culture [115]. By distinguishing between actively growing and inactive (non-replicating) taxa, qSIP also enables us to investigate shifts in the active community composition. This, for instance, revealed the impact of water limitation and its interactions with the presence of fungi on the active bacterial community, a pattern masked at the total community level [116]. A handful of qSIP studies have examined the effects of warming on bacterial growth [69, 71, 73, 117]. However, only one reported data from a long-term warming experiment [69] or simulated a rise in atmospheric CO_2 [118]. How indirect warming effects mediated by plants affect taxon-specific growth rates remains mostly elusive.

One of the shortcomings of qSIP is that soil samples are usually air-dried before heavy water is directly added to ensure sufficiently high ^{18}O soil water enrichment. This alters the soil moisture and may render growth estimates less representative of in situ conditions. Besides these artificial fluctuations in soil moisture, the addition of liquid water represents a big challenge for drought studies. Adding liquid water to dry soils drastically changes the conditions and simulates a rewetting event. While this can be intentional to study how soil microbes respond to rainfalls after a dry spell [108], it confounds microbial growth measurements in dry soils. Rewetting stimulates microbial activities ('birch effect' [119]) and may lead to growth overestimates of up to 250 % [120]. Due to this methodological limitation, we don't know which microbes are growing in drought-affected soils and can withstand the challenging conditions. This knowledge is highly relevant though. Active microbes in dry soils set the stage for the CO_2 emissions after rewetting [52] or may be useful for agriculture to alleviate drought stress in plants [121]. To circumvent the shortcomings of liquid water additions, soil water can be enriched in ^{18}O via the gas phase from an external water pool. This approach is called water vapor equilibration and was recently published by our group [120]. It allows us to enrich soil water with heavy water without changing the soil water content. So far, the water vapor equilibration method has only been used to measure microbial community growth and has not been adapted for qSIP applications yet.

Thesis outline and main goals

Soil microbial communities are arguably the most complex and diverse communities on Earth. With their activities, they control the direction of soil carbon fluxes and their response to climate change may have global repercussions. However, many aspects of the microbial response to climate change are not well understood yet and there remain many open questions. Four of the most pressing ones include:

- How does climate change alter the active and, thus, ecologically most relevant fraction of the microbial community?
- How do individual microbial taxa respond to climate change and can we use this information to better explain the mechanisms behind community-aggregated measurements?
- How do multiple climate change factors interact and modify microbial responses?
- What is the role of indirect climate change effects mediated by plants?

These questions represent the foundation of this thesis which aims to investigate how drought, warming, and elevated CO_2 concentrations, and their combination, affect the active communities of soil bacteria and archaea based on the growth response of their individual members. This work was divided into two separate studies for which I took advantage of a multifactorial climate change experiment situated in Central Austria and a natural long-term warming experiment located in Southern Iceland. In Austria, I examined the effects of drought and its interactions with higher temperatures and atmospheric CO_2. In Iceland, I focused on the direct and indirect effects of long-term warming. For both studies, I measured taxon-specific growth rates using quantitative stable isotope probing (qSIP). To accurately determine growth in dry soils, we developed vapor-qSIP by combining the water vapor equilibration method with ^{18}O-H_2O qSIP. This enabled us to enrich soil water with ^{18}O even in dry soil while maintaining its original moisture. I present the outcome of these studies in the following chapters (Chapter 2, Chapter 3).

Chapter 2 focuses on the impact of a six-week summer drought on the active community of soil bacteria and archaea and their taxon-specific growth rates. Drought was simulated under ambient as well as potential future climate conditions (higher temperatures and atmospheric CO_2) in a managed grassland in Central Austria. Using vapor-qSIP, I could determine taxon-specific microbial growth at in-situ soil moisture. My results demonstrate that microbial growth under drought is consolidated into a much smaller and less diverse active community, dominated by specific groups of the Actinobacteriota. Previous exposure to future climate conditions seemed to prime the active communities and alleviate drought effects.

In **Chapter 3**, I investigate the effects of more than 50 years of sustained soil warming (+ 6°C) on the active community of soil bacteria and archaea and their taxon-specific growth rates. This study was conducted in a Sub(Arctic) grassland with a natural soil temperature gradient that formed via geothermal activities. High-latitude soils and their carbon reservoirs may be particularly vulnerable to rising temperatures since microbial activities in these soils are likely temperature-limited. An acceleration of microbial activities was previously reported at the aggregated community level, and I aimed to elucidate which population-specific patterns underlie this observation. Indirect warming effects mediated by shifts in plant performance were examined with the aid of in situ root ingrowth and root exclusion cores, installed for 10 months. My results do not indicate that warming generally accelerated the growth rates of bacterial populations, as suggested before, but instead showed an increase in the number and diversity of active bacteria. Furthermore, roots stopped stimulating higher growth rates of associated taxa at warmed conditions.

References

1. Jansson JK, Hofmockel KS. Soil microbiomes and climate change. *Nature Reviews Microbiology* . 2020. , **18**: 35–46

2. Bar-On YM, Phillips R, Milo R. The biomass distribution on Earth. *Proceedings of the National Academy of Sciences* 2018; **115**: 6506–6511.

3. Polyanskaya LM, Gorodnichev RB, Zvyagintsev DG. Sizes of bacterial cells in soils determined by cascade filtration technique. *Biology Bulletin* 2013; **40**: 130–137.

4. Geisen S, Briones MJI, Gan H, Behan-Pelletier VM, Friman V-P, de Groot GA, et al. A methodological framework to embrace soil biodiversity. *Soil Biology and Biochemistry* 2019; **136**: 107536.

5. Jansson JK, Wu R. Soil viral diversity, ecology and climate change. *Nature Reviews Microbiology* 2023; **21**: 296–311.

6. Anthony MA, Bender SF, van der Heijden MGA. Enumerating soil biodiversity. *Proceedings of the National Academy of Sciences* 2023; **120**: e2304663120.

7. Falkowski PG, Fenchel T, Delong EF. The Microbial Engines That Drive Earth's Biogeochemical Cycles. *Science* 2008; **320**: 1034–1039.

8. Banerjee S, van der Heijden MGA. Soil microbiomes and one health. *Nature Reviews Microbiology* 2023; **21**: 6–20.

9. Hutchins DA, Jansson JK, Remais J V, Rich VI, Singh BK, Trivedi P. Climate change microbiology — problems and perspectives. *Nature Reviews Microbiology* 2019; **17**: 391–396.

10. Singh BK, Bardgett RD, Smith P, Reay DS. Microorganisms and climate change: terrestrial feedbacks and mitigation options. *Nature Reviews Microbiology* 2010; **8**: 779–790.

11. Todd-Brown KEO, Randerson JT, Post WM, Hoffman FM, Tarnocai C, Schuur EAG, et al. Causes of variation in soil carbon simulations from CMIP5 Earth system models and comparison with observations. *Biogeosciences* 2013; **10**: 1717–1736.

12. Karhu K, Auffret MD, Dungait JAJ, Hopkins DW, Prosser JI, Singh BK, et al. Temperature sensitivity of soil respiration rates enhanced by microbial community response. *Nature* 2014; **513**: 81–84.

13. Bardgett RD, van der Putten WH. Belowground biodiversity and ecosystem functioning. *Nature* 2014; **515**: 505–511.

14. Cavicchioli R, Ripple WJ, Timmis KN, Azam F, Bakken LR, Baylis M, et al. Scientists' warning to humanity: microorganisms and climate change. *Nature Reviews Microbiology* 2019; **17**: 569–586.

15. Shao P, Zeng X, Moore DJP, Zeng X. Soil microbial respiration from observations and Earth System Models. *Environmental Research Letters* 2013; **8**: 34034.

16. Miltner A, Bombach P, Schmidt-Brücken B, Kästner M. SOM genesis: microbial biomass as a significant source. *Biogeochemistry* 2012; **111**: 41–55.

17. Sokol NW, Slessarev E, Marschmann GL, Nicolas A, Blazewicz SJ, Brodie EL, et al. Life and death in the soil microbiome: how ecological processes influence biogeochemistry. *Nature Reviews Microbiology* 2022; **20**: 415–430.

18. Cox PM, Betts RA, Jones CD, Spall SA, Totterdell IJ. Acceleration of global warming due to carbon-cycle feedbacks in a coupled climate model. *Nature* 2000; **408**: 184–187.

19. Friedlingstein P, Cox P, Betts R, Bopp L, von Bloh W, Brovkin V, et al. Climate–carbon cycle feedback analysis: results from the C^4MIP model intercomparison. *Journal of Climate* 2006; **19**: 3337–3353.

20. Melillo JM, Steudler PA, Aber JD, Newkirk K, Lux H, Bowles FP, et al. Soil warming and carbon-cycle feedbacks to the climate system. *Science* 2002; **298**: 2173–2176.

21. Naylor D, Sadler N, Bhattacharjee A, Graham EB, Anderton CR, McClure R, et al. Soil Microbiomes Under Climate Change and Implications for Carbon Cycling. *Annual Review of Environment and Resources* 2020; **45**: 29–59.

22. Bradford MA, Wieder WR, Bonan GB, Fierer N, Raymond PA, Crowther TW. Managing uncertainty in soil carbon feedbacks to climate change. *Nature Climate Change* 2016; **6**: 751–758.

23. Wieder WR, Allison SD, Davidson EA, Georgiou K, Hararuk O, He Y, et al. Explicitly representing soil microbial processes in Earth system models. *Global Biogeochemical Cycles* 2015; **29**: 1782–1800.

24. Wieder WR, Bonan GB, Allison SD. Global soil carbon projections are improved by modelling microbial processes. *Nature Climate Change* 2013; **3**: 909–912.

25. Luo Y, Ahlström A, Allison SD, Batjes NH, Brovkin V, Carvalhais N, et al. Toward more realistic projections of soil carbon dynamics by Earth system models. *Global Biogeochemical Cycles* 2016; **30**: 40–56.

26. Allison SD, Wallenstein MD, Bradford MA. Soil-carbon response to warming dependent on microbial physiology. *Nature Geoscience* 2010; **3**: 336–340.

27. Liang C, Schimel JP, Jastrow JD. The importance of anabolism in microbial control over soil carbon storage. *Nature Microbiology* 2017; **2**: 1–6.

28. Williams AP, Cook ER, Smerdon JE, Cook BI, Abatzoglou JT, Bolles K, et al. Large contribution from anthropogenic warming to an emerging North American megadrought. *Science* 2020; **368**: 314–318.

29. Intergovernmental Panel on Climate Change (IPCC) (ed). Impacts of 1.5°C Global Warming on Natural and Human Systems. *Global Warming of 1.5°C: IPCC Special Report on Impacts of Global Warming of 1.5°C above Pre-industrial Levels in Context of Strengthening Response to Climate Change, Sustainable Development, and Efforts to Eradicate Poverty*. 2022. Cambridge University Press, Cambridge, pp 175–312.

30. Cook BI, Mankin JS, Anchukaitis KJ. Climate Change and Drought: From Past to Future. *Current Climate Change Reports* 2018; **4**: 164–179.

31. Senf C, Buras A, Zang CS, Rammig A, Seidl R. Excess forest mortality is consistently linked to drought across Europe. *Nature Communications* 2020; **11**: 6200.

32. Brookshire ENJ, Weaver T. Long-term decline in grassland productivity driven by increasing dryness. *Nature Communications* 2015; **6**: 7148.

33. Gampe D, Zscheischler J, Reichstein M, O'Sullivan M, Smith WK, Sitch S, et al. Increasing impact of warm droughts on northern ecosystem productivity over recent decades. *Nature Climate Change* 2021; **11**: 772–779.

34. Samaniego L, Thober S, Kumar R, Wanders N, Rakovec O, Pan M, et al. Anthropogenic warming exacerbates European soil moisture droughts. *Nature Climate Change* 2018; **8**: 421–426.

35. Copernicus Climate Change Service (C3S). European State of the Climate 2022, Summary: 2023. https://doi.org/10.24381/gvaf-h066.

36. IPCC. Summary for Policymakers. In: Climate Change 2023: Synthesis Report. Contribution of Working Groups I, II and III to the Sixth Assessment Report of the Intergovernmental Panel on Climate Change [Core Writing Team, H. Lee and J. Romero (eds.)]. 2023. Geneva, Switzerland.

37. WMO. State of the Climate in Europe 2022. 2023. WMO-No. 1320. Geneva, Switzerland.

38. Rantanen M, Karpechko AY, Lipponen A, Nordling K, Hyvärinen O, Ruosteenoja K, et al. The Arctic has warmed nearly four times faster than the globe since 1979. *Communications Earth & Environment* 2022; **3**: 168.

39. Cheng W, Dan L, Deng X, Feng J, Wang Y, Peng J, et al. Global monthly gridded atmospheric carbon dioxide concentrations under the historical and future scenarios. *Scientific Data* 2022; **9**: 83.

40. Or D, Smets BF, Wraith JM, Dechesne A, Friedman SP. Physical constraints affecting bacterial habitats and activity in unsaturated porous media – a review. *Advances in Water Resources* 2007; **30**: 1505–1527.

41. Malik AA, Bouskill NJ. Drought impacts on microbial trait distribution and feedback to soil carbon cycling. *Functional Ecology* 2022; **36**: 1442–1456.

42. Schimel JP. Life in Dry Soils: Effects of Drought on Soil Microbial Communities and Processes. *Annual Review of Ecology, Evolution, and Systematics* 2018; **49**: 409–432.

43. Carbone MS, Still CJ, Ambrose AR, Dawson TE, Williams AP, Boot CM, et al. Seasonal and episodic moisture controls on plant and microbial contributions to soil respiration. *Oecologia* 2011; **167**: 265–278.

44. Wu Z, Dijkstra P, Koch GW, Penuelas J, Hungate BA. Responses of terrestrial ecosystems to temperature and precipitation change: a meta-analysis of experimental manipulation. *Global Change Biology* 2011; **17**: 927–942.

45. Davidson EA, Belk E, Boone RD. Soil water content and temperature as independent or confounded factors controlling soil respiration in a temperate mixed hardwood forest. *Global Change Biology* 1998; **4**: 217–227.

46. Fuchslueger L, Bahn M, Hasibeder R, Kienzl S, Fritz K, Schmitt M, et al. Drought history affects grassland plant and microbial carbon turnover during and after a subsequent drought event. *Journal of Ecology* 2016; **104**: 1453–1465.

47. Fuchslueger L, Bahn M, Fritz K, Hasibeder R, Richter A. Experimental drought reduces the transfer of recently fixed plant carbon to soil microbes and alters the bacterial community composition in a mountain meadow. *New Phytologist* 2014; **201**: 916–927.

48. Canarini A, Schmidt H, Fuchslueger L, Martin V, Herbold CW, Zezula D, et al. Ecological memory of recurrent drought modifies soil processes via changes in soil microbial community. *Nature Communications* 2021; **12**: 1–14.

49. Ochoa-Hueso R, Collins SL, Delgado-Baquerizo M, Hamonts K, Pockman WT, Sinsabaugh RL, et al. Drought consistently alters the composition of soil fungal and bacterial communities in grasslands from two continents. *Global Change Biology* 2018; **24**: 2818–2827.

50. Bastida F, Torres IF, Andrés-Abellán M, Baldrian P, López-Mondéjar R, Větrovský T, et al. Differential sensitivity of total and active soil microbial communities to drought and forest management. *Global Change Biology* 2017; **23**: 4185–4203.

51. Naylor D, Coleman-Derr D. Drought Stress and Root-Associated Bacterial Communities. *Frontiers in Plant Science* 2018; **8**: 2223.

52. Barnard RL, Osborne CA, Firestone MK. Responses of soil bacterial and fungal communities to extreme desiccation and rewetting. *ISME Journal* 2013; **7**: 2229–2241.

53. Martiny AC, Treseder K, Pusch G. Phylogenetic conservatism of functional traits in microorganisms. *The ISME Journal* 2013; **7**: 830–838.

54. Malik AA, Swenson T, Weihe C, Morrison EW, Martiny JBH, Brodie EL, et al. Drought and plant litter chemistry alter microbial gene expression and metabolite production. *ISME Journal* 2020; **14**: 2236–2247.

55. Malik AA, Martiny JBH, Brodie EL, Martiny AC, Treseder KK, Allison SD. Defining trait-based microbial strategies with consequences for soil carbon cycling under climate change. *ISME Journal* 2020; **14**: 1–9.

56. Bradford M. Thermal adaptation of decomposer communities in warming soils. *Frontiers in Microbiology* 2013; **4:** 333**.**

57. Pold G, Melillo JM, DeAngelis KM. Two decades of warming increases diversity of a potentially lignolytic bacterial community. *Frontiers in Microbiology* 2015; **6**: 480.

58. Melillo JM, Frey SD, DeAngelis KM, Werner WJ, Bernard MJ, Bowles FP, et al. Long-term pattern and magnitude of soil carbon feedback to the climate system in a warming world. *Science* 2017; **358**.

59. Walker TWN, Kaiser C, Strasser F, Herbold CW, Leblans NIW, Woebken D, et al. Microbial temperature sensitivity and biomass change explain soil carbon loss with warming. *Nature Climate Change* 2018; **8**: 885–889

60. Walker TWN, Janssens IA, Weedon JT, Sigurdsson BD, Richter A, Peñuelas J, et al. A systemic overreaction to years versus decades of warming in a subarctic grassland ecosystem. *Nature Ecology & Evolution* 2020; **4**: 101–108.

61. Marañón-Jiménez S, Soong JL, Leblans NIW, Sigurdsson BD, Peñuelas J, Richter A, et al. Geothermally warmed soils reveal persistent increases in the respiratory costs of soil microbes contributing to substantial C losses. *Biogeochemistry* 2018; **138**: 245–260.

62. Söllinger A, Séneca J, Borg Dahl M, Motleleng LL, Prommer J, Verbruggen E, et al. Down-regulation of the bacterial protein biosynthesis machinery in response to weeks, years, and decades of soil warming. *Science Advances* 2022; **8**: eabm3230.

63. Rijkers R, Dekker M, Aerts R, Weedon JT. Maximum summer temperatures predict the temperature adaptation of Arctic soil bacterial communities. *Biogeosciences* 2023; **20**: 767–780.

64. Pugnaire FI, Morillo JA, Peñuelas J, Reich PB, Bardgett RD, Gaxiola A, et al. Climate change effects on plant-soil feedbacks and consequences for biodiversity and functioning of terrestrial ecosystems. *Science Advances* 2023; **5**: eaaz1834.

65. Bardgett RD, Freeman C, Ostle NJ. Microbial contributions to climate change through carbon cycle feedbacks. *The ISME Journal* 2008; **2**: 805–814.

66. Malhotra A, Brice DJ, Childs J, Graham JD, Hobbie EA, Vander Stel H, et al. Peatland warming strongly increases fine-root growth. *Proceedings of the National Academy of Sciences* 2020; **117**: 17627–17634.

67. Fang C, Verbrigghe N, Sigurdsson BD, Ostonen I, Leblans NIW, Marañón-Jiménez S, et al. Decadal soil warming decreased vascular plant above and belowground production in a subarctic grassland by inducing nitrogen limitation. *New Phytologist* 2023; **240**: 565–576.

68. Bhattarai B, Sigurdsson BD, Sigurdsson P, Leblans N, Janssens I, Meynzer W, et al. Soil warming duration and magnitude affect dynamics of fine roots and rhizomes and associated C and N pools in subarctic grasslands. *Annals of Botany* 2023; **132**: 269–279.

69. R. PJ, Egbert S, Michaela H, Samantha M, Victoria M-Q, J. KB, et al. Distinct Growth Responses of Tundra Soil Bacteria to Short-Term and Long-Term Warming. *Applied and Environmental Microbiology* 2023; **89**: e01543-22.

70. Simon E, Canarini A, Martin V, Séneca J, Böckle T, Reinthaler D, et al. Microbial growth and carbon use efficiency show seasonal responses in a multifactorial climate change experiment. *Communications biology* 2020; **3**: 1–10.

71. Purcell AM, Dijkstra P, Hungate BA, McMillen K, Schwartz E, van Gestel N. Rapid growth rate responses of terrestrial bacteria to field warming on the Antarctic Peninsula. *The ISME Journal* 2023; **17**: 2290–2302.

72. Liu XJA, Pold G, Domeignoz-Horta LA, Geyer KM, Caris H, Nicolson H, et al. Soil aggregate-mediated microbial responses to long-term warming. *Soil Biology and Biochemistry* 2021; **152**: 108055.

73. Purcell AM, Hayer M, Koch BJ, Mau RL, Blazewicz SJ, Dijkstra P, et al. Decreased growth of wild soil microbes after 15 years of transplant-induced warming in a montane meadow. *Global Change Biology* 2021; **28**: 128–139.

74. Högberg P, Nordgren A, Buchmann N, Taylor AFS, Ekblad A, Högberg MN, et al. Large-scale forest girdling shows that current photosynthesis drives soil respiration. *Nature* 2001; **411**: 789–792.

75. Clemmensen KE, Bahr A, Ovaskainen O, Dahlberg A, Ekblad A, Wallander H, et al. Roots and associated fungi drive long-term carbon sequestration in boreal forest. *Science* 2013; **339**: 1615–1618.

76. Norby RJ, Zak DR. Ecological lessons from free-air CO2 enrichment (FACE) experiments. *Annual Review of Ecology, Evolution, and Systematics* 2011; **42**: 181–203.

77. Blagodatskaya E, Blagodatsky S, Dorodnikov M, Kuzyakov Y. Elevated atmospheric CO2 increases microbial growth rates in soil: results of three CO2 enrichment experiments. *Global Change Biology* 2010; **16**: 836–848.

78. Sulman BN, Phillips RP, Oishi AC, Shevliakova E, Pacala SW. Microbe-driven turnover offsets mineral-mediated storage of soil carbon under elevated CO2. *Nature Climate Change* 2014; **4**: 1099–1102.

79. Keiluweit M, Bougoure JJ, Nico PS, Pett-Ridge J, Weber PK, Kleber M. Mineral protection of soil carbon counteracted by root exudates. *Nature Climate Change* 2015; **5**: 588–595.

80. Rillig MC, Ryo M, Lehmann A, Aguilar-Trigueros CA, Buchert S, Wulf A, et al. The role of multiple global change factors in driving soil functions and microbial biodiversity. *Science* 2019; **366**: 886–890.

81. Meeran K, Ingrisch J, Reinthaler D, Canarini A, Müller L, Pötsch EM, et al. Warming and elevated CO2 intensify drought and recovery responses of grassland carbon allocation to soil respiration. *Global Change Biology* 2021; **27**: 3230–3243.

82. Lennon JT, Jones SE. Microbial seed banks: the ecological and evolutionary implications of dormancy. *Nature Reviews Microbiology* 2011; **9**: 119–130.

83. Couradeau E, Sasse J, Goudeau D, Nath N, Hazen TC, Bowen BP, et al. Probing the active fraction of soil microbiomes using BONCAT-FACS. *Nature Communications* 2019; **10**: 1–10.

84. Blagodatskaya E, Kuzyakov Y. Active microorganisms in soil: Critical review of estimation criteria and approaches. *Soil Biology and Biochemistry* 2013; **67**: 192–211.

85. Jansson JK, Hofmockel KS. The soil microbiome—from metagenomics to metaphenomics. *Current Opinion in Microbiology* 2018; **43**: 162–168.

86. Joergensen RG, Wichern F. Alive and kicking: Why dormant soil microorganisms matter. *Soil Biology and Biochemistry* 2018; **116**: 419–430.

87. Dyckmans J, Chander K, Joergensen RG, Priess J, Raubuch M, Sehy U. Adenylates as an estimate of microbial biomass C in different soil groups. *Soil Biology and Biochemistry* 2003; **35**: 1485–1491.

88. Jones SE, Lennon JT. Dormancy contributes to the maintenance of microbial diversity. *Proceedings of the National Academy of Sciences* 2010; **107**: 5881 LP – 5886.

89. Dijkstra P, Martinez A, Thomas SC, Seymour CO, Wu W, Dippold MA, et al. On maintenance and metabolisms in soil microbial communities. *Plant and Soil* 2022; **476**: 385–396.

90. Singer E, Wagner M, Woyke T. Capturing the genetic makeup of the active microbiome in situ. *The ISME Journal* 2017; **11**: 1949–1963.

91. Ramin KI, Allison SD. Carbon Cycle Implications of Soil Microbial Interactions. In: Hurst CJ (eds). *Understanding Terrestrial Microbial Communities*. 2019. Springer, pp 1–29.

92. Neill C, Gignoux J. Soil organic matter decomposition driven by microbial growth: A simple model for a complex network of interactions. *Soil Biology and Biochemistry* 2006; **38**: 803–811.

93. Stone BW, Blazewicz SJ, Koch BJ, Dijkstra P, Hayer M, Hofmockel KS, et al. Nutrients strengthen density dependence of per-capita growth and mortality rates in the soil bacterial community. *Oecologia* 2023; **201**: 771–782.

94. Roller BRK, Stoddard SF, Schmidt TM. Exploiting rRNA operon copy number to investigate bacterial reproductive strategies. *Nature Microbiology* 2016; **1**: 16160.

95. Wolf AB, Vos M, de Boer W, Kowalchuk GA. Impact of Matric Potential and Pore Size Distribution on Growth Dynamics of Filamentous and Non-Filamentous Soil Bacteria. *PLOS ONE* 2014; **8**: e83661.

96. Roller BRK, Schmidt TM. The physiology and ecological implications of efficient growth. *The ISME Journal* 2015; **9**: 1481–1487.

97. Vasi F, Travisano M, Lenski RE. Long-Term Experimental Evolution in Escherichia coli. II. Changes in Life-History Traits During Adaptation to a Seasonal Environment. *The American Naturalist* 1994; **144**: 432–456.

98. Alteio L V, Séneca J, Canarini A, Angel R, Jansa J, Guseva K, et al. A critical perspective on interpreting amplicon sequencing data in soil ecological research. *Soil Biology and Biochemistry* 2021; **160**: 108357.

99. Carini P, Marsden PJ, Leff JW, Morgan EE, Strickland MS, Fierer N. Relic DNA is abundant in soil and obscures estimates of soil microbial diversity. *Nature Microbiology* 2016; **2**: 16242.

100. Radujkovic D, Verbruggen E, Sigurdsson BD, Leblans NIW, Janssens IA, Vicca S, et al. Prolonged exposure does not increase soil microbial community compositional response to warming along geothermal gradients. *FEMS Microbiology Ecology* 2018; **94**.

101. Séneca J, Pjevac P, Canarini A, Herbold CW, Zioutis C, Dietrich M, et al. Composition and activity of nitrifier communities in soil are unresponsive to elevated temperature and CO2, but strongly affected by drought. *ISME Journal* 2020; **14**: 3038–3053.

102. Isobe K, Bouskill NJ, Brodie EL, Sudderth EA, Martiny JBH. Phylogenetic conservation of soil bacterial responses to simulated global changes. *Philosophical Transactions of the Royal Society B: Biological Sciences* 2020; **375**.

103. Blazewicz SJ, Barnard RL, Daly RA, Firestone MK. Evaluating rRNA as an indicator of microbial activity in environmental communities: limitations and uses. *The ISME Journal* 2013; **7**: 2061–2068.

104. Spohn M, Klaus K, Wanek W, Richter A. Microbial carbon use efficiency and biomass turnover times depending on soil depth – Implications for carbon cycling. *Soil Biology and Biochemistry* 2016; **96**: 74–81.

105. Koch BJ, McHugh TA, Hayer M, Schwartz E, Blazewicz SJ, Dijkstra P, et al. Estimating taxon-specific population dynamics in diverse microbial communities. *Ecosphere* 2018; **9**: 1–15.

106. Morrissey EM, Mau RL, Hayer M, Liu X-JA, Schwartz E, Dijkstra P, et al. Evolutionary history constrains microbial traits across environmental variation. *Nature Ecology & Evolution* 2019; **3**: 1064–1069.

107. Stone BW, Li J, Koch BJ, Blazewicz SJ, Dijkstra P, Hayer M, et al. Nutrients cause consolidation of soil carbon flux to small proportion of bacterial community. *Nature Communications* 2021; **12**: 1–9.

108. Blazewicz SJ, Hungate BA, Koch BJ, Nuccio EE, Morrissey E, Brodie EL, et al. Taxon-specific microbial growth and mortality patterns reveal distinct temporal population responses to rewetting in a California grassland soil. *ISME Journal* 2020; **14**: 1520–1532.

109. Abs E, Chase AB, Allison SD. How do soil microbes shape ecosystem biogeochemistry in the context of global change? *Environmental Microbiology* 2023; **25**: 780–785.

110. Hall EK, Bernhardt ES, Bier RL, Bradford MA, Boot CM, Cotner JB, et al. Understanding how microbiomes influence the systems they inhabit. *Nature Microbiology* 2018; **3**: 977–982.

111. Hungate BA, Mau RL, Schwartz E, Gregory Caporaso J, Dijkstra P, van Gestel N, et al. Quantitative microbial ecology through stable isotope probing. *Applied and Environmental Microbiology* 2015; **81**: 7570–7581.

112. Mayali X, Weber PK, Brodie EL, Mabery S, Hoeprich PD, Pett-Ridge J. High-throughput isotopic analysis of RNA microarrays to quantify microbial resource use. *The ISME Journal* 2012; **6**: 1210–1221.

113. Purcell AM, Dijkstra P, Finley B, Hayer M, Koch BJ, Mau RL, et al. Quantitative stable isotope probing with H218O to measure taxon-specific microbial growth. *Soil Science Society of America Journal* 2020; **84**: 1503–1518.

114. Dang C, Walkup JG V, Hungate BA, Franklin RB, Schwartz E, Morrissey EM. Phylogenetic organization in the assimilation of chemically distinct substrates by soil bacteria. *Environmental Microbiology* 2022; **24**: 357–369.

115. Li J, Mau RL, Dijkstra P, Koch BJ, Schwartz E, Liu X-JA, et al. Predictive genomic traits for bacterial growth in culture versus actual growth in soil. *The ISME Journal* 2019; **13**: 2162–2172.

116. Hestrin R, Kan M, Lafler M, Wollard J, Kimbrel JA, Ray P, et al. Plant-associated fungi support bacterial resilience following water limitation. *The ISME Journal* 2022; **16**: 2752–2762.

117. Wang C, Morrissey EM, Mau RL, Hayer M, Piñeiro J, Mack MC, et al. The temperature sensitivity of soil: microbial biodiversity, growth, and carbon mineralization. *The ISME Journal* 2021; **15**: 2738–2747.

118. Bell SL, Zimmerman AE, Stone BW, Chang CH, Blumer M, Renslow RS, et al. Effects of warming on bacterial growth rates in a peat soil under ambient and elevated CO2. *Soil Biology and Biochemistry* 2023; **178**: 108933.

119. Birch HF. The effect of soil drying on humus decomposition and nitrogen availability. *Plant and Soil* 1958; **10**: 9–31.

120. Canarini A, Wanek W, Watzka M, Sandén T, Spiegel H, Šantrůček J, et al. Quantifying microbial growth and carbon use efficiency in dry soil environments via ^{18}O water vapor equilibration. *Global Change Biology* 2020; **26**: 5333–5341.

121. de Vries FT, Griffiths RI, Knight CG, Nicolitch O, Williams A. Harnessing rhizosphere microbiomes for drought-resilient crop production. *Science* 2020; **368**: 270–274.

Chapter II

Microbial growth under drought is confined to distinct taxa and modified by potential future climate conditions

nature communications

Article

https://doi.org/10.1038/s41467-023-41524-y

Microbial growth under drought is confined to distinct taxa and modified by potential future climate conditions

Received: 1 March 2023

Accepted: 7 September 2023

Published online: 22 September 2023

Check for updates

Dennis Metze[1,2] ✉, Jörg Schnecker[1], Alberto Canarini[1], Lucia Fuchslueger[1], Benjamin J. Koch[3], Bram W. Stone[4], Bruce A. Hungate[3], Bela Hausmann[5,6], Hannes Schmidt[1], Andreas Schaumberger[7], Michael Bahn[8], Christina Kaiser[1] & Andreas Richter[1,9] ✉

Climate change increases the frequency and intensity of drought events, affecting soil functions including carbon sequestration and nutrient cycling, which are driven by growing microorganisms. Yet we know little about microbial responses to drought due to methodological limitations. Here, we estimate microbial growth rates in montane grassland soils exposed to ambient conditions, drought, and potential future climate conditions (i.e., soils exposed to 6 years of elevated temperatures and elevated CO_2 levels). For this purpose, we combined ^{18}O-water vapor equilibration with quantitative stable isotope probing (termed 'vapor-qSIP') to measure taxon-specific microbial growth in dry soils. In our experiments, drought caused >90% of bacterial and archaeal taxa to stop dividing and reduced the growth rates of persisting ones. Under drought, growing taxa accounted for only 4% of the total community as compared to 35% in the controls. Drought-tolerant communities were dominated by specialized members of the Actinobacteriota, particularly the genus *Streptomyces*. Six years of pre-exposure to future climate conditions (3 °C warming and + 300 ppm atmospheric CO_2) alleviated drought effects on microbial growth, through more drought-tolerant taxa across major phyla, accounting for 9% of the total community. Our results provide insights into the response of active microbes to drought today and in a future climate, and highlight the importance of studying drought in combination with future climate conditions to capture interactive effects and improve predictions of future soil-climate feedbacks.

Droughts can have detrimental effects on ecosystems and human societies, threatening food production and forest survival[1,2]. In the last two decades, some areas of the world have experienced the driest period since the late 1500 s[3] and ongoing global warming is expected to increase the frequency, intensity, and duration of drought events even more[4]. Droughts will have strong effects on soils which not only harbor nearly 80% of terrestrial carbon stocks but are also home to about 25% of the global biodiversity[5,6]. Soil carbon fluxes and nutrient cycling are under the direct control of the growth and activity of soil microorganisms, governing, for instance, how much carbon will be lost to the atmosphere[7–9]. Shifts in microbial activity due to drought, warming, or elevated CO_2 concentrations may thus affect the direction and magnitude of these processes with consequences for the global climate and soil health. Low soil water content can limit microbial

A full list of affiliations appears at the end of the paper. ✉e-mail: dennis.metze@univie.ac.at; andreas.richter@univie.ac.at

activities in several ways, for instance, by reducing substrate availability due to a decreased diffusion or increasing the risk of cell dehydration[10,11]. Soil microorganisms have different strategies to cope with drought. Those include tolerance strategies, such as osmolyte production and higher investments in substrate acquisition via enzyme synthesis, or avoidance strategies, such as dormancy[12,13]. These strategies vary across groups of microorganisms and will determine their ability to remain active and growing under drought. We consider bacterial and archaeal taxa that show growth in drought-affected soils to be drought-tolerant. While it is known that microbial community composition is sensitive to soil dry-down and drought duration[14–17], it remains poorly understood which soil microorganisms are active and growing in dry soils, despite their ecological importance.

One gram of soil harbors tens of thousands of different taxa and up to billions of microbial cells of which only a small fraction (0.1–2%) is thought to be active at any given time[18]. More recent evidence, however, suggests that this fraction might be substantially larger (25–70%)[19]. Elucidating which microbial taxa are active and how much they grow is key to understanding the mechanisms that underlie shifts in organic matter fluxes, especially under climate change. Recent calculations estimate that one growing cell is as active as 1000 starving or 1,000,000 dormant cells, indicating that growing microbes account for >95% of total community respiration[20]. Under drought conditions, the number of growing cells may be lower because of reduced soil connectivity[21]. A recent conceptual model proposes that drought forces microorganisms to allocate more energy to adjust to the water deficit, including osmolyte production, or optimized substrate uptake, potentially reducing their growth[22]. Which microbes remain growing during drought might also influence carbon losses in response to rewetting such as the well-known burst in soil CO_2 emissions called the Birch effect[23–25].

Drought is among the main global change factors and is predicted to occur more frequently in a future climate when it will act together with elevated temperatures and higher atmospheric CO_2. Hence, studying drought under future climate conditions is crucial to understanding how microorganisms will function in dry soils in the decades ahead. While this will likely improve predictions of ecosystem processes such as carbon fluxes, data from multifactorial experiments remains scarce[26].

Currently, the most reliable tool to measure growth rates of microbial taxa in soil is quantitative stable isotope probing (qSIP) with ^{18}O-labelled water[27,28]. In the presence of ^{18}O-labeled water, ^{18}O is incorporated into the DNA of growing (i.e., dividing) microorganisms, which can be used to estimate growth rates of individual taxa[27]. This method has been used to study microbial growth patterns upon soil rewetting[29,30], but it could not be applied to estimate growth rates in dry soils since it relies on the addition of liquid water which can lead to growth overestimations of up to 250%[31]. Consequently, the growth rates and identities of growing taxa under drought have not been measured to date.

Here, we estimate bacterial and archaeal taxon-specific growth rates from soils exposed to ambient conditions, drought, future climate conditions (i.e., soils exposed to 6 years of elevated temperatures and elevated CO_2), and a combination of the latter, by combining ^{18}O-qSIP with an approach to enrich soil water isotopically without adding liquid water[31]. This approach, called ´water-vapor equilibration qSIP" (vapor-qSIP), enabled us to identify growing bacterial and archaeal taxa during drought and explore the interaction of drought and future climate conditions. The study was undertaken at a multifactorial climate change experiment located in a montane grassland in the Austrian Alps, in which a 6-week-long summer drought was simulated under ambient and future climate conditions (i.e., elevated temperatures of + 3 °C above ambient, and elevated atmospheric CO_2 of + 300 ppm above ambient) and compared to respective drought-unaffected controls[32]. Our main goals were (i) to estimate the growth rates of soil bacteria and archaea under a severe summer drought and (ii) to assess how future climate conditions affect the microbial growth response to drought. We report the first analysis of the size, diversity, and composition of the growing microbial communities during drought, and how drought effects were altered and alleviated by six years of pre-exposure to future climate conditions. Using vapor-qSIP allowed us to infer growth rates of individual bacterial and archaeal taxa and to explore growth patterns at a high taxonomic resolution, ranging from phylum to genus and even ASV (amplicon sequence variant) level.

Results

Growing communities reveal the effects of future climate conditions, masked at the total community level

Drought and future climate conditions significantly reduced volumetric soil water contents across treatments by ~17% and ~1%, respectively (Two-way ANOVA; Drought: $F = 1485$, $df = 1$, $p < 0.001$; Climate: $F = 4.2$, $df = 1$, $p = 0.047$). We compared the effects of drought, future climate conditions, and their combination on the composition of the total and actively growing community of bacteria and archaea using principal component analysis on the absolute abundances of individual taxa (16 S rRNA gene copies per taxon) after centered log-ratio transformation. Total community composition shifted in response to drought (PERMANOVA: $R^2 = 0.13$), whereas it was unaffected by future climate conditions (Fig. 1a). Drought had an even stronger effect on the composition of the growing community (PERMANOVA: $R^2 = 0.24$) which, in contrast, was also shaped by future climate conditions (PERMANOVA: $R^2 = 0.11$) and their interaction with drought (PERMANOVA: $R^2 = 0.11$). Communities of growing bacteria and archaea were distinct in their composition across all four treatments with drought being the main driver of divergence. We found a similar pattern when using relative growth rates for PCA instead of absolute abundances, suggesting that taxon abundances reflected growth patterns (Supplementary Fig. 1). Overall, drought and future climate effects on community composition seemed to be only visible within the growing community but masked at the total community level, which only responded to drought.

Growing communities become smaller and less diverse in drought-affected soils

Drought exhibited a strong negative impact on the growing community which seemed alleviated under future climate conditions. Drought substantially reduced the richness of growing bacterial and archaeal taxa represented as amplicon sequence variants (ASVs). The number of growing ASVS, as defined by minimum ^{18}O enrichment (atom percent excess (APE) ^{18}O > 5%), dropped on average by ~65% compared to ambient conditions, representing a loss of approximately 1000 growing ASVs (Fig. 2a, Two-way ANOVA; Drought: $F = 39.1$, $df = 1$, $p < 0.001$; Climate: $F = 0.8$, $df = 1$, $p = 0.38$; Drought x Climate: $F = 4.1$, $df = 1$, $p = 0.06$). Still, more than 500 ASVs remained growing in dry soils despite soil water contents being as low as 6–8% of soil fresh mass. We considered taxa that were able to grow in drought-affected soils to be drought-tolerant. Soils subjected to both drought and future climate conditions had 66% greater ASV richness than soils subject to drought only ($p = 0.06$). Future climate conditions alone did not affect ASV richness.

The drought effect on the size of the growing community, or the percentage of the total community that was growing, was even stronger. To estimate this, we summed the 16 S rRNA gene copies of all growing taxa and divided them by the sum of the gene copies of the total community (Fig. 2b). The total sum of 16 S rRNA gene copies did not significantly differ across treatments (Two-way ANOVA; Drought: $F = 0.7$, $df = 1$, $p = 0.39$; Climate: $F = 2.6$, $df = 1$, $p = 0.12$; Drought x Climate: $F = 0.004$, $df = 1$, $p = 0.95$). The share of growing taxa, however, declined from 35% under ambient conditions to only 4% in dry soils

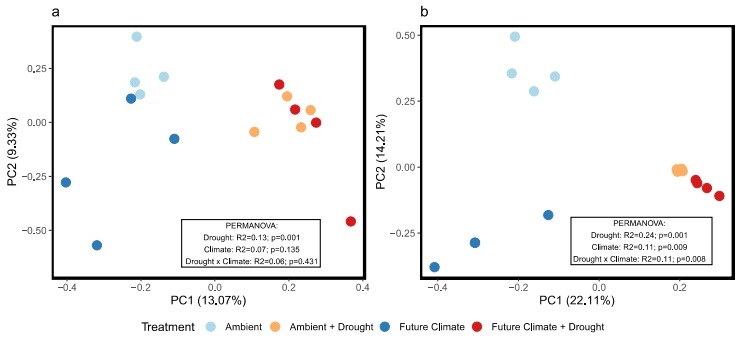

Fig. 1 | Effect of drought and future climate conditions on the composition of total and growing bacterial and archaeal communities. Principal component analysis (PCA) of total (**a**) and growing (**b**) bacterial and archaeal communities ($n = 4$ replicates) on centered log-ratio transformed amplicon sequence variant (ASV) absolute abundances. Absolute abundances were calculated by multiplying ASV-specific amplicon sequencing reads with 16 S rRNA gene copies inferred by digital droplet PCR. Absolute abundances were agglomerated over the density fractions of a sample gradient. Statistics from two-way permutation-based multivariate analysis of variance (PERMANOVA) testing a full two factorial design (Drought $_{Yes}$, Drought $_{No}$, Climate $_{Ambient}$, Climate $_{Future}$) are provided as inset panels. Source data are provided with this paper.

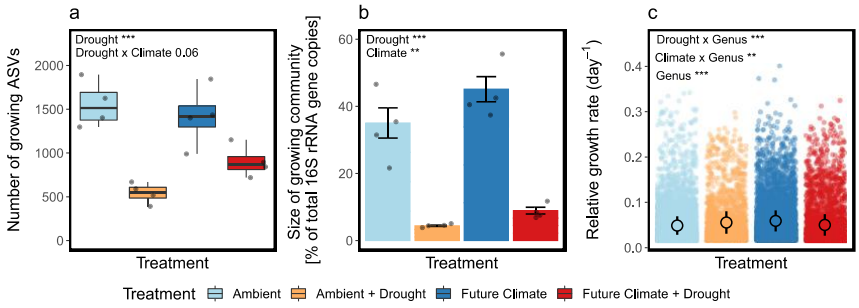

Fig. 2 | Diversity, population size, and mean relative growth rates of growing communities of bacteria and archaea across treatments. a Number of unique growing amplicon sequence variants (ASVs) ($n = 4$ replicates). **b** Population size of the growing community expressed as the percentage of growing taxa of the total community based on the sum of their 16 S rRNA gene copies ($n = 4$ replicates). **c** Mean taxon-level relative growth rates ($n = 4$ means of taxon-specific growth rates calculated per replicate). Asterisks depict significant results from either two-way ANOVA testing a full two factorial design (**a**, **b**: Drought $_{Yes}$, Drought $_{No}$, Climate $_{Ambient}$, Climate $_{Future}$) or a linear mixed model (**c**, $n = 391$–1845 taxon-specific growth rates per replicate). Light-colored dots represent replicate samples (**a**, **b**) or taxon-specific growth rates (**c**) across treatment replicates, used to calculate mean taxon-level relative growth rates and standard errors (points, error bars). Boxes show the interquartile range with a line representing the median and minimum/maximum whiskers (**a**). Error bars represent standard errors (**b**, **c**). Source data are provided with this paper.

(Fig. 2b, Two-way ANOVA; Drought: $F = 265$, $df = 1$, $p < 0.001$; Climate: $F = 17.4$, $df = 1$, $p = 0.001$; Drought x Climate: $F = 2.4$, $df = 1$, $p = 0.14$). Future climate conditions increased the size of the growing community compared to ambient conditions in drought–affected and drought-unaffected soils. While on average ~45% of the community was growing in future climate plots at regular precipitation, it was ~9% under drought.

Diverging growth responses under drought and future climate conditions

We investigated how drought and future climate conditions affected bacterial and archaeal growth rates from two perspectives. First, we calculated average relative growth rates for the growing community using data from all growing taxa per treatment. Second, we assessed how relative growth rates of specific taxa changed with treatment conditions. To this end, we filtered for taxa growing in more than one treatment and compared their average relative growth rates.

Although substantially fewer taxa were growing under drought, the mean relative growth rate of the growing community did not differ from ambient conditions (Fig. 2c). We found, however, that general growth patterns and growth responses to treatment conditions varied across genera (Fig. 2c, Linear mixed model; Genus: $F = 3.2$, $df = 376$, $p < 0.001$; Climate x Genus: $F = 1.3$, $df = 251$, $p = 0.001$; Drought x Genus: $F = 2.3$, $df = 222$, $p < 0.001$). When also taking non-growing taxa into account (defined as ^{18}O APE < 5%), representing the entire community, drought decreased mean relative growth rates while they increased in a future climate when precipitation was not manipulated (Supplementary Fig. 2, Two-way ANOVA; Drought: $F = 57$, $df = 1$, $p < 0.001$; Climate: $F = 7.6$, $df = 1$, $p = 0.01$).

To further understand how many taxa remained growing under drought and examine their growth response, we filtered for ASVs that consistently grew in at least two replicates per treatment (total growing in ≥2 replicates: 3553 ASVs, total growing: 5116 ASVs). The majority of taxa, representing about two-thirds (>2200 ASVs), were specific to

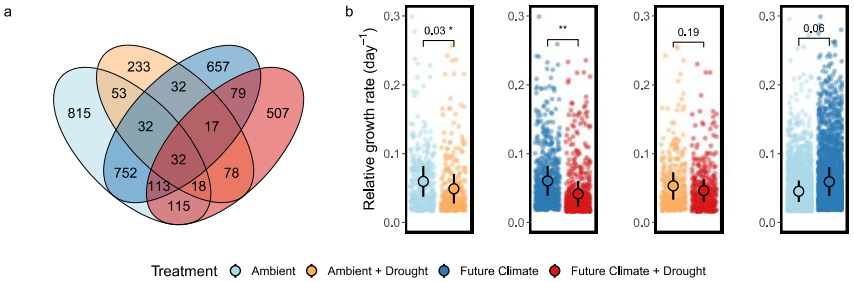

Fig. 3 | Overlap of growing ASVs between treatments and growth response of shared taxa. a Venn diagram of shared and unique amplicon sequence variants (ASVs) that were actively growing in at least two replicates per treatment. **b** Growth rates of shared taxa across four treatment comparisons: Ambient and Ambient + Drought (left panel), Future Climate and Future Climate + Drought (left center panel), Ambient + Drought and Future Climate + Drought (right center panel), Ambient and Future Climate (right panel). Asterisks represent significant differences between comparisons using two-sided Student's *t*-tests ($n = 4$ means of taxon-specific growth rates calculated per replicate). Light-colored dots represent taxon-specific growth rates across replicates used to calculate means and standard errors (points, error bars). Source data are provided with this paper.

only one treatment and found growing only there (Fig. 3a). In an ambient climate, only 7% of the original taxa continued to grow during drought (135 ASVs = 53 + 32 + 32 + 18 ASVs) as compared to 14% in a future climate (241 ASVs = 113 + 32 + 17 + 79 ASVs). If taxa managed to grow in both drought-affected and drought-unaffected soils, we considered them to be drought-enduring. Based on this assumption, more than twice as many ASVs were drought-enduring under simulated future climate conditions (374 ASVs = 79 + 17 + 32 + 113 + 115 + 18 ASVs) as compared to drought in an ambient climate (184 ASVs = 32 + 17 + 18 + 32 + 32 + 53 ASVs). Even though several ASVs were enduring drought conditions, their relative growth rates were reduced by 18.7% ± 5.3% (mean ± SD) in an ambient climate and by 31.2% ± 14.4% in a future climate (Fig. 3b: left panel, Ambient vs. Ambient + Drought, *t*-test: t (5.8) = 2.76, *p*-value = 0.03; Fig. 3b: left center panel, Future Climate vs. Future Climate + Drought, *t*-test: t (5.9) = 3.72, *p*-value = 0.009). At a phylum level, we observed the same response for Actinobacteriota and Bacteroidota but not Acidobacteriota and Proteobacteria (Supplementary Fig. 3A and C). If soils weren't exposed to drought, future climate conditions accelerated the growth of taxa shared with the ambient treatment by 34.7% ± 28.9% (Fig. 3b: right panel, Ambient vs. Future Climate, *t*-test: t (3.7) = −2.55, *p*-value = 0.06), which was mirrored by the Acidobacteriota, Actinobacteriota, and Bacteroidota (Supplementary Fig. 3E). This growth-promoting effect, however, was not detected in drought-affected soils (Fig. 3b: right center panel, Drought vs. Future Climate + Drought, *t*-test: t (4.9) = 1.49, *p*-value = 0.19).

Response patterns to drought are specific to taxonomic groups and altered by future climate conditions

We examined phylum- and family-specific drought response patterns by comparing how the number of growing taxa changed across treatments (Fig. 4). During drought, the number of growing taxa within most phyla, that fulfilled normality and homoscedasticity requirements for two-way ANOVA, decreased by >50%, including Acidobacteriota, Proteobacteria, Planctomycetota, and Verrucomicrobiota (Fig. 4a). Only Actinobacteriota showed a slightly positive response to drought. Their number of active ASVs increased on average by ~7%. This response was primarily driven by five families including Streptomycetaceae, Nocardiaceae, Nocardioidaceae, Intrasporangiaceae, and Solirubrobacteraceae (Supplementary Fig. 4A). It is worthwhile mentioning that several taxa within the Proteobacteria and Acidobacteriota remained growing even at comparatively high rates, despite a generally negative drought response at the phylum level.

In the combined drought and future climate treatment, more taxa were growing across major phyla and families as compared to drought only (Fig. 4b and Supplementary Fig. 4B, respectively). For instance, the loss of Proteobacteria and Acidobacteriota was alleviated resulting in almost twice as many growing taxa. This also applied to the Actinobacteriota although less pronounced. Some phyla did not show this alleviated drought response including Crenarchaeota, Latescibacterota (Fig. 4a), and Bacteroidota (Parametric pairwise Wilcoxon tests: Drought vs. Future Climate + Drought: $p = 0.58$).

Drought consolidates growth to fewer lineages and reduces growing bacterial predators

To examine which taxa contributed the most to the growth of the total community, we calculated their proportional ^{18}O assimilation (range: 0–1) by integrating relative growth rates and re-computed relative abundances for the growing community. We ranked taxa based on proportional ^{18}O assimilation and extracted the top five (Fig. 5) and top 50 assimilators (Supplementary Figs. 5, 6) of each sample. Across all respective samples, the top five assimilators represented 26 ASVs in drought-unaffected (Fig. 5a: ambient, future climate) and 19 ASVs in drought-affected soils (Fig. 5b: drought, future climate and drought) and accounted for 11.4 ± 4% and 23 ± 15% of the community growth (Supplementary Fig. 7A). At ambient precipitation, the top ^{18}O assimilating taxa included an unclassified member of the Bacteroidota (Family: env.OPS 17) and members of the genera *Pseudoduganella*, *Cavicella*, or *Bradyrhizobium* (Fig. 5a). During drought, the identity of dominant taxa shifted completely, and growth was more consolidated into fewer genera (Fig. 5b). These were mostly Actinobacteriota, belonging to the genera *Oryzihumus, Marmoricola*, *Rhodococcus*, and *Streptomyces*, but also included a member of the Proteobacteria. *Streptomyces* alone was responsible for on average 12.3 ± 11.1% (min: 2%, max = 38%) of the community growth in drought-affected soils (Fig. 5b). This response was primarily driven by one specific *Streptomyces* ASVs (ASV_rmw_7xq_0rh) (Supplementary Fig. 7B). This taxon maintained relative growth rates comparable to ambient conditions but increased in abundance by several magnitudes (Supplementary Fig. 8A, B).

Beyond the top ^{18}O assimilating taxa, we also aimed to understand the response of bacterial predators to drought. They play an important functional role in the microbial food web and might be more isolated from their prey in dry soils due to disconnected pores. Taxa were assigned a putative predatory lifestyle based on their taxonomy, for instance, if they belonged to the orders Myxococcales, Bdellovibrionales, Vampirovibrionales, Haliangiales, or Polyangiales. The vast

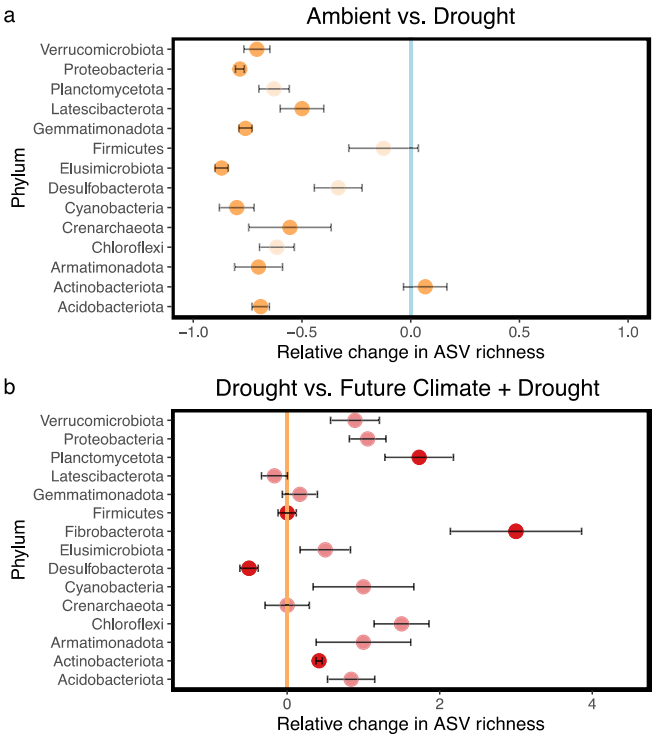

Fig. 4 | Relative changes in the number of growing taxa per phylum under drought and future drought conditions. a Relative change (0 = no change, 1 = increase by 100%) in the number of growing taxa per phylum comparing Ambient (reference) and Ambient + Drought conditions ($n = 4$ replicates). **b** Relative change in the number of growing taxa comparing Ambient + Drought (reference) and Future Climate + Drought conditions ($n = 4$ replicates). Points represent mean relative changes in the number of growing taxa per phylum including standard errors (error bars). Two-way ANOVA testing a full two factorial design (Drought $_{Yes}$, Drought $_{No}$, Climate $_{Ambient}$, Climate $_{Future}$) was performed on the number of growing amplicon sequence variants (ASVs) across all treatments for each phylum independently that fulfilled normality and homoscedasticity requirements. *P*-values were adjusted for multiple testing using false discovery rate correction. Bold colored points represent significant effects (**a**: Drought = $p < 0.05$, **b**: Climate = $p < 0.05$ or Drought x Climate = $p < 0.05$) and transparent points represent non-significant effects. Vertical lines depict the means of the respective reference treatment ($n = 4$ replicates) used to calculate relative changes. Source data and *p*-values are provided with this paper.

majority of these putative predatory bacteria stop growing under drought. While on average 146 ± 17 putative predatory taxa were growing at ambient precipitation, it was 15 ± 8 in drought-affected soils. With ~90%, this exceeded the drought response of the total community where the richness of growing taxa averaged over both drought treatments was approximately 50% lower as compared to ambient precipitation (ambient, future climate). The contribution of putative predatory bacteria to the total community's growth based on proportional ^{18}O assimilation also decreased with drought (Supplementary Fig. 9A, Two-way ANOVA; Drought: $F = 63$, $df = 1$, $p < 0.001$) along with a > 90% reduction in their abundance (Supplementary Fig. 9B, Two-way ANOVA; Drought: $F = 227$, $df = 1$, $p < 0.001$). Overall, most putative bacterial predators stopped growing in dry soils and even more as compared to the rest of the community. Putative predatory taxa that were still active under drought predominantly belonged to the Haliangiaceae family (Supplementary Fig. 10).

Discussion

Drought, warming, and elevated CO_2 concentrations are major global change factors that alter biogeochemical processes in soils, affecting global carbon cycling and possible climate feedbacks. Growing soil microbes are at the core of these processes. While several studies have investigated the effects of drought on microbial life[10,12,16,24,33–35], our knowledge about growing microbes and their dynamic activity patterns remains limited. Furthermore, much of what we know about microorganisms in dry soils is based on total community assessments, rarely differentiating between growing (i.e., dividing), inactive, dormant, or even dead microorganisms. This might explain why results are often ambiguous with regards to shifts in the community composition and seldomly report reductions in diversity[13,36–40] or even biomass[15,41,42]. Using vapor-qSIP, we could circumvent the limitations related to liquid tracer addition, allowing new insights into microbial life in dry soils. We observed that drought caused a large part of the bacterial and archaeal community to stop growing, resulting in smaller, less diverse, and distinct active communities dominated by specific members of Actinobacteriota. In a simulated future climate, we found these drought responses to be altered and even alleviated. Thus, experiments manipulating drought as a single factor might fail to realistically capture how soil microorganisms will react to drought in a future climate.

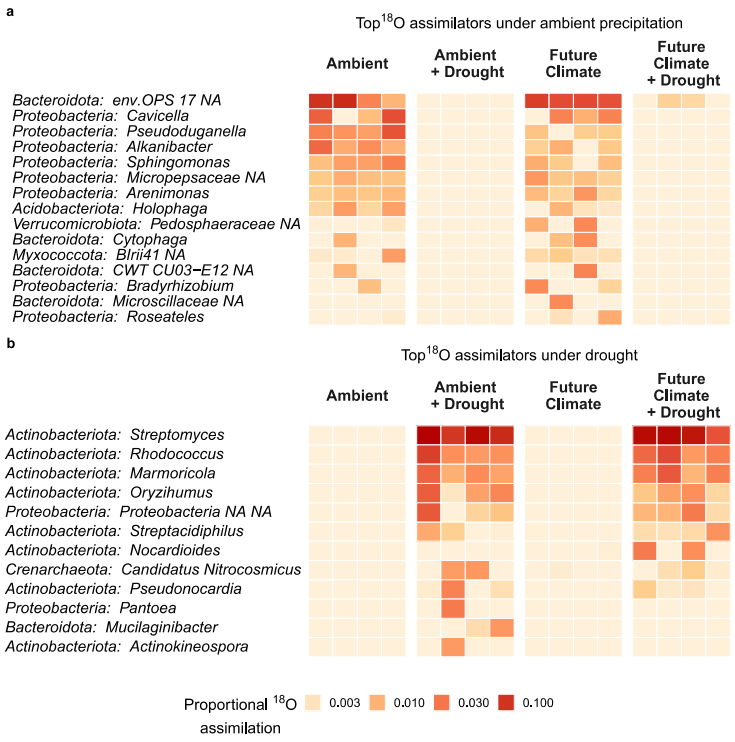

Fig. 5 | Drought-induced changes in the top ^{18}O assimilating taxa agglomerated at the genus level. Heatmap showing taxa with the highest proportional ^{18}O assimilation (contribution to the total community's growth) under ambient precipitation (**a**) and drought (**b**), visualized across all treatments and individual samples (rectangles, $n = 4$). Amplicon sequence variants (ASVs) were ranked based on their proportional ^{18}O assimilation, separately, for drought-unaffected (**a**: Ambient, Future Climate) and drought-affected samples (**b**: Ambient + Drought, Future Climate + Drought). The top five ASVs per sample were then selected (**a**: 26 total unique ASVs; **b**: 19 total unique ASVs) and visualized. Proportional ^{18}O assimilation ranges from 0–1 and estimates how much a single taxon contributes to the community's overall growth. It is calculated using re-computed relative abundances of only growing taxa (sum of growing taxa = 1) and their relative growth rates (RGR). ASVs had to be active in at least two samples if detected as growing in a treatment. ASV identities were agglomerated at the genus level and sorted in descending order based on proportional ^{18}O assimilation. If genus identity could not be assigned (NA), we agglomerated taxa at the family or phylum level. Source data are provided with this paper.

As soils dry down the water potential decreases, exposing microorganisms to an array of stressors including disconnectivity and, at local scales, resource limitation[13]. Our results suggest that most taxa active at ambient conditions are not well equipped for growth under drought conditions. Some taxa, however, were able to withstand drought and maintained growth in drought-affected soils but at on average 19% lower rates (Fig. 3b). We considered taxa to be drought-tolerant if they showed growth in drought affected-soils. We acknowledge that some taxa might have been drought-tolerant but did not grow, though these are likely to be less well-adapted. Drought adaptations include, for example, osmolyte production or biofilm formation. However, such strategies are energetically expensive[22] and reduce resources allocated to reproduction, leading to lower growth rates. Here, Actinobacteriota were the most drought-tolerant phylum with even slightly increasing numbers of growing taxa (Fig. 4a). This underlines the persistence of Actinobacteriota in dry soils previously indicated by higher relative abundances[17,24,43,44]. Extending such findings here, the positive response of Actinobacteriota was driven by a few families including the Streptomycetaceae, Nocardiaceae, Nocardioidaceae, and Intrasporangiaceae (Supplementary Fig. 4), and only a few genera within them, namely *Oryzihumus, Rhodococcus, Marmoricola*, and *Streptomyces*. Among these, *Streptomyces* accounted for most of the community's growth, underlining its paramount role under drought. A similar pattern of growth consolidation has been seen upon nutrient addition[45]. *Streptomyces* maintained the same growth rates as under ambient conditions while increasing in abundance. Their filamentous growth might be advantageous when pore spaces and resources become disconnected[21]. *Streptomyces* has been observed to persist in dry soils, alleviating drought stress in plants[44,46–52]. Interestingly, individual taxa from mostly drought-sensitive phyla also grew in dry soils such as one taxon assigned as Proteobacterium (Fig. 5b), despite more than 70% of the Proteobacteria becoming inactive. This indicates that although certain traits related to drought tolerance are phylogenetically conserved, others might be more widespread and even found in taxa of generally drought-sensitive groups where they might have evolved independently or were acquired via horizontal gene transfer[53,54].

Since pore spaces become increasingly disconnected with drought, leading to lower diffusion and mobility, microbe-feeding predators are expected to have less access to their prey, potentially

decreasing predatory pressure[13,21]. While this has been demonstrated for soil protists and nematodes before[55,56], we demonstrate here that most predatory bacteria almost completely ceased their growth, too. Although we could not differentiate between facultative and obligate predatory taxa, our results suggest a strong decrease in predation via predatory bacteria. Our growth data does not explain the reasons behind this decrease, but the disproportionate reduction of growing predatory bacteria as compared to the community's average might indicate that drought entails additional challenges for predatory bacteria such as restricted predator movement and lower prey accessibility due to drought.

In our study, microbial drought responses changed when soils had also been pre-exposed to future climate conditions (+3 °C and +300 ppm). Generally, future climate conditions allowed for larger active communities (Fig. 2b) and, at ambient precipitation, also higher relative growth rates (Fig. 3b: right panel). In drought-affected soils, future climate conditions alleviated the loss of growing taxa across many phyla. Furthermore, growing taxa under combined conditions formed distinct communities including many unique ASVs.

We hypothesize that the attenuated drought response of the growing community under future climate conditions might arise from (I) the 6-year-long pre-exposure of the microorganisms to higher temperatures and/or (II) larger carbon inputs from plants. It is well-known that previous exposure to drought often increases microbial resistance and resilience[17,57,58], but to our best knowledge, this is the first report that future climate conditions can alleviate negative drought effects on soil microorganisms. Compositional changes and associated shifts in the distribution of life-history traits in response to drying and rewetting can render microbial communities more drought-tolerant[54]. The simulation of future climate conditions significantly reduced the soil moisture content during the drought experiment and in the past, where they led to an earlier and more frequent drop in soil moisture[59,60], exposing the microbial community to longer and more frequent dry periods. This has likely caused a selection for more drought-enduring taxa and populations.

With regard to plants, higher concentrations of atmospheric CO_2 can increase leaf and root production[61] as well as exudation[62]. Higher carbon allocation belowground might explain why future climate conditions led to a larger growing community and higher growth rates at ambient precipitation. Drought generally reduces plant carbon transfer to soil bacteria[15] whereas moderate drought has been shown to increase rhizodeposition[63]. Furthermore, drought can affect root exudate properties, leading to higher microbial respiration compared to ambient soils[64]. We hypothesize that increased rhizodeposition, either preceding or in an early stage of the dry phase, partially reduced microbial drought stress by alleviating resource limitations[13]. In addition, elevated atmospheric CO_2 might have reduced plant water uptake due to lower stomatal conductance and transpiration[65], allowing more water to remain in the soil for longer, although we found only small differences in soil water content between ambient and future climate treatments.

Growing microbial taxa are key contributors to soil carbon cycling. They transform organic carbon to produce new biomass and release CO_2 produced for energy production back to the atmosphere, more than dormant and starving taxa combined[20]. Microbial growth rates inferred by ^{18}O-qSIP were found to be directly related to ecosystem-level respiration rates in soil[45]. Here, the growing community changed in both composition and size under drought and future climate conditions as well as their combination, which might explain previous results, reporting lower soil respiration under drought and slightly higher respiration when previously exposed to future climate conditions[66].

Our results illustrate that vapor-qSIP, i.e., the combination of ^{18}O water vapor equilibration and qSIP, allows for unprecedented insights into growing microbial communities in dry soils, revealing that future climate conditions increased their drought tolerance. Understanding which microorganisms persist to grow in dry soils and at what rates constitutes the basis of an in-depth understanding of how drought affects soil carbon cycling and soil organic matter persistence. Considering that microbes can alleviate drought stress in plants, understanding which taxa grow in dry soils, can be exploited to engineer rhizosphere microbiomes for future climatic conditions. While members of the genus *Streptomyces* are well known for reducing drought stress in plants, we present other drought-tolerant genera such as *Oryzihumus, Rhodococcus, and Marmoricola* which might prove interesting for future studies. With regards to soil functioning, the vast majority of taxa active at ambient conditions stopped growing under drought and were replaced by a substantially smaller number of drought-tolerant taxa. This will reduce the rate of many biogeochemical processes as well as the diversity of the active microbiome, rendering it more vulnerable to additional disturbances, such as environmental contamination. While this provides new directions for drought research, we highlight that it is important to study drought in combination with future climate conditions to capture interactive effects and improve predictions of future soil-climate feedbacks.

Methods

Study site and sample collection

This study was conducted within the ClimGrass experiment located at the Agricultural Research and Education Centre, Raumberg-Gumpenstein, Austria (47°29′38″N, 14°06′03″E, 710 m, MAT: 8.2 °C, MAT: 1056 mm). ClimGrass is a multifactorial climate change experiment established in a managed grassland and fully operational since 2014. It comprises 54 experimental plots and six treatment conditions characterized by joint or individual manipulations of temperature (ambient, +1.5 °C, +3 °C), atmospheric CO_2 (ambient, +150 ppm, +300 ppm), and severe summer drought events[32,66–68]. Soil temperatures and CO_2 concentrations were manipulated with infrared heaters and miniFACE systems since 2014 (Free Air CO_2 enrichment System), respectively. To simulate a summer drought event, automated rainout shelters were installed for six weeks (June 17th—August 3rd, 2020). The soil type was a Cambisol (pH ~5.5) with a loamy sand texture. Soil carbon and nitrogen content were 3.2 ± 0.3% (mean ± SD) and 0.3 ± 0.04% per gram of dry soil, respectively. Dominant plant species included the grasses *Arrhenatherum elatius* and *Festuca pratensis, the* legumes *Lotus corniculatus* and *Trifolium pratense*, and the non-leguminous forbs *Taraxacum officinale* and *Plantago lanceolata*[67].

At the end of July (July 29th, 2020), soil samples were collected from the top 10 cm with a corer (2 cm diameter) from four treatments and all four respective replicates plots each: (i) ambient conditions, (ii) ambient conditions & drought, (iii) future climate conditions (+3 °C and +300 ppm), and (iv) future climate conditions & drought. This represented peak drought for the plots where precipitation was manipulated using rainout shelters (ambient conditions & drought, future climate conditions & drought). At the time of sampling, all future climate plots have been exposed to warming and elevated atmospheric CO_2 for ~6 years. All drought plots experienced two previous summer drought simulations (2017, 2019).

Quantitative stable isotope probing via ^{18}O water vapor equilibration (vapor-qSIP)

Soils were passed through a 2 mm sieve to remove rocks, plant litter, and roots and stored for 48 h until the start of qSIP incubations. Soil water content was determined gravimetrically by drying 2 g of fresh soil at 105 °C for 24 h.

Samples for qSIP were incubated with ^{18}O-enriched water and water at natural abundance isotope concentrations using the ^{18}O water vapor equilibration method[31]. Typically, in qSIP experiments, soil samples are air-dried followed by the direct addition of a liquid tracer (e.g., ^{18}O water). While this is necessary to study, for instance, the

effects of rewetting on the physiology of soil microorganisms[30], this procedure changes the soil water content. Especially in dry soils, liquid water addition stimulates microbial respiration (‘birch effect”, Birch 1958) and growth[31,69], making it hard to derive ecologically relevant rates of microbial activity under dry conditions. In vivo ^{18}O water vapor equilibration avoids changes in soil water content by letting labeled water redistribute into the soil pore space from a spatially separated source in a closed system. To this end, sieved soil samples (~500 mg) were weighed in 1.2 ml cryovials and inserted into 27 ml glass headspace vials. The amount of water applied to the bottom of a headspace vial (here: 270–430 µl) was calculated using the following equation:

$$V_{^{18}O\text{–}H_2O\text{ to be added}} = \frac{V_{\text{soil water}} * {}^{18}O\,at\%_{NA} - V_{\text{soil water}} * {}^{18}O\,at\%_{target}}{{}^{18}O\,at\%_{target} - {}^{18}O\,at\%_{added}} \quad (1)$$

where $^{18}O\ at\%_{target}$ and $^{18}O\ at\%_{added}$ represent the target enrichment of the soil water (here: ~70 ^{18}O atom%) and the enrichment of the added water, while $V_{soil\ water} * {}^{18}O\ at\%_{NA}$ represents the soil water volume multiplied by its natural abundance of ^{18}O ($^{18}O\ at\%_{NA} = 0.2\%$). The volumetric water contents of our soils were 31.6 ± 1.8% under ambient precipitation and 6.9 ± 1.9% under drought. Drought-unaffected samples were incubated with 95 atom % ^{18}O labeled water and drought-affected samples were incubated with 75 atom % ^{18}O to make sure that enough remaining water could be collected after incubation for isotopic analysis.

After water addition, we closed the headspace vials air-tight with rubber septa and incubated them at field temperatures at the time of harvest (ambient = 20 °C, future climate = 23 °C) for five days. To monitor the ^{18}O soil water enrichment over time, we prepared four additional ^{18}O calibration samples using one soil sample per treatment. From the calibration samples, we collected the remaining water at the bottom of the headspace vial after 3, 6, 24, and 48 h, respectively. At the end of the 5-day incubation period, we performed the same for all primary ^{18}O labeled samples. The water samples were analyzed for their ^{18}O enrichment through equilibration of ^{18}O in H_2O with CO_2 on a Gasbench II headspace sampler connected to a Delta V Advantage isotope ratio mass spectrometer (Thermo Fisher). These values informed the mean ^{18}O enrichments of soil water over the course of the incubation by fitting a negative exponential function and determining its integral[31]. Based on these calculations, our samples reached the target enrichment after 24–48 h (Supplementary Fig. 11), resulting in an average soil water enrichment of 59.3 ± 3 atom% (mean ± SD). Soil water enrichments ranged between 55–64 atom% and we accounted for this variation while calculating relative growth rates.

After incubation, soil aliquots were flash-frozen and stored at −80 °C. We isolated DNA from soils using the FastDNA™ SPIN Kit for Soil (MO Biomedicals) following manufacturer’s instructions. DNA concentrations were quantified fluorometrically using the PicoGreen assay (Quant-iTTM PicoGreen dsDNA Reagent, Life Technologies). To measure ^{18}O isotope incorporation in microbial DNA, we subjected our samples to ultracentrifugation in a cesium chloride density gradient[27]. We loaded 2 µg DNA into a 4.7 mL OptiSeal ultracentrifuge tube (Beckman Coulter) with ~4 ml saturated CsCl solution and gradient buffer (100 mM Tris, 100 mM KCl, 1 mM EDTA). Samples were spun in a Beckman Optima ultracentrifuge using a Beckman VTi 65.2 rotor (50,000 rpm at 20 °C) for 72 h. We manually collected 24 fractions of 250 µl after puncturing the tubes with a cannula (Braun Sterican, 0.9 × 25 mm). Sterile distilled water served as a displacement medium. During fractionation, tubes were secured with a three-prong clamp attached to a retort stand. The density of each fraction was determined with a Krüss DR301-95 digital refractometer. DNA was purified from the CsCl solution by glycogen-aided isopropanol precipitation, resuspended in 50 µl of nuclease-free water, and quantified by the PicoGreen assay (see above).

Sequencing was performed on 15-16 fractions per sample at the Joint Microbiome Facility of the Medical University of Vienna and the University of Vienna (JMF project IDs: JMF-2104-06, JMF-2012-8). Fractions were selected based on DNA content and density, excluding those without detectable DNA and mostly consisting of displacement medium. A two-step barcoding approach was used to generate amplicon libraries of archaeal and bacterial communities using Illumina MiSeq (V3 Kit) in the 2 × 300 bp configuration[70]. Primer sequences (515F–806 R) and PCR amplification protocols (30 cycles) were used as specified by the Earth Microbiome Project[71] standard protocols (https://earthmicrobiome.org/protocols-and-standards/16s/). We used the following cycling conditions: initial denaturation at 94 °C for 4 min, 7 cycles of 94 °C for 30 s, 52 °C for 30 s, 72 °C for 60 s, and final elongation at 72 °C for 7 min[70]. Amplicon pools were extracted from the raw sequencing data using the FASTQ workflow in BaseSpace (Illumina) with default parameters. Demultiplexing was performed with the python package demultiplex (Laros JFJ, github.com/jfjlaros/demultiplex) allowing one mismatch for barcodes and two mismatches for linkers and primers[70]. Amplicon sequence variants (ASVs) were inferred using the DADA2 R package[72] applying the recommended workflow. FASTQ reads 1 and 2 were trimmed at 220 nt and 150 nt with allowed expected errors of 2 and 2, respectively. ASV sequences were subsequently classified using DADA2 and the SILVA database SSU Ref NR 99 release 138.1[73,74] with a confidence threshold of 0.5. Datasets were deposited in the NCBI Sequence Read Archive under BioProject accession number PRJNA937073.

We measured the concentration of archaeal and bacterial 16 S rRNA gene copies per fraction with the Bio-Rad QX200 Droplet Digital PCR (ddPCR) system using the same primers as for the sequencing. Individual PCR reactions comprised the following components: 11 µl 1× EvaGreen Droplet Generation Mix (Bio-Rad), 0.2 µl forward primer (10 µM), 0.2 µl reverse primer (10 µM), 8.6 µl nuclease-free water, and 2 µl diluted DNA template. Prior to ddPCR quantification, DNA samples were diluted to 0.05 ng/µl as 0.1 ng of total DNA per reaction was found optimal for the separation of negative and positive droplets. The following cycling conditions were used for ddPCR: 95 °C for 5 min, 5 cycles of 95 °C for 30 s, 57 °C for 2.5 min (−1 °C each step), followed by 35 cycles of 95 °C for 30 s, 52 °C for 2.5 min, followed by 4 °C for 5 min, and 90 °C for 5 min. Droplets were stored at 4 °C for a least one hour before reading. We used QuantaSoft software (Bio-Rad) to calculate 16 S rRNA gene copies.

qSIP and statistical analyses

All analyses were performed in R 4.1.1[75]. Amplicon sequencing data was manipulated using the phyloseq package[76]. We removed ASVs without taxonomic assignment at the phylum level as well as sequences classified as eukaryotes, mitochondria, or chloroplasts (2243 ASVs). In addition, we removed contaminant ASVs identified by decontam 1.6.0[77] using the prevalence method and a threshold setting of 0.01 (number of negative controls = 3). Negative controls from DNA extraction and dilution steps served as input data, resulting in the removal of 11 ASVs. Only samples within a density range of 1.614- – 1.753 and >2000 read pairs were retained for further analyses to exclude fractions contaminated with the fractionation medium (water) and of low sequencing yield. After filtering, we continued with 12-14 fractions per sample. Several low-density fractions of two replicates from the control treatment (ambient conditions) were lost during fractionation, resulting in higher weighted average density (WAD) values per tube. To account for this, we calculated the mean offset in weighted average density at the tube level and subtracted it from the measured densities of these samples. These procedures yielded a feature table with 15,565 ASVs and 4,342,798 read pairs.

Taxon-specific ^{18}O atom percent enrichment (APE ^{18}O), a proxy for relative microbial growth, was determined based on the relationships between ^{18}O incorporation, DNA density, GC-content, and DNA

molecular weight[37]. Although growth and activity do not always correspond, since non-growing microbes can still show low activity, we used both terms interchangeably for simplicity reasons. We used publicly available code to perform qSIP calculations (https://bitbucket.org/QuantitativeSIP/qsip_repo, https://github.com/bramstone/qsip). A prevalence filtering step was applied prior to qSIP analysis to exclude infrequent taxa[45]. Taxa had to occur in at least 4 fractions and two replicates per treatment, yielding 6,054 ASVs accounting for 84.9 % of all sequence read pairs. We calculated replicate-level APE ^{18}O values without bootstrapping, yielding 5,652 active ASVs (APE $^{18}O > 0$; min. APE $^{18}O = 0$; max. APE $^{18}O = 110\%$). We then applied a minimum enrichment threshold (APE $^{18}O > 5\%$) to ensure enrichment was due to isotopic incorporation and not caused by density variations between tubes, resulting in 5116 ASVs. Taxon-level relative growth rates per day (RGR) were calculated as follows assuming linear growth: RGR = APE $^{18}O_{taxon}$ / (Average APE $^{18}O_{soil\ water}$ * 5 days)[78,79]. For this, APE ^{18}O percent values were converted into decimals also called ^{18}O atom fraction excess (AFE ^{18}O) and commonly used in qSIP studies. We compared RGRs of shared taxa between treatments only if they were growing in at least two replicates each. To avoid pseudoreplication (multiple taxon-specific growth estimates per sample), we calculated mean relative growth rates for each sample and compared them using either two-way ANOVA (see details below) or Student's *t*-test for pairwise treatment comparisons.

Absolute abundances (16 S rRNA gene copies per ASV) were calculated by multiplying their sequencing-inferred relative abundances by the total number of 16 S rRNA gene copies accumulated over all density fractions of a sample. To determine the size, or percentage, of the growing community, we summed the absolute abundances of all growing taxa before dividing them by the total number of absolute abundances per sample.

Although some taxa might be growing faster than others, their contribution to the overall community-level growth will also depend on their abundance. Therefore, we estimated proportional ^{18}O-assimilation for each growing ASV by re-calculating their relative abundances (sum of relative abundances of growing taxa = 1) and multiplying them by their relative growth rate (RGR). These weighted enrichment values were then divided by their sum, producing a proportional ^{18}O-assimilation value ranging between 0–1. We ranked ASVs that were active in at least two replicates based on their proportional ^{18}O-assimilation to identify the top five and top 50 ^{18}O assimilating taxa per sample. The pool of the top five ^{18}O assimilating taxa consisted of 26 and 19 ASVs for samples exposed to ambient precipitation and drought, respectively. We visualized changes in proportional ^{18}O-assimilation with heatmaps using functions from the ampvis2 package[80]. For heatmaps, ASVs were agglomerated at the genus level. If genus identity could not be assigned (´NA"), we agglomerated taxa at the family or phylum level.

To compare the effect of drought and future climate treatments across phyla and families, we calculated their number of growing taxa in each sample. These numbers were used to perform two-way ANOVAs testing a full two factorial design (Drought $_{Yes}$, Drought $_{No}$, Climate $_{Ambient}$, Climate $_{Future}$) for each phylum and family individually if normality (Shapiro–Wilk test) and homoscedasticity (Levene's test) requirements were fulfilled. If these requirements were not met for a phylum, we used pairwise Wilcoxon signed-rank tests. Shifts in the number of growing taxa were visualized between treatment pairs using relative changes as compared to the mean of the respective reference (0 = no change, 1 = increase by 100%).

We compared treatment effects on the composition of total versus growing communities by computing Euclidean distances according to a new quantitative sequencing framework used when dealing with absolute abundances[81]. This was followed by two-way PERMANOVA testing a full two factorial design (Drought $_{Yes}$, Drought $_{No}$, Climate $_{Ambient}$, Climate $_{Future}$) using the ´adonis" function[82]. For the total and growing communities, we merged the absolute abundances of all density fractions per sample (only labeled) before centered log-ratio transformation. For the growing community, we additionally computed Euclidean distances based on relative growth rates to examine differences in activity patterns beyond abundance shift. Euclidean distances were visualized using PCA.

Due to the full two factorial design of our experiment, we used two-way ANOVA to test for the effects of drought (Drought $_{Yes}$, Drought $_{No}$,), climate (Climate $_{Ambient}$, Climate $_{Future}$), and their interaction on the richness, size, and mean relative growth rates (including ´non-growing" taxa) of the growing community. We also used two-way ANOVA to test for drought and climate effects on putative predators and the proportional ^{18}O-assimilation across the top five ^{18}O assimilating taxa including *Streptomyces* as well as on its abundance and RGR.

We examined the normality and homoscedasticity of our data and applied log transformation if necessary. False discovery rate (FDR) correction was employed to correct for multiple testing. To examine the impact of genus identity on mean relative growth rates (excluding ´non-growing" taxa) in addition to drought and climate, we used a hierarchical linear mixed model implemented in the 'lme4' package[83]. Our model had the following structure: lmer (formula = log (Relative growth rate$_{ASV}$) ~ Drought * Climate * Genus + (1|SampleID), data = data). By implementing 'Genus' in the fixed and 'Sample ID' in the random terms, we tried to limit pseudoreplication.

Reporting summary

Further information on research design is available in the Nature Portfolio Reporting Summary linked to this article.

Data availability

DNA sequence data generated in the frame of this study have been deposited in the NCBI Short-Read Archive under the BioProject accession number PRJNA937073. The data used in this study are available in the Zenodo database under accession code 8109566. Source data are provided with this paper.

Code availability

All code and data used to produce the analyses and figures of this study are openly available in the Zenodo database under accession code 8109566.

References

1. Cook, B. I., Mankin, J. S. & Anchukaitis, K. J. Climate change and drought: from past to future. *Curr. Clim. Change Rep.* **4**, 164–179 (2018).
2. Senf, C., Buras, A., Zang, C. S., Rammig, A. & Seidl, R. Excess forest mortality is consistently linked to drought across Europe. *Nat. Commun.* **11**, 6200 (2020).
3. Williams, A. P. et al. Large contribution from anthropogenic warming to an emerging North American megadrought. *Science* **368**, 314–318 (2020).
4. Impacts of 1.5 °C Global Warming on Natural and Human Systems. in *Global Warming of 1.5 °C: IPCC Special Report on Impacts of Global Warming of 1.5 °C above Pre-industrial Levels in Context of Strengthening Response to Climate Change, Sustainable Development, and Efforts to Eradicate Poverty* (ed. Intergovernmental Panel on Climate Change (IPCC)) 175–312 (Cambridge University Press, 2022). https://doi.org/10.1017/9781009157940.005.
5. Lal, R. Carbon sequestration. *Philos. Trans. R. Soc. B: Biol. Sci.* **363**, 815–830 (2007).
6. Ontl, T. A. & Schulte, L. A. Soil carbon storage. *Nat. Educ. Knowl.* **3**, 35 (2012).
7. Falkowski, P. G., Fenchel, T. & Delong, E. F. The microbial engines that drive earth's biogeochemical cycles. *Science* **320**, 1034–1039 (2008).

8. Bardgett, R. D., Freeman, C. & Ostle, N. J. Microbial contributions to climate change through carbon cycle feedbacks. *ISME J.* **2**, 805–814 (2008).
9. Melillo, J. M. et al. Soil warming and carbon-cycle feedbacks to the climate system. *Science* **298**, 2173–2176 (2002).
10. Manzoni, S., Schimel, J. P. & Porporato, A. Responses of soil microbial communities to water stress: results from a meta-analysis. *Ecology* **93**, 930–938 (2012).
11. Stark, J. M. & Firestone, M. K. Mechanisms for soil moisture effects on activity of nitrifying bacteria. *Appl. Environ. Microbiol.* **61**, 218–221 (1995).
12. Manzoni, S., Schaeffer, S. M., Katul, G., Porporato, A. & Schimel, J. P. A theoretical analysis of microbial eco-physiological and diffusion limitations to carbon cycling in drying soils. *Soil Biol. Biochem.* **73**, 69–83 (2014).
13. Schimel, J. P. Life in dry soils: effects of drought on soil microbial communities and processes. *Annu. Rev. Ecol. Evol. Syst.* **49**, 409–432 (2018).
14. Fuchslueger, L. et al. Drought history affects grassland plant and microbial carbon turnover during and after a subsequent drought event. *J. Ecol.* **104**, 1453–1465 (2016).
15. Fuchslueger, L., Bahn, M., Fritz, K., Hasibeder, R. & Richter, A. Experimental drought reduces the transfer of recently fixed plant carbon to soil microbes and alters the bacterial community composition in a mountain meadow. *N. Phytol.* **201**, 916–927 (2014).
16. Evans, S. E., Wallenstein, M. D. & Burke, I. C. Is bacterial moisture niche a good predictor of shifts in community composition under long-term drought? *Ecology* **95**, 110–122 (2014).
17. Canarini, A. et al. Ecological memory of recurrent drought modifies soil processes via changes in soil microbial community. *Nat. Commun.* **12**, 1–14 (2021).
18. Blagodatskaya, E. & Kuzyakov, Y. Active microorganisms in soil: critical review of estimation criteria and approaches. *Soil Biol. Biochem.* **67**, 192–211 (2013).
19. Couradeau, E. et al. Probing the active fraction of soil microbiomes using BONCAT-FACS. *Nat. Commun.* **10**, 1–10 (2019).
20. Dijkstra, P. et al. On maintenance and metabolisms in soil microbial communities. *Plant Soil* https://doi.org/10.1007/s11104-022-05382-9 (2022).
21. Bickel, S. & Or, D. Soil bacterial diversity mediated by microscale aqueous-phase processes across biomes. *Nat. Commun.* **11**, 116 (2020).
22. Malik, A. A. & Bouskill, N. J. Drought impacts on microbial trait distribution and feedback to soil carbon cycling. *Funct. Ecol.* **36**, 1442–1456 (2022).
23. Barnard, R. L., Blazewicz, S. J. & Firestone, M. K. Rewetting of soil: revisiting the origin of soil CO2 emissions. *Soil Biol. Biochem.* **147**, 107819 (2020).
24. Barnard, R. L., Osborne, C. A. & Firestone, M. K. Responses of soil bacterial and fungal communities to extreme desiccation and rewetting. *ISME J.* **7**, 2229–2241 (2013).
25. Birch, H. F. The effect of soil drying on humus decomposition and nitrogen availability. *Plant Soil* **10**, 9–31 (1958).
26. Rillig, M. C. et al. The role of multiple global change factors in driving soil functions and microbial biodiversity. *Science* **366**, 886–890 (2019).
27. Hungate, B. A. et al. Quantitative microbial ecology through stable isotope probing. *Appl. Environ. Microbiol.* **81**, 7570–7581 (2015).
28. Berry, D. et al. Tracking heavy water (D2O) incorporation for identifying and sorting active microbial cells. *Proc. Natl Acad. Sci.* **112**, E194–E203 (2015).
29. Koch, B. J. et al. Estimating taxon-specific population dynamics in diverse microbial communities. *Ecosphere* **9**, 1–15 (2018).
30. Blazewicz, S. J. et al. Taxon-specific microbial growth and mortality patterns reveal distinct temporal population responses to rewetting in a California grassland soil. *ISME J.* **14**, 1520–1532 (2020).
31. Canarini, A. et al. Quantifying microbial growth and carbon use efficiency in dry soil environments via 18O water vapor equilibration. *Glob. Change Biol.* **26**, 5333–5341 (2020).
32. Piepho, H.-P., Herndl, M., Pötsch, E. M. & Bahn, M. Designing an experiment with quantitative treatment factors to study the effects of climate change. *J. Agron. Crop Sci.* **203**, 584–592 (2017).
33. Barnard, R. L., Osborne, C. A. & Firestone, M. K. Changing precipitation pattern alters soil microbial community response to wet-up under a Mediterranean-type climate. *ISME J.* **9**, 946–957 (2015).
34. Schaeffer, S. M., Homyak, P. M., Boot, C. M., Roux-Michollet, D. & Schimel, J. P. Soil carbon and nitrogen dynamics throughout the summer drought in a California annual grassland. *Soil Biol. Biochem.* **115**, 54–62 (2017).
35. Bouskill, N. J. et al. Pre-exposure to drought increases the resistance of tropical forest soil bacterial communities to extended drought. *ISME J.* **7**, 384–394 (2013).
36. Bastida, F. et al. Differential sensitivity of total and active soil microbial communities to drought and forest management. *Glob. Change Biol.* **23**, 4185–4203 (2017).
37. Naylor, D. & Coleman-Derr, D. Drought stress and root-associated bacterial communities. *Front. Plant Sci.* **8**, 2223 (2018).
38. Acosta-Martínez, V. et al. Predominant bacterial and fungal assemblages in agricultural soils during a record drought/heat wave and linkages to enzyme activities of biogeochemical cycling. *Appl. Soil Ecol.* **84**, 69–82 (2014).
39. Armstrong, A. et al. Temporal dynamics of hot desert microbial communities reveal structural and functional responses to water input. *Sci. Rep.* **6**, 34434 (2016).
40. Tóth, Z. et al. Extreme effects of drought on composition of the soil bacterial community and decomposition of plant tissue. *Eur. J. Soil Sci.* **68**, 504–513 (2017).
41. Parker, S. S. & Schimel, J. P. Soil nitrogen availability and transformations differ between the summer and the growing season in a California grassland. *Appl. Soil Ecol.* **48**, 185–192 (2011).
42. Hartmann, M. et al. A decade of irrigation transforms the soil microbiome of a semi-arid pine forest. *Mol. Ecol.* **26**, 1190–1206 (2017).
43. Ochoa-Hueso, R. et al. Drought consistently alters the composition of soil fungal and bacterial communities in grasslands from two continents. *Glob. Change Biol.* **24**, 2818–2827 (2018).
44. Naylor, D., DeGraaf, S., Purdom, E. & Coleman-Derr, D. Drought and host selection influence bacterial community dynamics in the grass root microbiome. *ISME J.* **11**, 2691–2704 (2017).
45. Stone, B. W. et al. Nutrients cause consolidation of soil carbon flux to small proportion of bacterial community. *Nat. Commun.* **12**, 1–9 (2021).
46. Kour, D. et al. Drought adaptive microbes as bioinoculants for the horticultural crops. *Heliyon* **8**, e09493 (2022).
47. Abbasi, S., Sadeghi, A. & Safaie, N. Streptomyces alleviate drought stress in tomato plants and modulate the expression of transcription factors ERF1 and WRKY70 genes. *Sci. Hortic.* **265**, 109206 (2020).
48. Schrey, S. D. & Tarkka, M. T. Friends and foes: streptomycetes as modulators of plant disease and symbiosis. *Antonie van. Leeuwenhoek* **94**, 11–19 (2008).
49. Breitkreuz, C., Buscot, F., Tarkka, M. & Reitz, T. Shifts between and among populations of wheat Rhizosphere pseudomonas, streptomyces and phyllobacterium suggest consistent phosphate mobilization at different wheat growth stages under abiotic stress. *Front. Microbiol.* **10**, 3109 (2020).

50. Fitzpatrick, C. R. et al. Assembly and ecological function of the root microbiome across angiosperm plant species. *Proc. Natl Acad. Sci.* **115**, E1157–E1165 (2018).
51. Xu, L. & Coleman-Derr, D. Causes and consequences of a conserved bacterial root microbiome response to drought stress. *Curr. Opin. Microbiol.* **49**, 1–6 (2019).
52. Xu, L. et al. Drought delays development of the sorghum root microbiome and enriches for monoderm bacteria. *Proc. Natl Acad. Sci.* **115**, E4284–E4293 (2018).
53. Isobe, K., Bouskill, N. J., Brodie, E. L., Sudderth, E. A. & Martiny, J. B. H. Phylogenetic conservation of soil bacterial responses to simulated global changes. *Philos. Trans. R. Soc. B: Biol. Sci.* **375**, 20190242 (2020).
54. Evans, S. E. & Wallenstein, M. D. Climate change alters ecological strategies of soil bacteria. *Ecol. Lett.* **17**, 155–164 (2014).
55. Franco, A. L. C. et al. Drought suppresses soil predators and promotes root herbivores in mesic, but not in xeric grasslands. *Proc. Natl Acad. Sci.* **116**, 12883–12888 (2019).
56. Hu, Z. et al. Precipitation changes, warming, and N input differentially affect microbial predators in an alpine meadow: Evidence from soil phagotrophic protists. *Soil Biol. Biochem.* **165**, 108521 (2022).
57. Brangari, A. C., Manzoni, S. & Rousk, J. The mechanisms underpinning microbial resilience to drying and rewetting—a model analysis. *Soil Biol. Biochem.* **162**, 108400 (2021).
58. Leizeaga, A., Hicks, L. C., Manoharan, L., Hawkes, C. V. & Rousk, J. Drought legacy affects microbial community trait distributions related to moisture along a savannah grassland precipitation gradient. *J. Ecol.* **109**, 3195–3210 (2021).
59. Reinthaler, D. et al. Responses of grassland soil CO2 production and fluxes to drought are shifted in a warmer climate under elevated CO2. *Soil Biol. Biochem.* **163**, 108436 (2021).
60. Simon, E. et al. Microbial growth and carbon use efficiency show seasonal responses in a multifactorial climate change experiment. *Commun. Biol.* **3**, 1–10 (2020).
61. Norby, R. J. & Zak, D. R. Ecological lessons from free-air CO2 enrichment (FACE) experiments. *Annu. Rev. Ecol. Evol. Syst.* **42**, 181–203 (2011).
62. Phillips, R. P., Finzi, A. C. & Bernhardt, E. S. Enhanced root exudation induces microbial feedbacks to N cycling in a pine forest under long-term CO2 fumigation. *Ecol. Lett.* **14**, 187–194 (2011).
63. Preece, C. & Peñuelas, J. Rhizodeposition under drought and consequences for soil communities and ecosystem resilience. *Plant Soil* **409**, 1–17 (2016).
64. de Vries, F. T. et al. Changes in root-exudate-induced respiration reveal a novel mechanism through which drought affects ecosystem carbon cycling. *N. Phytol.* **224**, 132–145 (2019).
65. Leakey, A. D. B., Bernacchi, C. J., Dohleman, F. G., Ort, D. R. & Long, S. P. Will photosynthesis of maize (Zea mays) in the US Corn Belt increase in future [CO2] rich atmospheres? An analysis of diurnal courses of CO2 uptake under free-air concentration enrichment (FACE). *Glob. Change Biol.* **10**, 951–962 (2004).
66. Meeran, K. et al. Warming and elevated CO_2 intensify drought and recovery responses of grassland carbon allocation to soil respiration. *Glob. Change Biol.* **27**, 3230–3243 (2021).
67. Séneca, J. et al. Composition and activity of nitrifier communities in soil are unresponsive to elevated temperature and CO_2, but strongly affected by drought. *ISME J.* **14**, 3038–3053 (2020).
68. Maxwell, T. L. et al. Contrasting drivers of belowground nitrogen cycling in a montane grassland exposed to a multifactorial global change experiment with elevated CO_2, warming, and drought. *Glob. Change Biol.* **28**, 2425–2441 (2022).
69. Blazewicz, S. J., Schwartz, E. & Firestone, M. K. Growth and death of bacteria and fungi underlie rainfall-induced carbon dioxide pulses from seasonally dried soil. *Ecology* **95**, 1162–1172 (2014).
70. Pjevac, P. et al. An economical and flexible dual barcoding, two-step PCR approach for highly multiplexed amplicon sequencing. *Front. Microbiol.* **12**, 669776 (2021).
71. Gilbert, J. A., Jansson, J. K. & Knight, R. The earth microbiome project: successes and aspirations. *BMC Biol.* **12**, 69 (2014).
72. Callahan, B. J. et al. DADA2: high-resolution sample inference from Illumina amplicon data. *Nat. Methods* **13**, 581 (2016).
73. Quast, C. et al. The SILVA ribosomal RNA gene database project: improved data processing and web-based tools. *Nucleic Acids Res.* **41**, D590–D596 (2013).
74. McLaren, M. R. & Callahan, B. J. Silva 138.1 prokaryotic SSU taxonomic training data formatted for DADA2 [Data set]. *Zenodo* https://doi.org/10.5281/zenodo.4587955 (2021).
75. R Core Team. R: A language and environment for statistical computing. http://www.R-project.org/. *R Foundation for Statistical Computing*, Vienna, Austria (2021).
76. McMurdie, P. J. & Holmes, S. phyloseq: an R package for reproducible interactive analysis and graphics of microbiome census data. *PLoS One* **8**, e61217 (2013).
77. Davis, N. M., Proctor, D. M., Holmes, S. P., Relman, D. A. & Callahan, B. J. Simple statistical identification and removal of contaminant sequences in marker-gene and metagenomics data. *Microbiome* **6**, 226 (2018).
78. Purcell, A. M. et al. Decreased growth of wild soil microbes after 15 years of transplant-induced warming in a montane meadow. *Glob. Change Biol.* **28**, 128–139 (2021).
79. Li, J. et al. Predictive genomic traits for bacterial growth in culture versus actual growth in soil. *ISME J.* **13**, 2162–2172 (2019).
80. Andersen, K. S., Kirkegaard, R. H., Karst, S. M. & Albertsen, M. ampvis2: an R package to analyse and visualise 16S rRNA amplicon data. *bioRxiv* 299537 https://doi.org/10.1101/299537 (2018).
81. Barlow, J. T., Bogatyrev, S. R. & Ismagilov, R. F. A quantitative sequencing framework for absolute abundance measurements of mucosal and lumenal microbial communities. *Nat. Commun.* **11**, 2590 (2020).
82. Oksanen, J. et al. Vegan: Community Ecology Package. R Package Version. 2.5-6. http://CRAN.R-project.org/package=vegan (2019).
83. Bates, D., Mächler, M., Bolker, B. & Walker, S. Fitting linear mixed-effects models using lme4. *J. Stat. Softw.* **67**, 1–48 (2015).

Acknowledgements

DM was financially supported by FutureArctic, a European Union's Horizon 2020 research and innovation program under the Marie Skłodowska-Curie Actions (grant no. 813114). We thank Jasmin Schwarz and Gudrun Kohl for 16 S rRNA gene amplification and sequencing. We also thank Joana Senéca Silva for handling the submission of the sequencing data to the NCBI Short-Read Archive, Petra Pjevac for her helpful comments on the manuscript, and Leila Hadziabdic for optimizing the conditions for 16 S rRNA gene amplification using ddPCR. Furthermore, we thank Stephanie Eichorst for her support with the ultracentrifuge.

Author contributions

AR, DM, JS, LF, AC, and CK conceived the study, and AS, MB, and AR established the field site. AC, LF, and JS carried out fieldwork and incubations. DM performed the lab experiments and data analyses, with important inputs from BWS, BJK, HS, and BAH. BH processed the raw amplicon sequencing data.

Competing interests

The authors declare no competing interests.

Additional information

Supplementary information The online version contains supplementary material available at https://doi.org/10.1038/s41467-023-41524-y.

Correspondence and requests for materials should be addressed to Dennis Metze or Andreas Richter.

Peer review information *Nature Communications* thanks Eric Morrison, and the other, anonymous, reviewers for their contribution to the peer review of this work. A peer review file is available.

Reprints and permissions information is available at http://www.nature.com/reprints

Publisher's note Springer Nature remains neutral with regard to jurisdictional claims in published maps and institutional affiliations.

[1]Centre for Microbiology and Environmental Systems Science, University of Vienna, Vienna, Austria. [2]Doctoral School in Microbiology and Environmental Science, University of Vienna, Vienna, Austria. [3]Center for Ecosystem Science and Society and Department of Biological Sciences, Northern Arizona University, Flagstaff, AZ, USA. [4]Earth and Biological Sciences Directorate, Pacific Northwest National Laboratory, Richland, WA, USA. [5]Joint Microbiome Facility of the Medical University of Vienna and the University of Vienna, Vienna, Austria. [6]Division of Clinical Microbiology, Department of Laboratory Medicine, Medical University of Vienna, Vienna, Austria. [7]Agricultural Research and Education Centre Raumberg-Gumpenstein, Irdning, Austria. [8]Department of Ecology, University of Innsbruck, Innsbruck, Austria. [9]International Institute for Applied Systems Analysis, Advancing Systems Analysis Program, Laxenburg, Austria. ✉e-mail: dennis.metze@univie.ac.at; andreas.richter@univie.ac.at

Supplementary Material

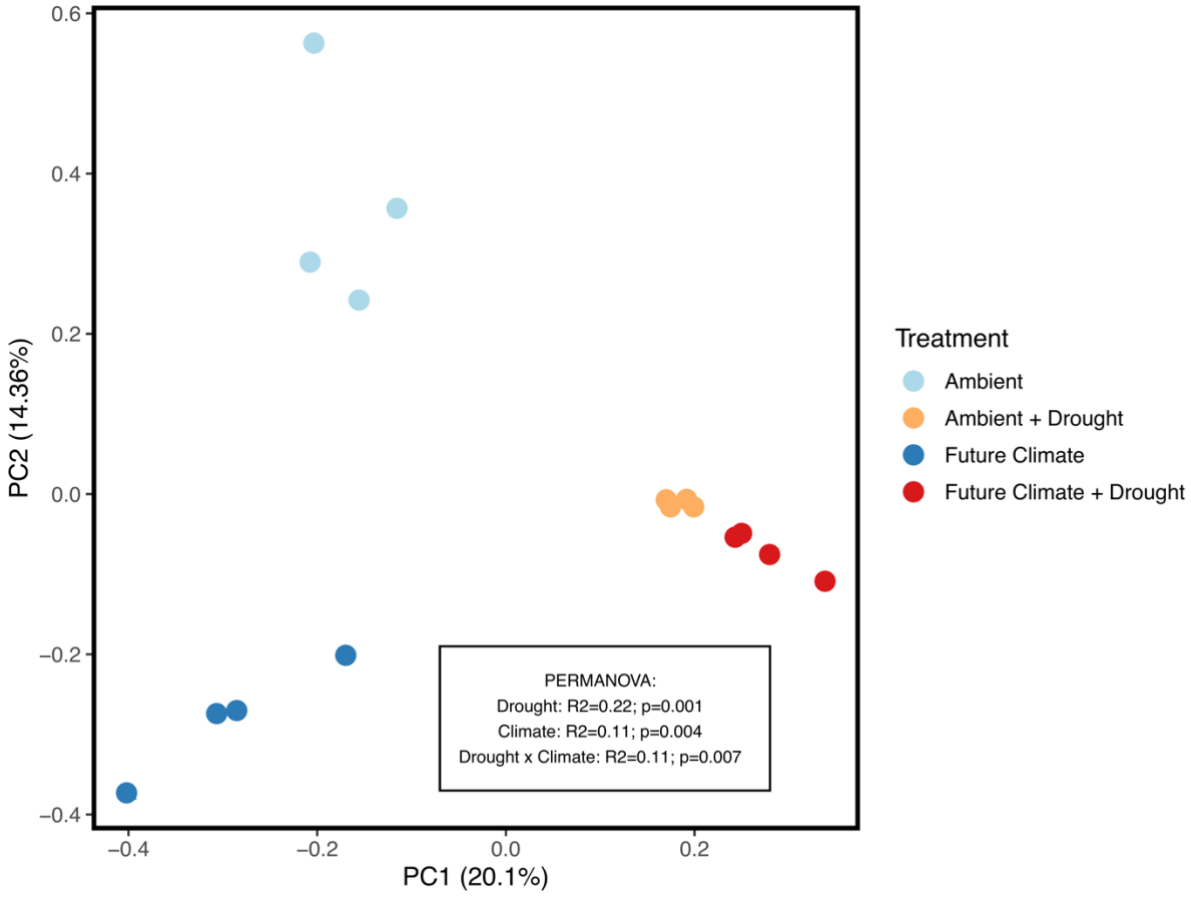

Supplementary Figure 1: Effect of drought and future climate conditions on the growth patterns of bacterial and archaeal communities. Principal component analysis (PCA) of taxon-specific relative growth rates (RGR) of the growing fraction of bacterial and archaeal communities (n=4 replicates). Statistics from two-way permutation-based multivariate analysis of variance (PERMANOVA) testing a full two factorial design (Drought $_{Yes}$, Drought $_{No}$, Climate $_{Ambient}$, Climate $_{Future}$) are provided as inset panels.

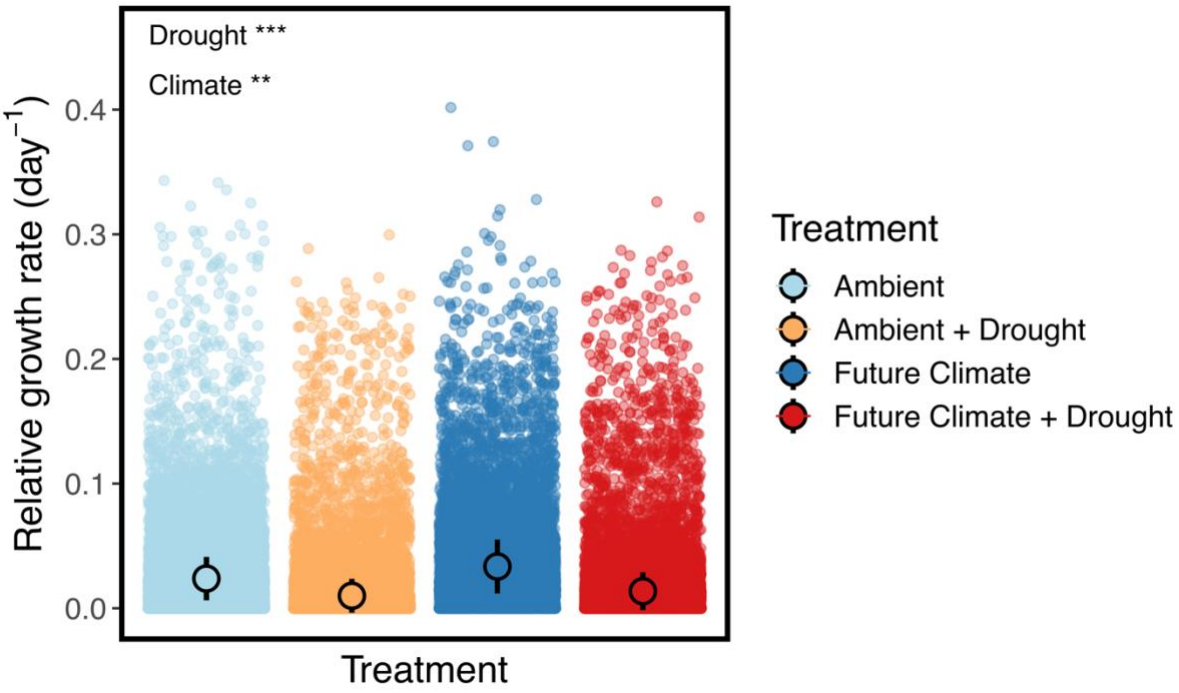

Supplementary Figure 2: Mean taxon-level relative growth rates of bacterial and archaea across treatments including growing and non-growing members. Mean taxon-level relative growth rates (RGR) were calculated using relative growth rates from all taxa that passed prevalence filtering (6054 amplicon sequencing variants (ASVs)). Non-growing taxa as defined per our minimum enrichment threshold (APE ^{18}O > 5 %) were assigned RGR = 0. Asterisks depict significant results from two-way ANOVA testing a full two factorial design (Drought $_{Yes}$, Drought $_{No}$, Climate $_{Ambient}$, Climate $_{Future}$). Light-colored dots represent ASV-level relative growth rates from all replicates used to calculate means (n=4 means of taxon-specific growth rates calculated per replicate) and standard errors (points, error bars).

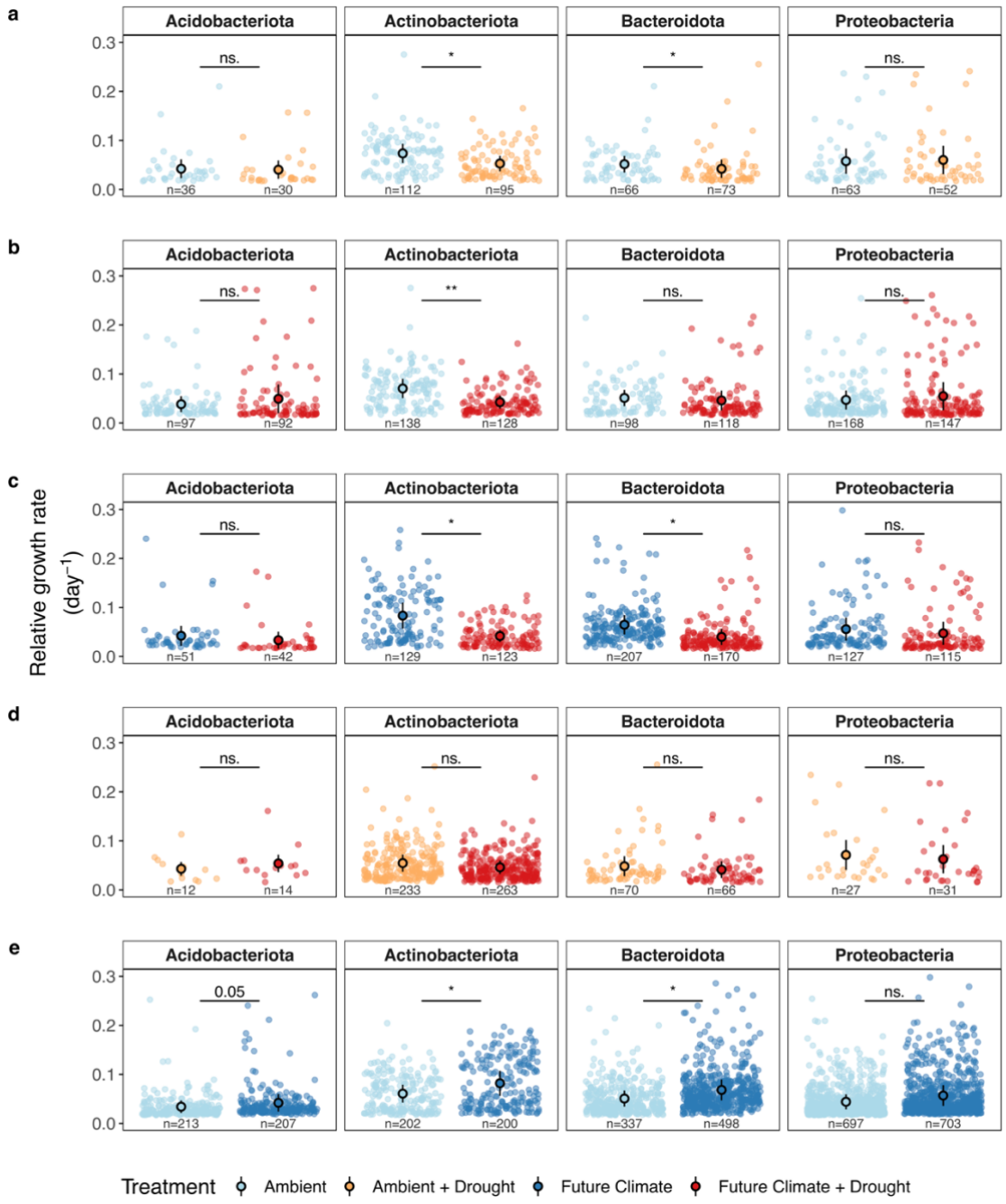

Supplementary Figure 3: Phylum-specific growth differences between treatments. Phylum-resolved comparison of mean taxon-level relative growth rates of shared ASVs between five treatment pairs **(a-e)**. ASVs belonged to the phyla Acidobacteriota, Actinobacteriota, Bacteroidota, and Proteobacteria. Light-colored dots represent ASV-level growth rates of all replicates used to calculate means and standard errors (points, error bars). P-values of pairwise comparisons are given as insert text. When data fulfilled normality and homoscedasticity requirements, t-tests were performed. If these criteria were not met, Wilcoxon tests were performed. The number of actively growing ASVs across all replicates used to calculate mean growth rates (n=4 means of taxon-specific growth rates calculated per replicate) is given below. ASVs had to grow in at least two replicates per treatment to be included.

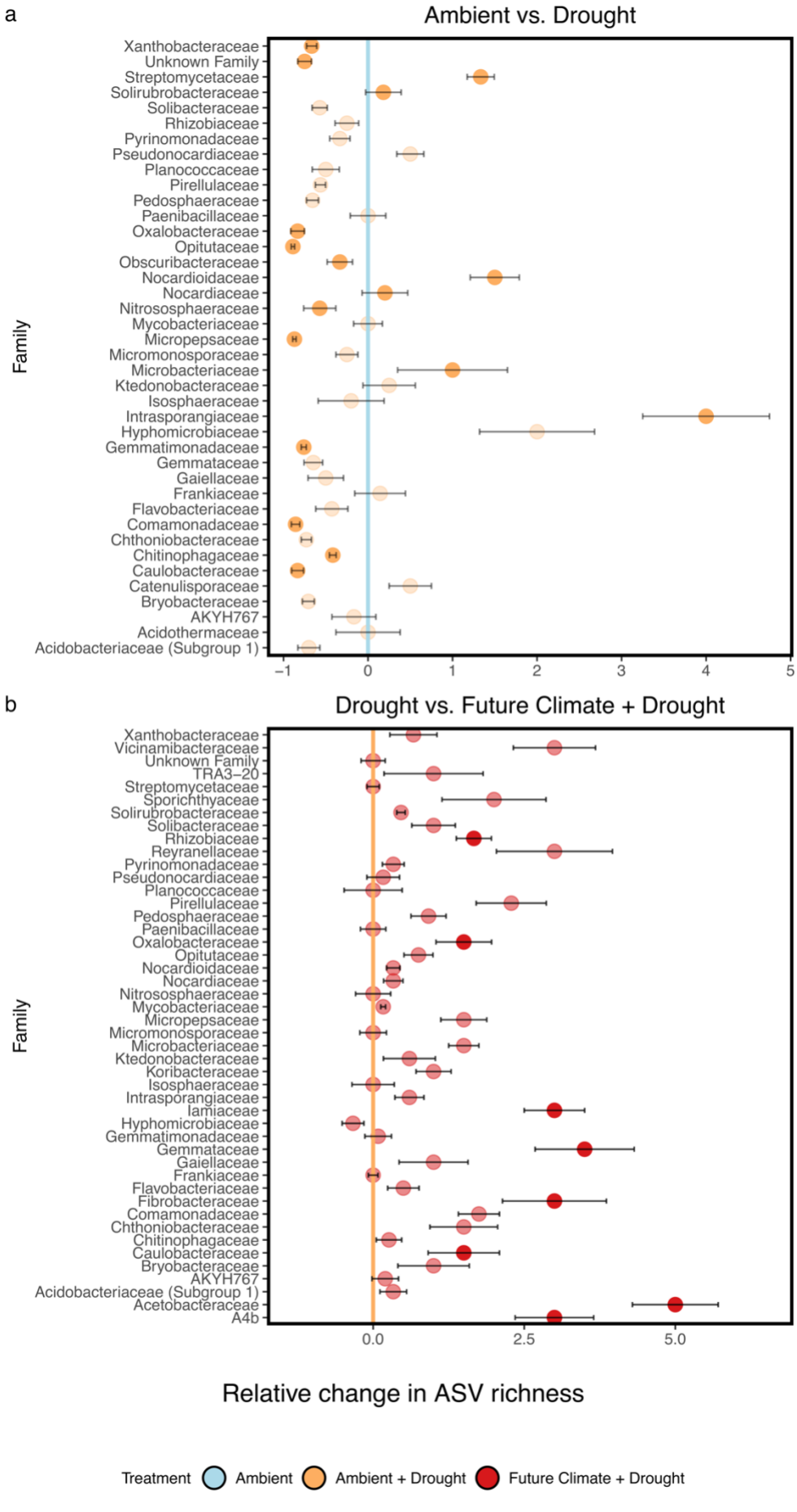
a
Ambient vs. Drought
Family
Xanthobacteraceae
Unknown Family
Streptomycetaceae
Solirubrobacteraceae
Solibacteraceae
Rhizobiaceae
Pyrinomonadaceae
Pseudonocardiaceae
Planococcaceae
Pirellulaceae
Pedosphaeraceae
Paenibacillaceae
Oxalobacteraceae
Opitutaceae
Obscuribacteraceae
Nocardioidaceae
Nocardiaceae
Nitrososphaeraceae
Mycobacteriaceae
Micropepsaceae
Micromonosporaceae
Microbacteriaceae
Ktedonobacteraceae
Isosphaeraceae
Intrasporangiaceae
Hyphomicrobiaceae
Gemmatimonadaceae
Gemmataceae
Gaiellaceae
Frankiaceae
Flavobacteriaceae
Comamonadaceae
Chthoniobacteraceae
Chitinophagaceae
Caulobacteraceae
Catenulisporaceae
Bryobacteraceae
AKYH767
Acidothermaceae
Acidobacteriaceae (Subgroup 1)
−1
0
1
2
3
4
5
b
Drought vs. Future Climate + Drought
Family
Xanthobacteraceae
Vicinamibacteraceae
Unknown Family
TRA3−20
Streptomycetaceae
Sporichthyaceae
Solirubrobacteraceae
Solibacteraceae
Rhizobiaceae
Reyranellaceae
Pyrinomonadaceae
Pseudonocardiaceae
Planococcaceae
Pirellulaceae
Pedosphaeraceae
Paenibacillaceae
Oxalobacteraceae
Opitutaceae
Nocardioidaceae
Nocardiaceae
Nitrososphaeraceae
Mycobacteriaceae
Micropepsaceae
Micromonosporaceae
Microbacteriaceae
Ktedonobacteraceae
Koribacteraceae
Isosphaeraceae
Intrasporangiaceae
Iamiaceae
Hyphomicrobiaceae
Gemmatimonadaceae
Gemmataceae
Gaiellaceae
Frankiaceae
Flavobacteriaceae
Fibrobacteraceae
Comamonadaceae
Chthoniobacteraceae
Chitinophagaceae
Caulobacteraceae
Bryobacteraceae
AKYH767
Acidobacteriaceae (Subgroup 1)
Acetobacteraceae
A4b
0.0
2.5
5.0
Relative change in ASV richness
Treatment
Ambient
Ambient + Drought
Future Climate + Drought

Supplementary Figure 4: Relative changes in the number of growing taxa per family under drought and future drought conditions. a Relative change (0 = no change, 1 = increase by 100 %) in the number of growing taxa per family comparing Ambient (reference) and Ambient + Drought conditions. **b** Relative change in the number of growing taxa comparing Ambient + Drought (reference) and Future Climate + Drought conditions. Points represent mean relative changes in the number of growing taxa per family including standard errors (n=4). Two-way ANOVA testing a full two factorial design (Drought $_{Yes}$, Drought $_{No}$, Climate $_{Ambient}$, Climate $_{Future}$) was performed on the number of growing amplicon sequence variants (ASVs) across all treatments for each family independently that fulfilled normality and homoscedasticity requirements. Bold colored points represent significant effects (A: Drought = $p < 0.05$, B: Climate = $p < 0.05$ or Drought x Climate = $p < 0.05$), and transparent points non-significant ones. Vertical lines depict the means of the respective reference treatment used to calculate relative changes.

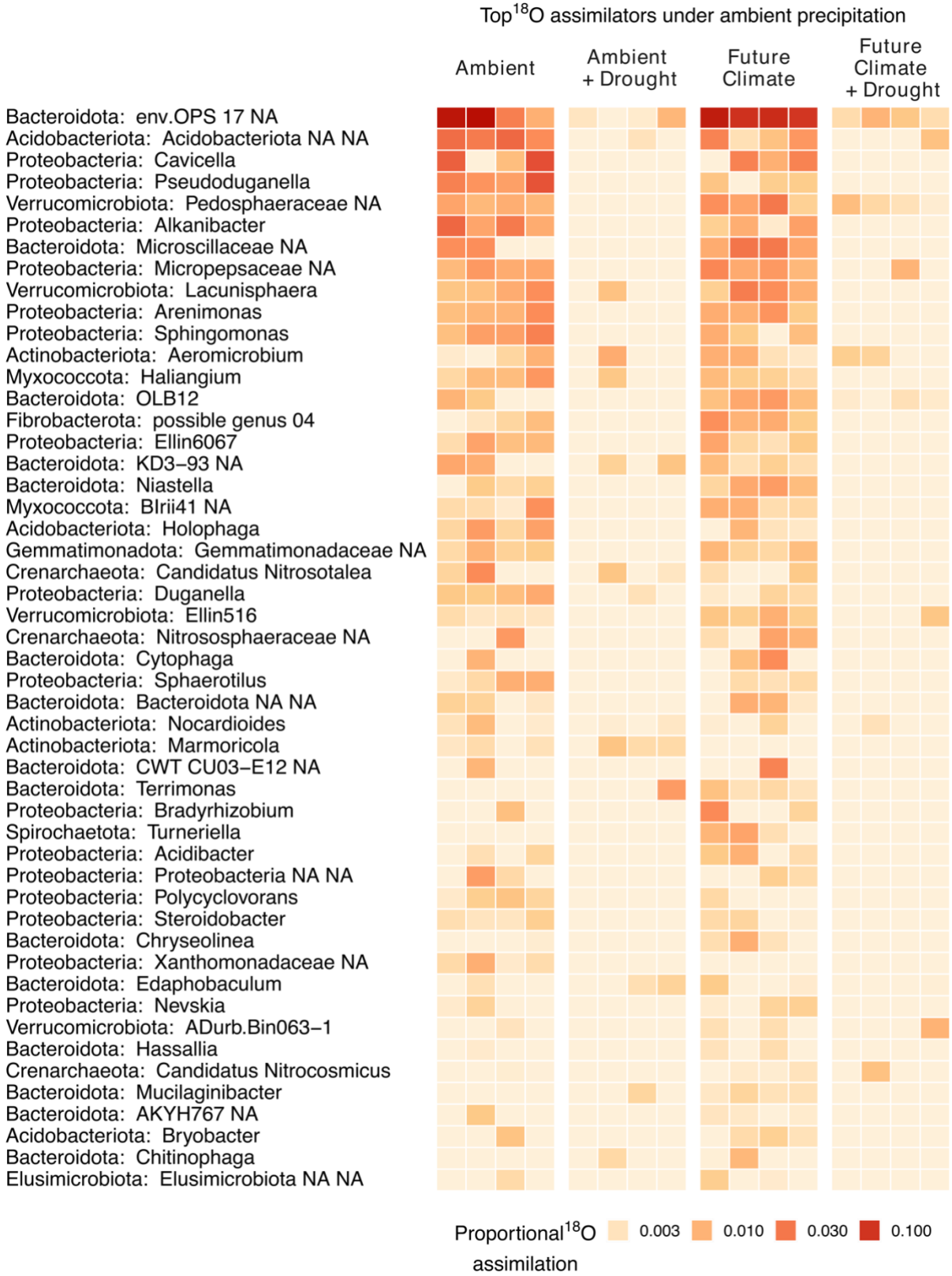
Top18O assimilators under ambient precipitation
Ambient
Ambient + Drought
Future Climate
Future Climate + Drought
Bacteroidota: env.OPS 17 NA
Acidobacteriota: Acidobacteriota NA NA
Proteobacteria: Cavicella
Proteobacteria: Pseudoduganella
Verrucomicrobiota: Pedosphaeraceae NA
Proteobacteria: Alkanibacter
Bacteroidota: Microscillaceae NA
Proteobacteria: Micropepsaceae NA
Verrucomicrobiota: Lacunisphaera
Proteobacteria: Arenimonas
Proteobacteria: Sphingomonas
Actinobacteriota: Aeromicrobium
Myxococcota: Haliangium
Bacteroidota: OLB12
Fibrobacterota: possible genus 04
Proteobacteria: Ellin6067
Bacteroidota: KD3−93 NA
Bacteroidota: Niastella
Myxococcota: BIrii41 NA
Acidobacteriota: Holophaga
Gemmatimonadota: Gemmatimonadaceae NA
Crenarchaeota: Candidatus Nitrosotalea
Proteobacteria: Duganella
Verrucomicrobiota: Ellin516
Crenarchaeota: Nitrososphaeraceae NA
Bacteroidota: Cytophaga
Proteobacteria: Sphaerotilus
Bacteroidota: Bacteroidota NA NA
Actinobacteriota: Nocardioides
Actinobacteriota: Marmoricola
Bacteroidota: CWT CU03−E12 NA
Bacteroidota: Terrimonas
Proteobacteria: Bradyrhizobium
Spirochaetota: Turneriella
Proteobacteria: Acidibacter
Proteobacteria: Proteobacteria NA NA
Proteobacteria: Polycyclovorans
Proteobacteria: Steroidobacter
Bacteroidota: Chryseolinea
Proteobacteria: Xanthomonadaceae NA
Bacteroidota: Edaphobaculum
Proteobacteria: Nevskia
Verrucomicrobiota: ADurb.Bin063−1
Bacteroidota: Hassallia
Crenarchaeota: Candidatus Nitrocosmicus
Bacteroidota: Mucilaginibacter
Bacteroidota: AKYH767 NA
Acidobacteriota: Bryobacter
Bacteroidota: Chitinophaga
Elusimicrobiota: Elusimicrobiota NA NA
Proportional 18O assimilation
0.003
0.010
0.030
0.100

Supplementary Figure 5: Top 200 taxa based on their proportional ^{18}O assimilation in soils unaffected by drought, agglomerated at the genus level. Heatmap showing taxa with the highest proportional ^{18}O assimilation under ambient precipitation visualized across all treatments and individual samples (rectangles, n=4). Taxa were ranked based on their proportional ^{18}O assimilation (contribution to the total community's growth) for each drought-unaffected sample (Ambient, Future Climate). The top 50 amplicon sequence variants (ASVs) per sample were then selected (total across all samples due to overlap: 200 ASVS) and visualized. Proportional ^{18}O assimilation ranges from 0 - 1 and estimates how much a single taxon contributes to the community's overall growth. It is calculated using re-computed relative abundances of only growing taxa (sum of growing taxa = 1) and their relative growth rates (RGR). ASVs had to be active in at least two samples if detected as growing in a treatment. ASV identities were agglomerated at the genus level and sorted in descending order based on proportional ^{18}O assimilation. If genus identity could not be assigned (NA), we agglomerated taxa at the family or phylum level.

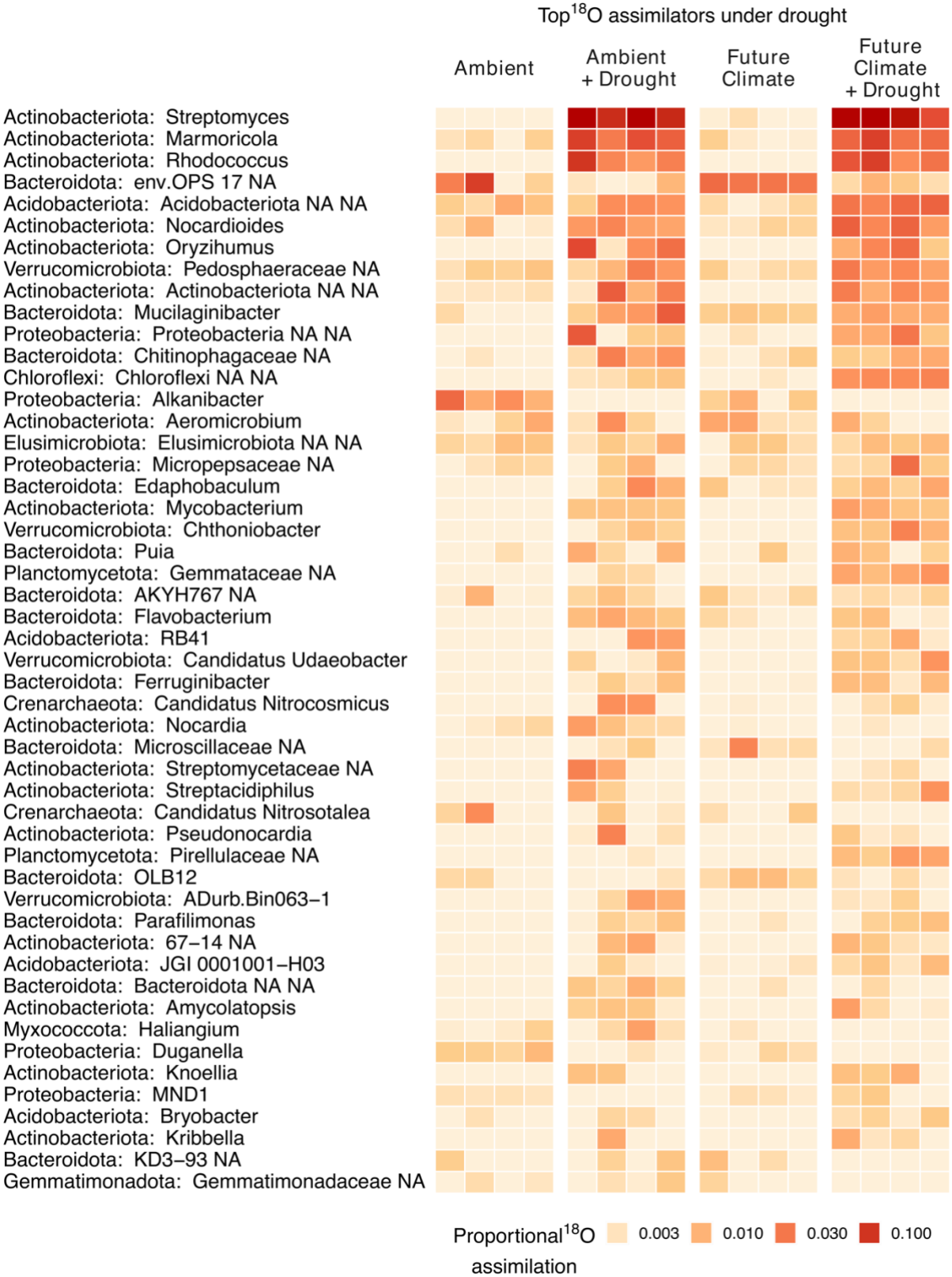
Top 18O assimilators under drought
Ambient
Ambient + Drought
Future Climate
Future Climate + Drought
Actinobacteriota: Streptomyces
Actinobacteriota: Marmoricola
Actinobacteriota: Rhodococcus
Bacteroidota: env.OPS 17 NA
Acidobacteriota: Acidobacteriota NA NA
Actinobacteriota: Nocardioides
Actinobacteriota: Oryzihumus
Verrucomicrobiota: Pedosphaeraceae NA
Actinobacteriota: Actinobacteriota NA NA
Bacteroidota: Mucilaginibacter
Proteobacteria: Proteobacteria NA NA
Bacteroidota: Chitinophagaceae NA
Chloroflexi: Chloroflexi NA NA
Proteobacteria: Alkanibacter
Actinobacteriota: Aeromicrobium
Elusimicrobiota: Elusimicrobiota NA NA
Proteobacteria: Micropepsaceae NA
Bacteroidota: Edaphobaculum
Actinobacteriota: Mycobacterium
Verrucomicrobiota: Chthoniobacter
Bacteroidota: Puia
Planctomycetota: Gemmataceae NA
Bacteroidota: AKYH767 NA
Bacteroidota: Flavobacterium
Acidobacteriota: RB41
Verrucomicrobiota: Candidatus Udaeobacter
Bacteroidota: Ferruginibacter
Crenarchaeota: Candidatus Nitrocosmicus
Actinobacteriota: Nocardia
Bacteroidota: Microscillaceae NA
Actinobacteriota: Streptomycetaceae NA
Actinobacteriota: Streptacidiphilus
Crenarchaeota: Candidatus Nitrosotalea
Actinobacteriota: Pseudonocardia
Planctomycetota: Pirellulaceae NA
Bacteroidota: OLB12
Verrucomicrobiota: ADurb.Bin063–1
Bacteroidota: Parafilimonas
Actinobacteriota: 67–14 NA
Acidobacteriota: JGI 0001001–H03
Bacteroidota: Bacteroidota NA NA
Actinobacteriota: Amycolatopsis
Myxococcota: Haliangium
Proteobacteria: Duganella
Actinobacteriota: Knoellia
Proteobacteria: MND1
Acidobacteriota: Bryobacter
Actinobacteriota: Kribbella
Bacteroidota: KD3–93 NA
Gemmatimonadota: Gemmatimonadaceae NA
Proportional 18O assimilation
0.003
0.010
0.030
0.100

Supplementary Figure 6: Top 217 taxa based on their proportional ^{18}O assimilation in drought-affected soils, agglomerated at the genus level. Heatmap showing taxa with the highest proportional ^{18}O assimilation under drought visualized across all treatments and individual samples (rectangles, n=4). Taxa were ranked based on their proportional ^{18}O assimilation (contribution to the total community's growth) for each drought-affected sample (Ambient + Drought, Future Climate + Drought). The top 50 amplicon sequence variants (ASVs) per sample were then selected (total across all samples due to overlap: 217 ASVS) and visualized. Proportional ^{18}O assimilation ranges from 0 - 1 and estimates how much a single taxon contributes to the community's overall growth. It is calculated using re-computed relative abundances of only growing taxa (sum of growing taxa = 1) and their relative growth rates (RGR). ASVs had to be active in at least two samples if detected as growing in a treatment. ASV identities were agglomerated at the genus level and sorted in descending order based on proportional ^{18}O assimilation. If genus identity could not be assigned (NA), we agglomerated taxa at the family or phylum level.

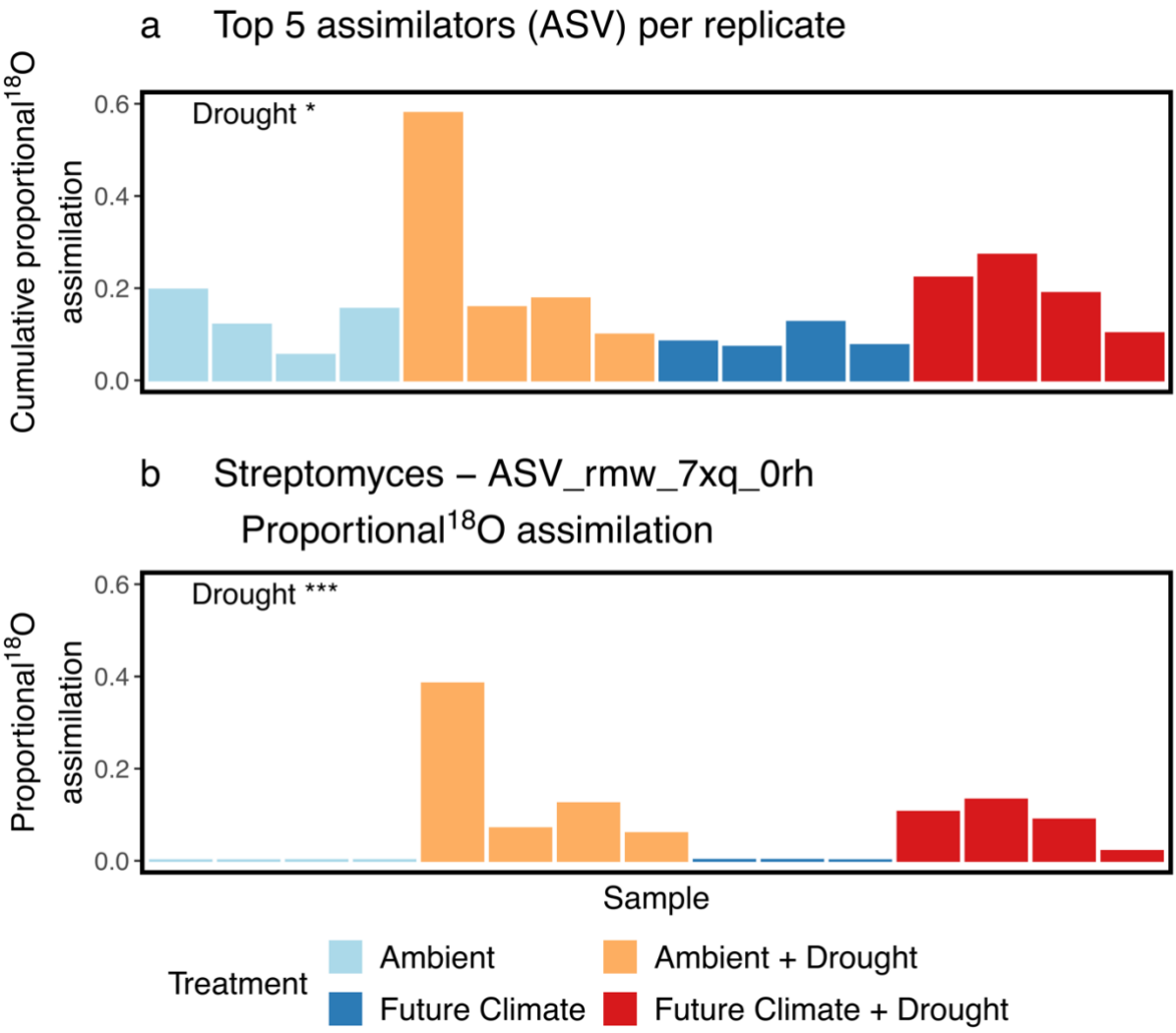

Supplementary Figure 7: Contribution of the top five assimilators and a drought-resistant taxon of the genus *Streptomyces* to the overall community growth. Cumulative proportional ^{18}O assimilation across all samples, calculated as the sum of the proportional ^{18}O assimilation of the top five amplicon sequence variants (ASVs) per replicate (**a**; Drought: F = 7.3, df = 1, p = 0.019) and ASV_rmw_7xq_0rh (Genus: *Streptomyces*; **b**; Drought: F = 159.9, df = 1, p < 0.001). Results of two-way ANOVA (n=4 replicates) are given as insert text (factors: Drought $_{Yes}$, Drought $_{No}$, Climate $_{Ambient}$, Climate $_{Future}$).

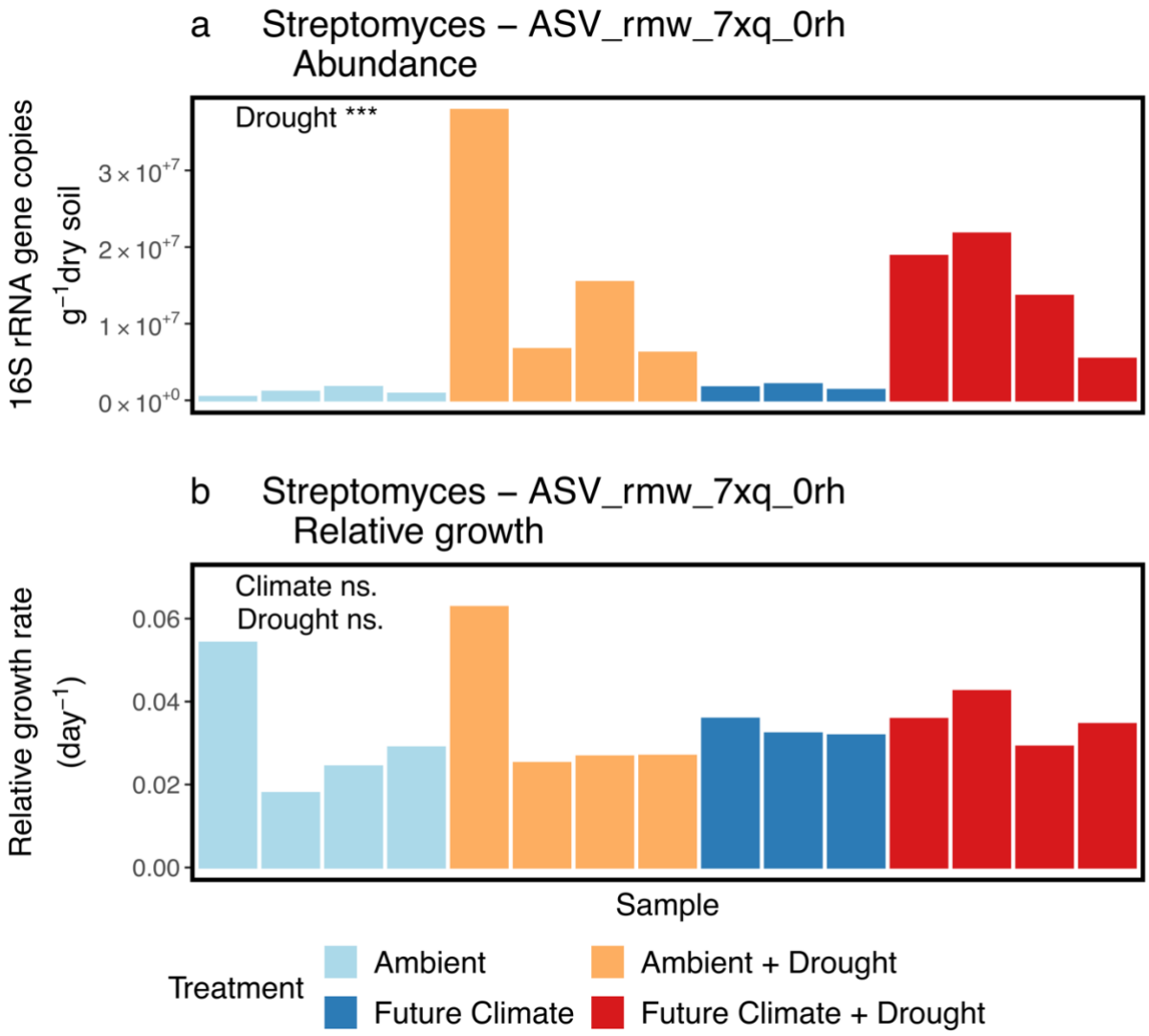

Supplementary Figure 8: Abundance and relative growth of a drought-resistant taxon of the genus *Streptomyces*. a Absolute abundance of ASV_rmw_7xq_0rh (Genus: *Streptomyces*) expressed as 16S rRNA gene copies per gram soil dry weight (Drought: F = 52.4, df = 1, p < 0.001). **b** Relative growth rates of ASV_rmw_7xq_0rh (Genus: *Streptomyces*). Results of two-way ANOVA (n=4 replicates) are given as insert text (factors: Drought $_{Yes}$, Drought $_{No}$, Climate $_{Ambient}$, Climate $_{Future}$).

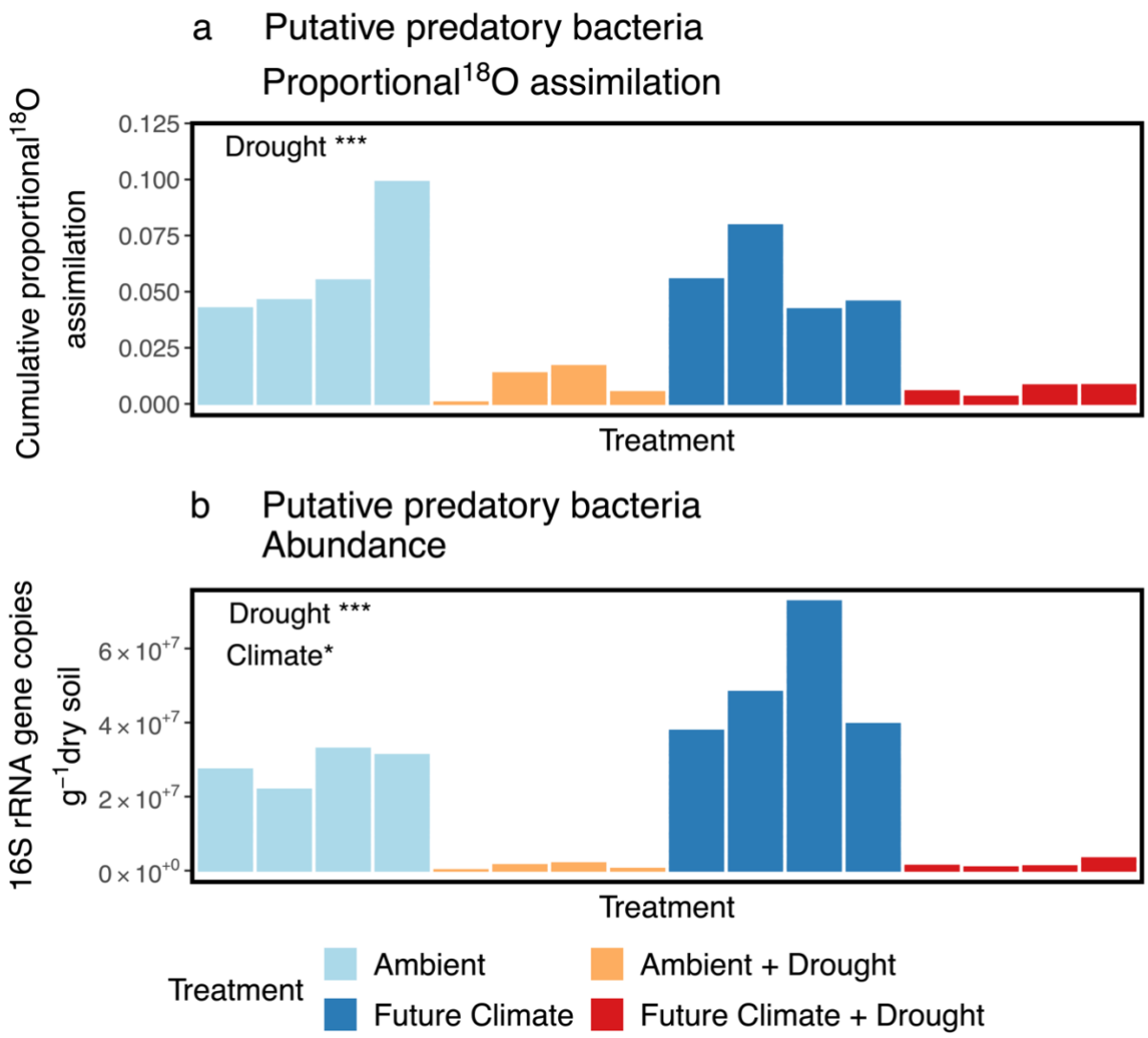

Supplementary Figure 9: Proportional ^{18}O assimilation and abundance of putative predatory bacteria. a Cumulative proportional ^{18}O assimilation across all samples, calculated as the sum of the proportional ^{18}O assimilation of putative predatory amplicon sequence variants (ASVs) per replicate (Drought: F = 63.4, df = 1, p < 0.001). **b** Absolute abundance of growing putative predatory ASVs expressed as 16S rRNA gene copies per gram soil dry weight (Drought: F = 227.9, df = 1, p < 0.001; Climate: F = 8.9, df = 1, p = 0.01). Results of two-way ANOVA (n=4 replicates) are given as insert text (factors: Drought $_{Yes}$, Drought $_{No}$, Climate $_{Ambient}$, Climate $_{Future}$).

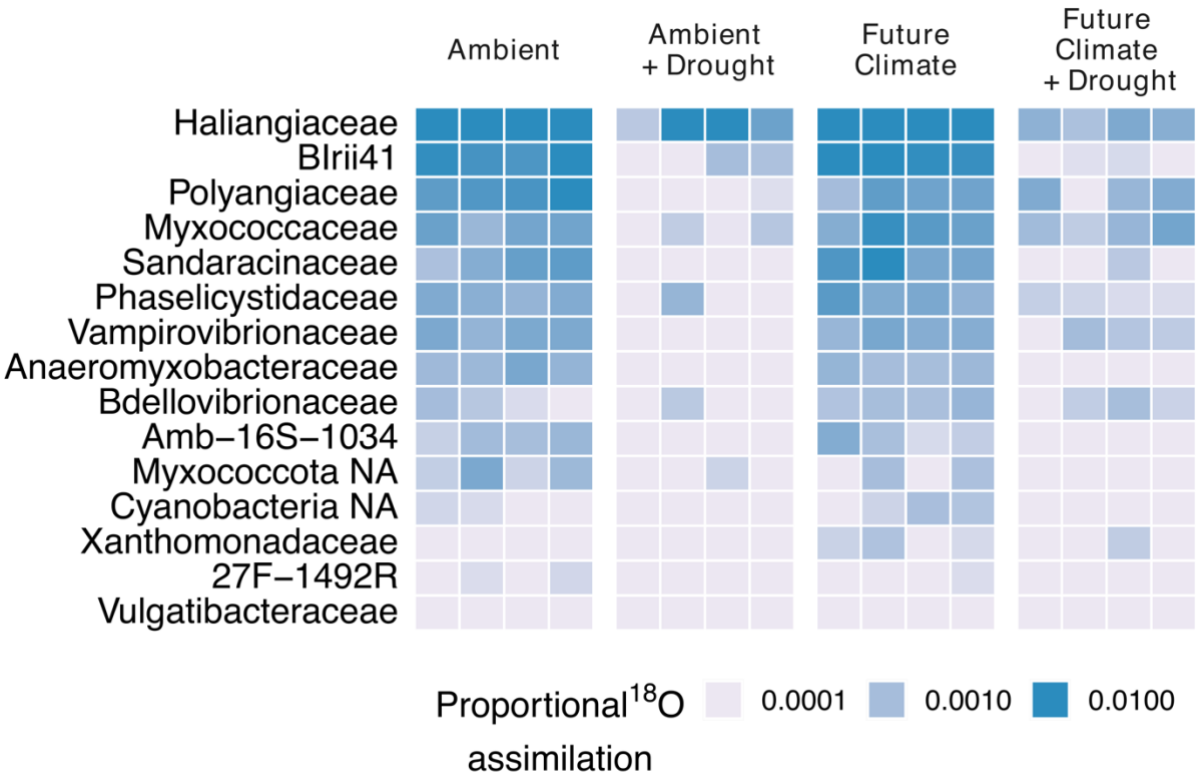

Supplementary Figure 10: Drought-induced changes in the proportional ^{18}O assimilation of putative bacterial predators agglomerated at the family level. Heatmap showing the proportional ^{18}O assimilation of putatively predatory taxa agglomerated at the family level and visualized across all treatments and individual samples (rectangles, n=4 replicates). Taxa were classified as putatively predatory if they belonged to the following orders and genera: Myxococcales, Bdellovibrionales, Vampirovibrionales, Haliangiales, Polyangiales*, Lysobacter, Daptobacter*, and *Vampirococcus*. Proportional ^{18}O assimilation ranges from 0 - 1 and estimates how much a single taxon contributes to the community's overall growth. It is calculated using re-computed relative abundances of only growing taxa (sum of growing taxa = 1) and their relative growth rates (RGR). If family identity could not be assigned (NA), phylum names were provided.

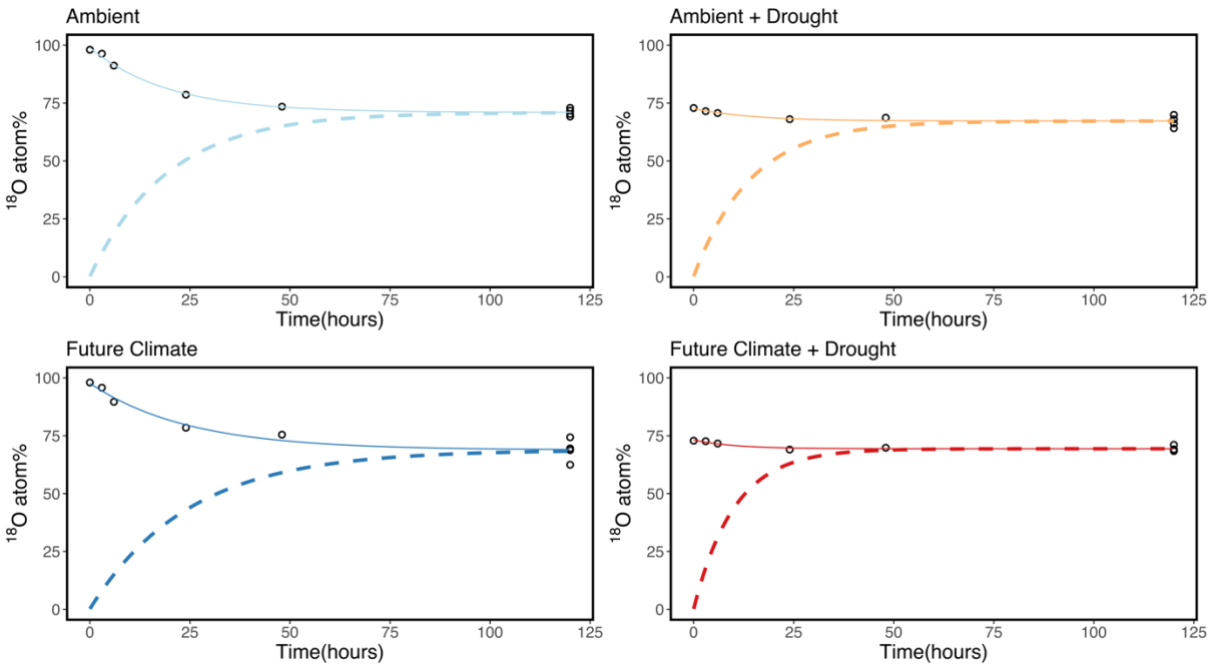

Supplementary Figure 11: Development of ^{18}O soil water enrichment over incubation time. Isotopic equilibration between the externally added ^{18}O labeled source water (solid line) and soil water (dashed line) over five days for all four treatments. Points represent measured ^{18}O atom% values of the added water pool. Data were fitted using a negative exponential model (solid line) and used to predict ^{18}O enrichment of the soil water.

Chapter III

Soil warming increases the number of growing bacterial taxa but not their growth rates

Full title:

Soil warming increases the number of growing bacterial taxa but not their growth rates

Short title :

More bacterial taxa start growing with soil warming

Authors

Dennis Metze [1,2*], Jörg Schnecker[1], Coline Le Noir de Carlan[3], Biplabi Bhattarai[4], Erik Verbruggen[3], Ivika Ostonen[4], Ivan A. Janssens[3], Bjarni D. Sigurdsson[5], Bela Hausmann[7,8], Christina Kaiser[1], and Andreas Richter[1,6*]

Affiliations

[1] Centre for Microbiology and Environmental Systems Science, University of Vienna, Vienna, Austria

[2] Doctoral School in Microbiology and Environmental Science, University of Vienna, Vienna, Austria

[3] Research Group Plants and Ecosystems, University of Antwerp, Antwerp, Belgium

[4] Department of Geography, Institute of Ecology and Earth Sciences, University of Tartu, Tartu, Estonia

[5] Faculty of Environmental and Forest Sciences, Agricultural University of Iceland, Hvanneyri, Borgarnes, Iceland

[6] International Institute for Applied Systems Analysis, Advancing Systems Analysis Program, Laxenburg, Austria

[7] Joint Microbiome Facility of the Medical University of Vienna and the University of Vienna, Vienna, Austria

[8] Division of Clinical Microbiology, Department of Laboratory Medicine, Medical University of Vienna, Vienna, Austria

*Corresponding authors. Email: dennis.metze@univie.ac.at; andreas.richter@univie.ac.at

Abstract

Soil microorganisms control the fate of soil organic carbon. Warming may accelerate their activities putting large carbon stocks at risk of decomposition. Existing knowledge about microbial responses to warming is based on community-level measurements, leaving the underlying mechanisms unexplored and hindering predictions.

In a long-term soil warming experiment in a Subarctic grassland, we investigated how active populations of bacteria and archaea responded to elevated soil temperatures (+6 °C) and the influence of plant roots, by measuring taxon-specific growth rates using quantitative stable isotope probing and ^{18}O water vapor equilibration.

Contrary to prior assumptions, increased community growth was associated with a greater number of active bacterial taxa rather than generally faster-growing populations. We also found that root presence enhanced bacterial growth at ambient temperatures but not at elevated temperatures, indicating a shift in plant-microbe interactions.

Our results, thus, reveal a mechanism of how soil bacteria respond to warming, that cannot be inferred from community-level measurements.

Teaser

More active taxa, not faster growth rates, drive warming-induced increases in bacterial community growth.

Introduction

One major challenge in climate change research is understanding its effects on the soil microbiome which is crucial for global climate projections [1–3]. Soil microorganisms are important climate regulators, governing carbon fluxes an order of magnitude larger than anthropogenic CO_2 emissions [4, 5]. Accelerated microbial activities due to warming might increase soil carbon losses, and thereby exacerbate climate change. Carbon stocks in high-latitude soils are particularly vulnerable to microbial decomposition since the microbes inhabiting them are often temperature-limited and tend to be more responsive to warming [6, 7]. Whether a soil microorganism becomes more active with warming depends on the complex interplay of many factors such as its genetic makeup, substrate availability [8, 9], or its interactions with plants and predators. Although accounting for microbial responses is important for improving predictions of soil carbon dynamics [3], many aspects remain elusive. Specifically, we lack an understanding of the physiological response of individual microbial taxa to warming and have major knowledge gaps on how warming affects plant-microbe interactions [1, 2, 10–13].

Growth is the central component of a microorganism's physiology and is closely linked to soil carbon fluxes [14–16]. Growth is restricted to the active part of the soil microbial community. Despite constituting only a few percent of the total community [17], the active microbial community is the main driver of soil carbon and nutrient cycling [11, 17, 18]. Recent estimates suggest that growing microorganisms in soil account for > 95 % of the respiration of the entire community with growing cells being 1,000 times more active than starved ones [19]. Rising temperatures have a large impact on the physiological processes of soil microbes including their growth rates and, therefore, soil carbon fluxes.

Microbial growth in warmed soils has been predominantly measured at the total community level, aggregating over thousands of different populations. Growth responses to warming (measured as relative community growth; mass-specific growth) range from positive [9, 20], over neutral [9] to negative [20, 21] with seasonal variation. Short-term warming often accelerates microbial process rates. Over time, however, many of these rates tend to return to their initial state which is thought to be mediated by community shifts, substrate loss, or physiological acclimation [22–24]. In a (Sub)Arctic grassland, which is also subject of this study, long-term warming has caused significant losses of soil carbon and nitrogen resulting

in a reduction of microbial biomass [8]. While this did not affect microbial growth and respiration rates per unit of soil mass, rates of relative community growth and respiration per unit of microbial biomass (mass-specific) increased with temperature and stayed elevated even after more than 50 years of warming. This was interpreted as a persistent acceleration of microbial activities without signs of thermal acclimation [8]. In this system, warming caused a downregulation of the microbial protein biosynthesis machinery which possibly freed energy available for accelerated activity [25]. However, warming was also found to increase maintenance and respiratory costs [25, 26].

Community-aggregated measurements of growth and respiration are useful to indicate directions of warming responses. Nonetheless, they integrate over thousands of microbial populations with varying growth and carbon use characteristics [27] which hampers their capacity to detect underlying microbial mechanisms. Detecting these mechanisms is crucial to comprehend the dynamic processes that underlie microbial warming responses and is needed to improve their prediction. Quantitative stable isotope probing (qSIP) using ^{18}O water can hereby be a powerful tool since it allows estimating growth rates of individual microbial populations based on the incorporation of ^{18}O into microbial DNA [28]. qSIP can be used to quantify the growth response of distinct microbial taxa to warming from which shifts in ecosystem-scale rates ultimately emerge. A recent improvement of this technique, vapor-SIP, allows us to label soil water without the addition of liquid water and, thus, enables us to estimate taxon-resolved microbial growth near in situ conditions [29].

Plants are another important factor impacting and controlling microbial activities by providing primary carbon resources through litter production and root exudates. Soil microorganisms that live in association with roots consume plant-derived carbon and show higher potential growth rates [30, 31]. Climate change alters plant performance, including litter and exudate production and litter quality, with potential repercussions for the soil microbiome and the carbon cycle [32]. For instance, warming can increase plant productivity, causing greater carbon allocation belowground and promoting microbial activities [33]. On the other hand, warming can compromise plant performance, reducing rhizodeposition or inducing plant-microbe competition, for instance, when nitrogen is limiting [34]. The effects of soil warming on roots seem to differ between ecosystems. While warming has been found to increase either fine root production or biomass in a boreal peatland [35] and a mountainous forest [36], it caused a reduction in both in the (Sub)Arctic grassland also examined here [37, 38].

Fine root biomass is particularly important for root-associated taxa since it determines the root surface where exudates are released. Warming might also affect root exudate quality and seasonality if it causes shifts in the plant community structure. Overall, indirect warming effects mediated by plants can have a strong impact on soil microorganisms. In some cases, these effects might be stronger than direct warming effects, especially if microbes are adapted to live in association with roots. Yet, it remains elusive how climate change shapes the direction of plant-microbe interactions [2, 12, 13].

To better understand the microbial warming response and more accurately predict microbial activities in a future climate, we need to look beyond community-aggregated growth estimates and acknowledge that these activities emerge from a diverse set of active populations, shaped by direct and indirect warming effects. Studying them accordingly will allow us to scrutinize interpretations derived from community-aggregated measurements and might lead to new insights into how soil microbes respond to warming.

Here, we investigated the impact of more than 50 years of natural geothermal soil warming on the growing populations of bacteria and archaea in a (Sub)Arctic grassland in Iceland. We also examined how their responses were shaped by indirect warming effects mediated by roots. We used water-vapor equilibration ^{18}O-qSIP (vapor-qSIP) to identify growing (hereafter also: active) taxa of bacteria and archaea in soil and quantify their growth rates at ambient and elevated soil temperatures (+ 6 °C). Root-ingrowth (1 mm mesh) and root exclusion cores (30 µm mesh) were used to elucidate the impact of plants on microbial growth. We installed these cores in the field for ten months and extracted them at peak vegetation season, along with an undisturbed soil core. Using these three soil core types, we aimed to disentangle direct and indirect warming effects. We had three primary objectives. First, we aimed to decipher the growth patterns of individual bacterial and archaeal populations following long-term warming and compare them to community-level estimates. Second, we aimed to investigate how the presence of roots impacted their growth patterns and whether plant-microbe interactions change under long-term warmed conditions, particularly considering previously reported decreases in fine root biomass and production. Third, we aimed to examine if taxa of the same genus or family showed similar growth responses to warming and root presence, possibly elucidating group-specific traits.

Results

Soil carbon and nitrogen are lost with long-term warming while relative community growth increases

We took three different soil cores (undisturbed, root ingrowth, root exclusion) across four replicated temperature gradients in a long-term warmed (Sub)Arctic grassland (fig. S1) to differentiate between direct warming effects (undisturbed) and indirect warming effects mediated by roots (root ingrowth, root exclusion) on soil biogeochemical and microbial parameters (Fig. 1 A). Long-term warming (+ 6 °C) and root presence altered soil carbon and nitrogen pools, soil water content, extracellular enzyme activities, and relative community

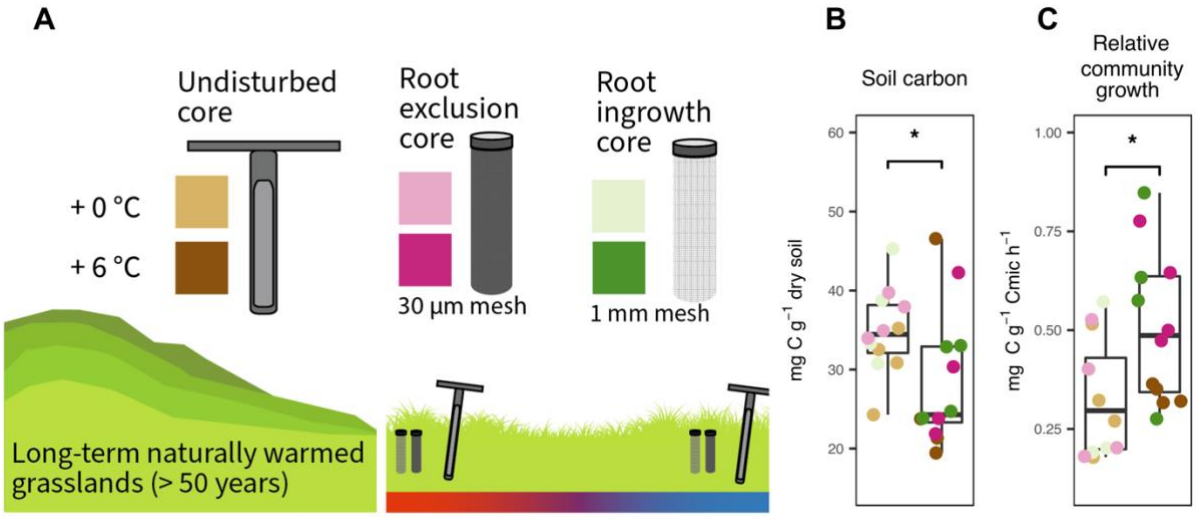

Figure 1: Experimental design, soil carbon, and relative microbial community growth. (A) Soil samples were taken from four replicated temperature gradients (n=4 biological replicates) in a (Sub)arctic grassland in Iceland. This grassland experienced at least 50 years of soil warming established by natural geothermal activity. Root ingrowth and root exclusion cores were installed in situ for 10 months (October 2019 – August 2020) at two temperature levels (ambient temperatures, + 6°C above ambient temperatures). We aimed to investigate how root presence or absence affects microbial growth under warmed conditions. While extracting the in situ installed cores, we also took a fresh soil core (hereafter: undisturbed core) to examine warming effects without the disturbances associated with core installation (e.g., soil extraction, mixing, and root/ stone removal). Squares depict treatment colors used for graphs. (B) Concentrations of soil carbon decreased with warming (t= 2.1, df= 18.3, p= 0.049, n= 12) while (C) relative microbial community growth (mass-specific) increased (t= -2.5, df= 20.7, p= 0.019, n=12). The median is represented by the center line of the box, while the upper and lower quartiles are indicated by the box limits. The whiskers represent 1.5 times the interquartile range; any outliers are shown as separate points. We utilized two-sided Student's t-tests to infer differences between warming levels.

growth rates. Long-term warming reduced the concentrations of soil carbon (Fig. 1 B) and soil nitrogen (table S1) by 18 % and 19 %, respectively, and decreased soil moisture by 5 % compared to ambient conditions (F= 12.9, p= 0.002). Warming and root presence increased exoglucanase (Warming: F= 8.8, p= 0.01; Core $_{\text{root presence/absence}}$: F= 5.7, p= 0.033) and exochitinase activities (Warming: F= 21.5, p < 0.001; Core $_{\text{root presence/ absence}}$: F= 4.6, p= 0.05) but did not affect phosphatase and protease activities. Measurements of more dynamic pools such as dissolved organic carbon (DOC) and total dissolved nitrogen (TDN) did not differ between cores and warming levels (table S1). Also, microbial biomass carbon and total 16S rRNA gene copy numbers did not significantly differ between warmed and control plots. However, relative community growth rates increased with warming (Fig. 1 C), similar to previous reports. These microbial community growth rates were determined based on the ^{18}O enrichment of the unfractionated DNA and, thus, inherently also included other microorganisms such as fungi. When averaging relative community growth across cores for each warming level, we found it to rise by 53 % with long-term warming of 6 °C.

Root effects on community composition are only captured when differentiating between active and inactive taxa

After 10 months of field incubations, the absence of roots did not affect total community composition estimated via amplicon sequencing. However, roots affected which members of the total community were active and growing. To compare the composition of total and growing communities of bacteria and archaea, we performed a principal component analysis (PCA) using Euclidean distances based on ASV absolute abundances (16S rRNA gene copies per ASV, centered-log transformed). Hereafter, 'bacteria' is used for both bacteria and archaea for brevity.

Long-term warming caused significant shifts in the composition of the total communities which also became more variable as compared to ambient conditions (Fig. 2 A). Root presence, however, did not affect the composition of the total communities. This changed when subsetting total communities for their growing taxa. We found growing communities to be distinct in each treatment with roots and warming having significant effects on their composition (Fig. 2 B). In contrast to the total communities, core type (= root presence; R^2 = 0.26) and its interaction with warming (R^2 = 0.25) had a greater impact on the composition of the growing communities than warming alone (R^2 = 0.15). The composition of the growing

communities that formed in the absence of roots was particularly different from those cores where roots were present (undisturbed cores, root ingrowth cores). Overall, this highlights that analyses only based on amplicon sequencing data without additional growth information were not able to capture root effects.

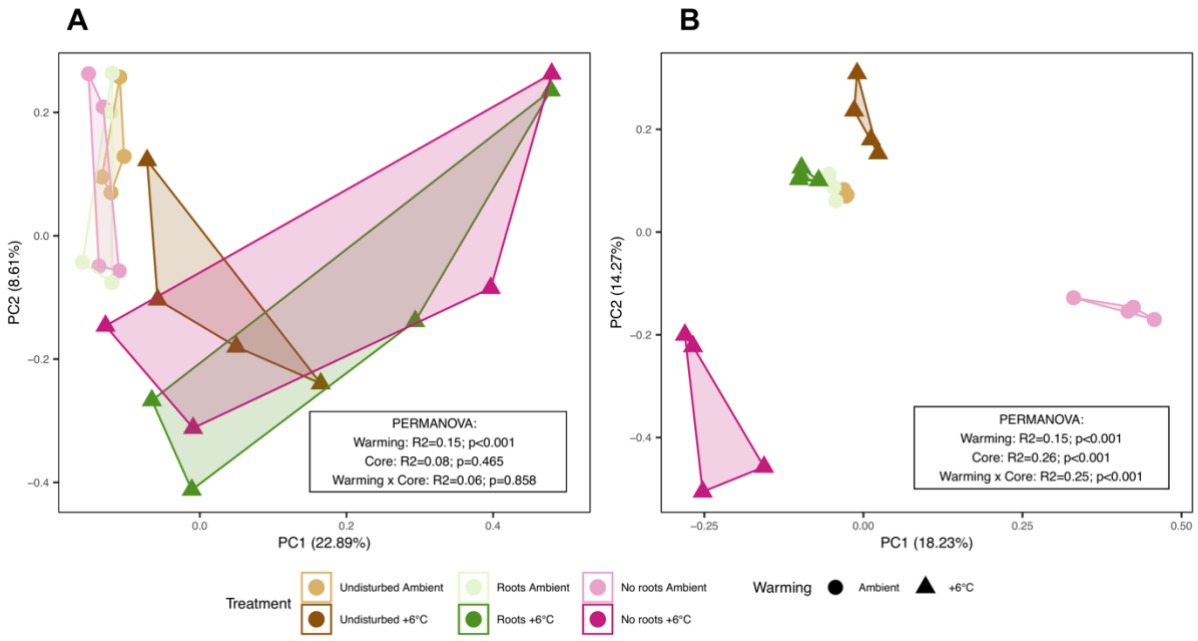

Figure 2: Root effects are only captured when examining growing communities. Principal component analysis (PCA) of total (A) and growing (B) bacterial and archaeal communities from fresh undisturbed soil cores (brown), root ingrowth cores (mesh size: 1 mm, green), and root exclusion cores (mesh size: 30 µm, pink). PCA was performed using Euclidean distances based on centered log-ratio transformed amplicon sequence variant (ASV) absolute abundances (digital droplet PCR inferred 16S rRNA gene copies multiplied by amplicon sequencing reads). Absolute abundances were aggregated over the density fractions of each sample gradient. Statistics from two-way permutation-based multivariate analysis of variance (PERMANOVA, n=4 biological replicates) are provided as inset panels (factors: Warming $_{\text{ambient/ +6°C}}$, Core $_{\text{undisturbed/ root ingrowth/ root exclusion}}$).

Long-term warming does not increase average bacterial growth rates but causes twice as many taxa to become active

To describe the general effects of long-term warming, we focused on samples from the undisturbed cores since they were not exposed to any disturbances connected to core installation. The number of growing taxa, their contribution to the total community, and their relative growth rates served as indicators for microbial shifts in response to long-term warming. The number of growing ASVs (Fig. 3 A) almost doubled with warming (ambient: 342

± 32 ASVs, warmed: 797 ± 115 ASVs, mean ± SD), also increasing the percentage of the total community that was growing (Fig. 3 B) from on average 1.64 % to 4.75 %. The increase in the number of growing taxa was reflected across most major phyla but differed in extent (Fig. 3 D). While Actinobacteriota, Bacteroidota, and Chloroflexi harbored twice as many growing taxa under long-term warming, there were almost three times as many Acidobacteriota and

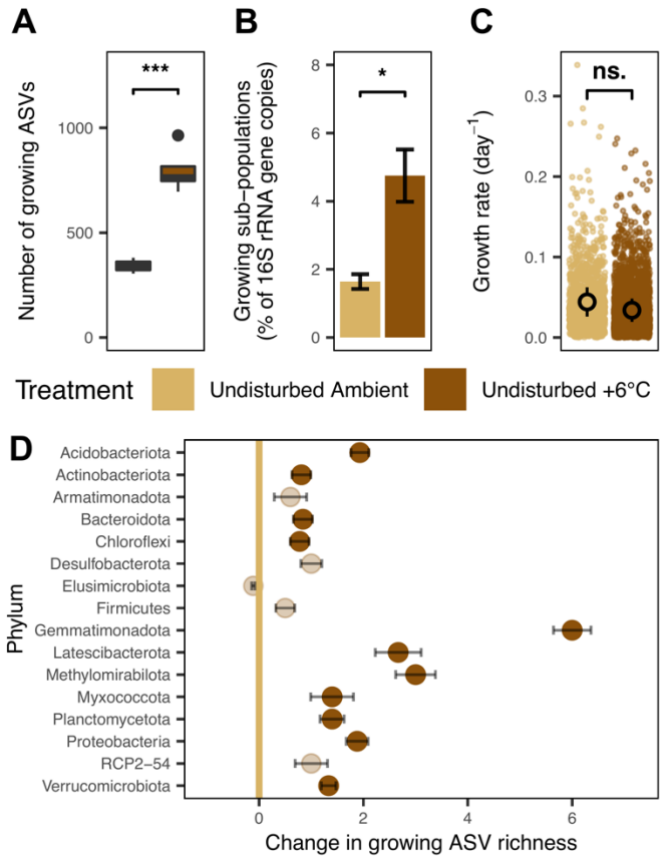

Figure 3: Warming increases the richness of growing taxa and their share of the total community but not their mean growth rates. Number of unique growing amplicon sequence variants (ASVs) (A), their proportion of the total community expressed as the share of 16S rRNA gene copies (B), mean taxon-level growth rates (C), and warming-induced relative changes in the number of growing taxa within major phyla (D). Light-colored dots in (C) represent ASV-level growth rates from all replicates used to calculate means (n=4 biological replicates) and standard errors (points, error bars). Points in (D) represent relative changes (0 = no change, 1 = increase by 100 %) in the number of growing taxa per phylum including standard errors. Bold colored points denote significant shifts (Kruskal-Wallis test and false detection rate (fdr) correction for multiple comparisons, n= 4) and transparent points non-significant ones. The vertical line depicts the mean of the reference treatment (Undistributed core at ambient conditions) used to calculate relative changes. Asterisks (A,B,C) represent significant differences (n=4) inferred by two-way ANOVA (Supplementary Table 1, factors: Warming $_{\text{ambient/ +6°C}}$, Core $_{\text{undisturbed/ root ingrowth/ root exclusion}}$) followed by Tukey post hoc tests.

Proteobacteria. We found that many of these shifts were driven by specific families (fig. S2). For instance, the Xanthobacteraceae, a family of the Proteobacteria, showed a more than 8 times higher richness of growing taxa at elevated temperatures (fig. S2). The Xanthobacteraceae also contributed to a larger proportion of community growth at higher temperatures (fig. S3).

Despite higher microbial community growth (Fig. 1 C), long-term warming did not accelerate average taxon-specific growth rates (Fig. 3 C), so bacterial populations were generally not growing faster. This was supported by directly comparing relative growth rates of ASVs active at both temperatures which did not increase either (fig. S4 B). If we included non-growing taxa (APE $^{18}O = 0$) in these calculations, average taxon-specific growth increased slightly but not significantly (fig. S4 A). At the level of the whole bacterial community, we observed that total and relative growth approximately doubled at higher temperatures (fig. S5 A, B). Although this increase was only significant for the relative growth ($p = 0.042$), these bacterial community patterns corresponded to the rise in microbial community growth (Fig. 1 C) and the increase in the richness of growing bacterial taxa (Fig. 3 A). Community growth correlated with the number of growing bacterial taxa (Fig. S6). This held for the whole microbial community ($R^2 = 0.13$, $p = 0.082$, Fig. S6 A) as well as the bacterial community ($R^2 = 0.81$, $p > 0.001$, Fig. S6 A), albeit only significant for the latter. In addition, taxa that became only active with elevated temperatures did not grow faster than populations exclusively active in ambient soils (Fig. S7 B)

Different bacterial taxa become dominant with long-term warming

Although average growth rates did not increase, individual taxa showed clear responses to warming. Since the contribution of soil microorganisms to biogeochemical processes is not only connected to their growth rates but also their abundance, we integrated both by calculating proportional ^{18}O assimilation rates. Proportional ^{18}O assimilation (range: 0 - 1) is a relative value, expressing how much a single ASV contributes to the total growth of the active community. Hence, it can also be considered as the proportion of bacterial growth an ASV is responsible for.

At ambient temperatures, the top 20 ASVs based on their proportional ^{18}O assimilation accounted for 36 - 46 % of the community growth (Fig. 4 A). Most of these taxa lost their dominant role with long-term warming where they were only responsible for 3 - 11 % of the

community growth. Dominant growing taxa at ambient temperatures belonged to the genera *Collimonas, Flavisolibacter, Granulicella, Kitatospora, Pseudomonas, Puia, Streptoacidiphilus, Terracidiphilus,* and *Undibacterium*, showing a high proportion of Bacteroidota. Three ASVs remained amongst the top ^{18}O assimilators (*Collimonas* ASV 2, *Kitatospora* ASV 5, *Streptoacidiphilus* ASV 10) even after long-term warming (bold ASV names, Fig. 4 B). Their contribution to the total community's growth was lower though and less consistent across replicates. Many top assimilatory taxa at elevated temperatures were uncharacterized

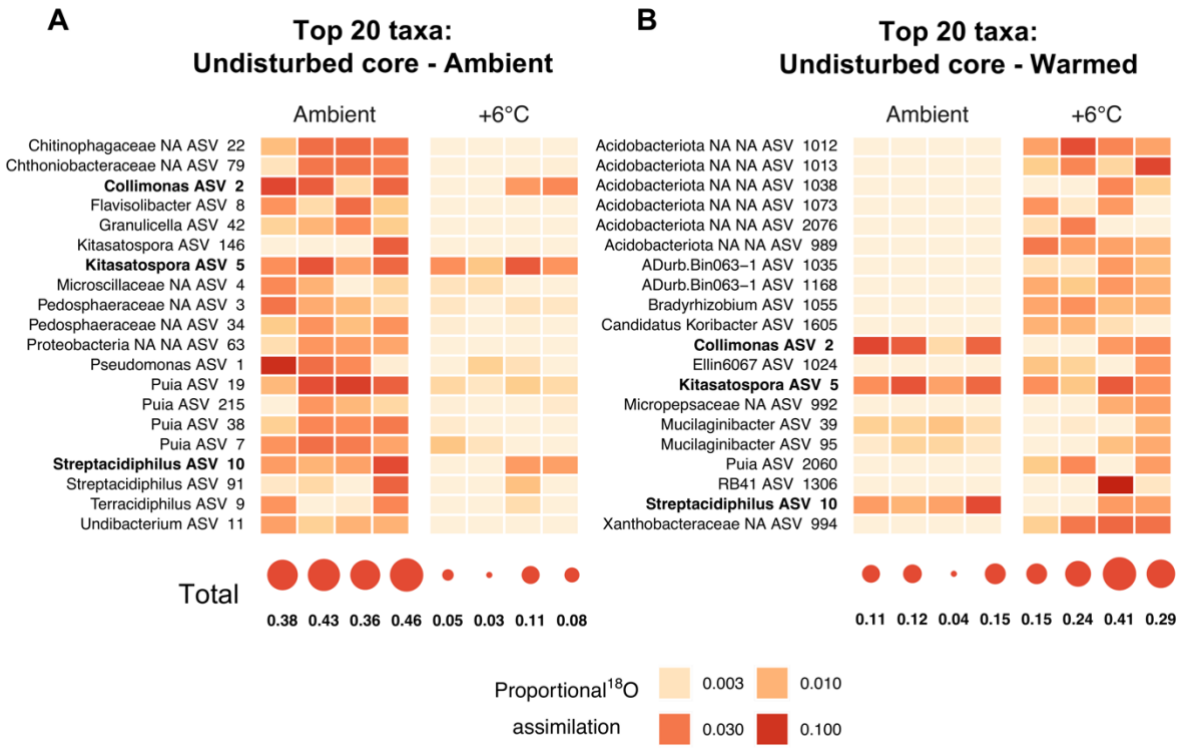

Figure 4: Different taxa become dominant contributors to the total community's growth with long-term warming in undisturbed cores. Heatmap showing taxa (amplicon sequence variants, ASVs) with the highest proportional ^{18}O assimilation in undisturbed cores at ambient (A) and warmed (B) conditions, visualized across individual samples (boxes n=4 biological replicates). Proportional ^{18}O assimilation is calculated using re-computed relative abundances of only growing taxa (sum: relative abundances $_{growing\ taxa}$ = 1) and their relative growth rates (RGR); it represents the contribution of an ASV to the total community's growth. Hence, it can also be considered as the proportion of bacterial growth an ASV is responsible for. ASVs were ranked based on their proportional ^{18}O assimilation per replicate. After retaining the top 15 ASVs across all replicates per treatment (total $_{ambient}$: 33 ASVs, total $_{warmed}$: 39 ASVs), we visualized the top 20 ASVs using heatmaps. (A) shows the top taxa at ambient temperatures whereas (B) depicts the top taxa under warming. Bubbles below each replicate show the cumulative growth summarized over all displayed ASVs. ASVs were only considered if they were growing in at least two samples per treatment. If genus or family identity could not be assigned (NA), phylum names were provided.

members of the Acidobacteriota which lacked taxonomic assignment at the order level. Other ASVs belonged to the genera *Bradyrhizobium, Mucilaginibacter, Puia*, and the unclassified Acidobacteriota RB41. At higher temperatures, community growth was more evenly distributed among a larger number of taxa. The top 20 ASVs accounted for less community growth than at ambient conditions with only 13 - 40 %. Under long-term warming, community growth generally comprised fewer dominant taxa indicating a larger evenness across active taxa. For instance, more than twice as many taxa were required to account for 50 % of the community growth in warmed plots (59 ± 25 ASVs (mean ± SD), fig. S8) than at ambient temperatures (26 ± 5 ASVs).

Long-term warming alters root effects on bacterial growth

To disentangle how roots impact the growth of soil bacteria and archaea today and in a warmer climate, we installed root in-growth and root exclusion cores *in situ* for 10 months. At ambient conditions, root presence accelerated growth rates on average ~ 2.5 times as compared to root-exclusion cores (Fig. 5 A, Two-way ANOVA; Warming: $F = 2.4$, $df = 1$, $p = 0.138$; Core: $F = 8.85$, $df = 2$, $p = 0.002$; Warming x Core: $F = 10.98$, $df = 2$, $p = 0.0007$). In long-term warmed soils, however, this effect was lost (Fig. 5 A). In fact, warming significantly decreased relative growth rates in root inclusion cores, so they were indistinguishable from those estimated from root exclusion cores (Fig. 5 A). Most growing taxa were exclusively active in one specific core type, indicating a closer association with either roots or bulk soil (fig. S9). We defined putative root-associated and bulk-soil-associated taxa as those exclusively growing in either the presence or absence of roots. We found that root-associated were growing faster than bulk-soil-associated taxa at ambient temperatures whereas this effect was not significant for shared taxa growing in both cores (fig. S7 A). The two functional groups also differed in their warming response. Putative root-associated taxa showed a negative growth response to warming (fig. S7 B) indicated by a decrease in mean growth rates (Fig. 5 B). Putative bulk-soil-associated taxa responded to long-term warming in an opposite manner. Their mean growth rates either increased with warming (Fig. 5 C) or remained constant (fig. S7 B).

At ambient conditions, the richness of growing taxa in root ingrowth cores was comparable to undisturbed cores (302 ± 106 ASVs, fig. S7) but lower than in root-exclusion cores (968 ± 88 ASVs). Root ingrowth cores responded to long-term warming with larger and more diverse

growing communities, supporting our findings from the undisturbed cores (fig. S10 A, B). In contrast, the diversity and size of growing communities in root exclusion cores remained unchanged.

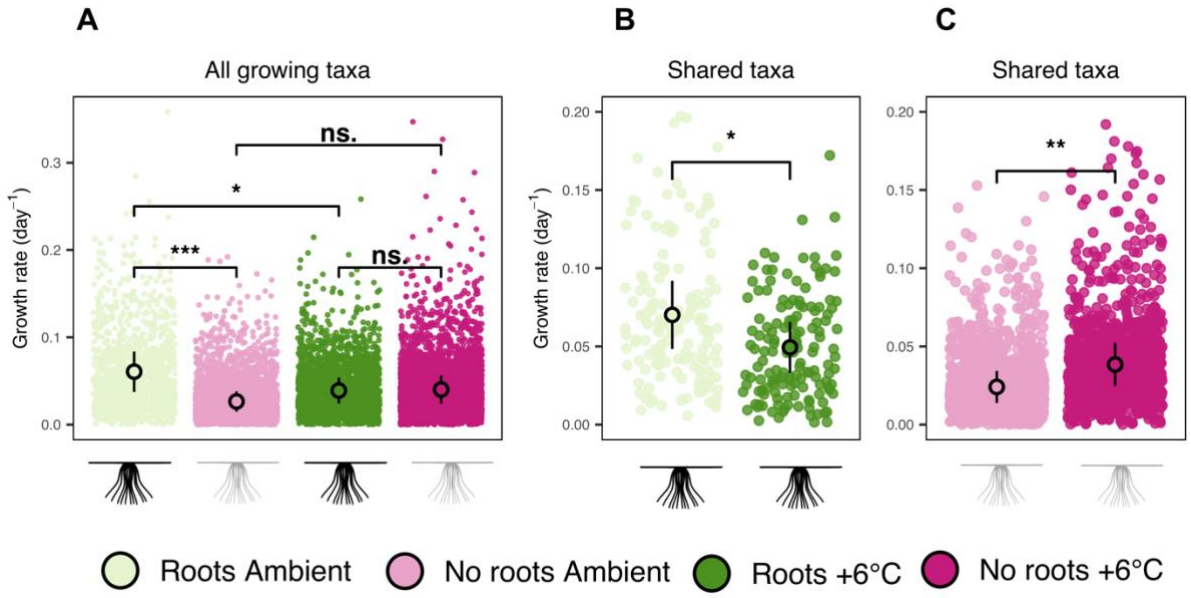

Figure 5: Warming alters the effect of roots on bacterial and archaeal growth rates. Mean taxon-level relative growth rates of all taxa growing in root ingrowth and root exclusion cores at ambient and warmed conditions (A). Mean taxon-level relative growth rates of shared growing taxa between ambient and warmed conditions in root ingrowth (B; Student's t-test: t= 2.8, df= 4.05, p= 0.046) and root exclusion cores (C; Student's t-test: t= -4.9, df= 5.41, p= 0.003). Light-colored dots represent ASV-level growth rates across all replicates used to calculate means (n=4 biological replicates) and standard errors (points, error bars). Asterisks represent significant differences (n=4) inferred from two-way ANOVA (Factors: Warming $_{\text{ambient/ +6°C}}$, Core $_{\text{undisturbed/ root ingrowth/ root exclusion}}$) followed by Tukey post hoc tests (A) or inferred from Student's t-test (B, C).

Members of the Chitinophagaceae profit from root presence

The growth of several taxa was influenced by the presence or absence of roots. Based on their proportional ^{18}O assimilation, we observed specific ASVs from different genera to be linked with the presence roots such as *Alkanindiges, Mucilaginibacter, Puia*, and *Cytophaga* (fig. S11 A). However, most of these taxa stopped growing at higher temperatures. Other taxa showed larger contributions to the community's growth when roots were absent such as unclassified members of the Acidobacteriota, Micropepsaceae, and Xanthobacteraceae (fig. S11 B). Few root-specific patterns could be observed at the family level (Fig. 6). We found that the top-^{18}O assimilating families accounted for similar amounts of community growth across both

core types and warming levels, ranging between 42 – 72 %. Only Chitinophagaceae and Streptomycetaceae members seemed to consistently profit from the presence of roots with significantly higher proportional growth as compared to root exclusion cores (Fig. 6). In contrast, proportional ^{18}O assimilation of the Nitrosomonadaceae was larger in root exclusion cores. Overall, although root association patterns were evident at the ASV level, they were not consistent at the family level, except for Chitinophagaceae and Streptomycetaceae.

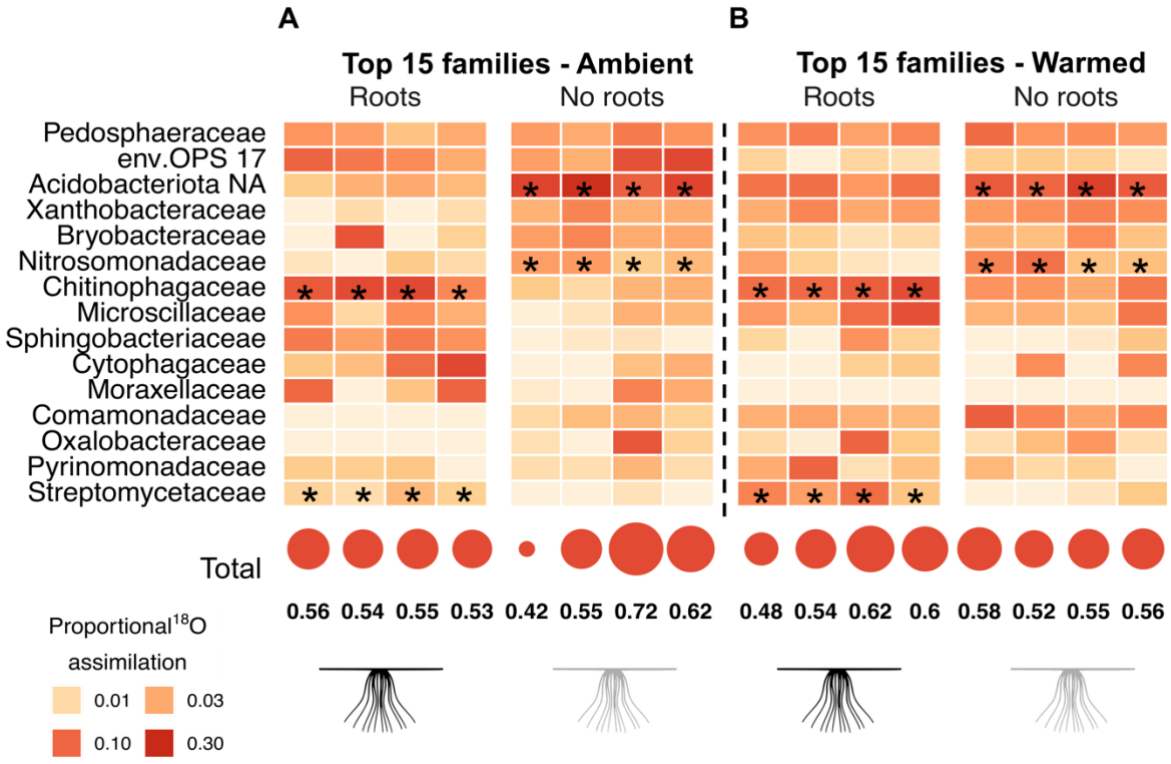

Figure 6: Chitinophagaceae show a higher contribution to the total community's growth in the presence of roots. Heatmap showing the top 15 families based on their proportional ^{18}O assimilation across root ingrowth and exclusion cores at ambient (A) and long-term warmed conditions (B). Individual boxes represent replicates per treatment (n= 4 biological replicates). Proportional ^{18}O assimilation ranges from 0 - 1 and estimates how much a single taxon contributes to the community's overall growth. Hence, it can also be considered as the proportion of bacterial growth an ASV is responsible for. It was calculated using re-computed relative abundances of only growing taxa (sum: relative abundances $_{growing\ taxa}$ = 1) and their relative growth rates (RGR). ASVs had to be active in at least two samples if detected as growing in a treatment. Proportional ^{18}O assimilation was then agglomerated at the family level and visualized for the top 15 families. If family identity could not be assigned (NA), phylum names were provided. Bubbles below each replicate box show the cumulative growth summarized over all displayed families. Asterisks represent significant differences between root ingrowth and root exclusion cores agglomerated over both temperature regimes based on Wilcoxon rank tests using false detection rate (fdr) correction for multiple comparisons (n= 4).

Discussion

High-latitude soils contain large carbon stocks that are vulnerable to being lost with warming due to accelerated microbial activities. Our understanding of the underlying mechanisms remains inadequate though, partly because microbial responses to climate change are often measured at an aggregated level, summing over the complexity of an entire community. Here, we disentangled the growth response of individual populations of active bacteria and archaea (hereafter: summarized as bacteria) to more than 50 years of long-term soil warming (+ 6 °C), also accounting for indirect warming effects mediated by roots. Our study demonstrates that accelerated community growth with warming is driven by a strong increase in the number of growing taxa, rather than by an increase in average bacterial growth rates, providing a different mechanistic explanation for the microbial warming response than inferred by community-aggregated measurements. We also show that root presence accelerates bacterial growth rates at ambient conditions, whereas this growth-promoting root effect was lost with long-term warming. Warming even seemed to decrease the growth rates of putative root-associated taxa. This indicates that for some microbial groups, indirect warming effects may be stronger than direct ones, depending on their life history strategy.

In the (Sub)Arctic, long-term warming has been shown to persistently increase relative microbial community growth and respiration [8]. This was explained by a permanent acceleration of microbial activities with no signs of thermal acclimation, defined as the return of microbial activities towards pre-warmed rates. We also observed higher microbial community growth rates (including fungi) in long-term warmed soils. For archaea and bacteria, however, the increase in community growth was not associated with generally faster-growing populations. This contrasts the idea that warming just accelerates the growth rates of already present populations (Fig. 3 C). Instead, higher bacterial community growth (fig. S5 A, B) in warmed soils was driven by a doubling of growing taxa (Fig. 3 A) as well as a larger proportion of the total community being active (Fig. 3 B). While warming led many bacterial taxa to transition from an inactive to an active state, taxa active at higher temperatures were not characterized by higher growth rates. Neither did warming accelerate the growth of taxa active at both temperatures (fig. S4 B) or give rise to generally faster-growing bacteria (fig. S7 B). Hence, long-term warming did not produce or foster faster

growing bacterial populations but rather caused more dormant cells to enter a state of activity.

Since taxon-specific growth rates were indistinguishable between temperatures, we cannot generally rule out the presence of thermal acclimation at the level of individual populations. Thermal acclimation can be evoked by direct and indirect factors such as physiological acclimation or substrate depletion. Physiological acclimation, possibly due to higher cellular maintenance [39] and respiratory costs [26], seems likely for those taxa that were shared between warming levels and did not differ in their growth rates. Most taxa, however, showed narrow environmental optima and were growing at either ambient or warmed conditions. Although many additional taxa became active at higher temperatures, they grew at average rates indistinguishable from ambient conditions. This might have been due to indirect factors such as substrate depletion [8, 9] and larger resource acquisition efforts associated with less energy allocated to growth [40, 41]. The latter was supported by higher potential extracellular enzyme activities involved in cellulose and chitin degradation in long-term warmed plots, which also points to a reduced availability of substrates. Overall, we could show that increases in bacterial community growth can be driven by a larger number of growing taxa rather than generally faster-growing populations, with the potential for thermal acclimation across several taxa. This highlights that studying individual microbial populations can reveal mechanisms of the soil microbiome's warming response that are masked at the aggregated community level.

Previous reports of higher relative community growth rates in response to long-term warming were inferred by measuring the incorporation of ^{18}O into total microbial DNA [8]. Hence, these growth measurements encompassed several groups of microorganisms but mostly bacteria, archaea, and fungi. While we observed the same increase in relative community growth (Fig. 1 C), we subsequently focused on the contribution of bacteria and archaea and, thus, cannot make assumptions about shifts in fungal growth rates. Our results shed light on the mechanisms of the bacterial warming response to long-term warming, allowing us to disentangle community aggregated measurements. We cannot rule out that fungi responded differently than bacteria and contributed to the rise in microbial community growth with higher growth rates. Our proposed mechanism, therefore, only applies to the bacterial and archaeal part of the microbial community. Nonetheless, we found that microbial community

growth also increases with the number of growing bacterial taxa (fig. S6 A) which is not surprising since bacteria and archaea constitute a large part of soil microbial communities.

Many taxa only became active and started growing at higher temperatures. Warming has been reported to increase soil microbiome diversity based on amplicon sequencing of the 16S rRNA gene [42–45]. Optimal growth temperatures of Artic soil microorganisms can range between 23 – 34 °C [46] which by far exceeds regular temperature in high latitude soils. It is possible that the + 6 °C (ambient: 10.7 °C; warmed: 16.7 °C) of soil warming studied in our experiment crossed a minimum temperature threshold which enabled many additional taxa to start growing. Warming-induced losses of nitrogen and carbon might have also decreased the competitiveness of taxa adapted to more nutrient-rich environments, as hypothesized for plants, allowing for a larger diversity of active bacteria [47]. Mean growth rates remained comparable to unwarmed conditions though. Findings from other warming experiments using qSIP underline that local biogeochemical conditions have a strong impact on the microbial response to climate change. While 29 years of warming increased the mean growth of Tundra soil bacteria by more than 150 % [45], 15 years of warming along an elevational gradient in Arizona reduced the growth of various groups of bacteria by more than 70 % [48]. The diversity of growing taxa in response to warming in these studies either increased or remained unchanged. Similar to our results, field warming in the Antarctic doubled the number of active taxa [49]. This suggests that shifts in the number of active bacteria may be a fundamental component of the microbial warming response, but the strength of this mechanism might differ between ecosystems.

Plant-microbe interactions play an important role in shaping microbial activities but how they are affected by warming remains largely unknown. Warming of soil and air can increase plant carbon inputs and promote microbial activities [50–52]. On the other hand, it may also deplete available nutrients such as nitrogen and enhance competition between plants and soil microorganisms [34]. We found that plants promoted higher growth rates at ambient temperatures, but that this effect was lost with long-term warming, indicating a shift of plant-microbe interactions from positive to neutral (Fig. 5). Especially root-associated taxa showed lower growth rates in warmed plots. This response may be explained by warming-induced losses in fine-root biomass and production, which were reported from the study site [37, 38], also suggesting a reduction in belowground plant carbon allocation [53]. Root-associated taxa have been found to consume plant-derived carbon and show higher potential growth rates

than bulk-soil-associated taxa [30, 31]. Since there are indications from the same experimental site that plant carbon inputs did not increase but rather decreased with warming [37, 38], root-associated taxa may have been unable to maintain higher growth rates in warmed plots due to an insufficient supply of extra carbon, likely aggravated by a simultaneous rise in metabolic and respiratory costs [26, 39]. Interestingly, many bulk-soil-associated taxa showed a positive growth response to warming, indicating that their growth was rather limited by temperature than substrate availability. On the other hand, root exclusion could have also reduced competition with root-associated taxa or negative interactions with larger predatory organisms that could not overcome the small mesh size of the root exclusion cores. Root- and bulk-soil-associated taxa likely differ in their life history traits. Root-associated taxa are adapted to extra carbon provided by plants as indicated by higher potential growth rates and more genes associated with carbon metabolisms [30, 31]. Bulk-soil-associated taxa usually don't have access to root exudates and are adapted to a more carbon-limited environment and need to invest more into extracellular enzymes for soil organic matter decomposition. Hence, indirect warming effects driven by shifts in plant-microbe interactions might have had a negligible impact on the growth rates of bulk-soil-associated taxa. Overall, our study provides evidence that in a (Sub)Arctic grassland, the direction of plant-microbe interactions shifts from positive to neutral because of long-term warming. This also suggests that root effects on soil bacteria have become smaller with warming. The strength of the observed root effect differed between microbial groups, possibly due to differences in their life history strategies, since bulk-soil-associated taxa were largely unaffected by shifts in root-microbe interactions.

Do microbial genera or families show similar response patterns to climate change and, if so, could this help us to infer something about their traits? These are well-identified, yet open questions in climate change microbiology. We know that growth rates seem to be to conserved across taxonomic groups [54]. Whether a certain family performs better under warmed conditions remains elusive though. The growth rate of a microorganism is the major component of its fitness [55] and by measuring its change across different environmental conditions we may infer something about its adaptations and traits. We found that the top 20 taxa, based on their growth and abundance, accounted for > 30 % of the community growth at ambient temperatures. Most of these taxa lost their dominant role with long-term warming while other active taxa became dominant contributors to the community's growth,

likely better adapted to the conditions at higher temperatures (Fig. 4). Despite strong differences between warmed and control soils at the ASV level, few taxa managed to persist amongst the top ^{18}O assimilators (*Collimonas, Kitasatospora, Streptacidiphilus*) at warmed conditions, suggesting physiological plasticity with regards to temperature. It is worth mentioning that members of these genera show a wide range of defensive properties including the production of various bioactive and antibiotic compounds which might increase their competitiveness at both temperature regimes [56–58]. *Collimonas* is also known to be a fungus-eating genus [56].

The same families accounted for very similar proportions of bacterial growth (> 60 %) at both temperature regimes (fig. S3). Hence, we could not identify any family, except the Xanthobacteraceae, as particularly warming responsive. However, many ASVs and several genera within these families showed a clear warming response. This suggests that the temperature niche of several bacterial families was rather broad whereas the niche of the individual taxa within these families was considerably smaller.

Root effects were only visible when examining the actively growing community, highlighting the importance of using activity-based techniques such as qSIP to be able to capture indirect warming effects mediated by plants. Despite strong taxon-specific response patterns, which could be used to categorize ASVs into root- and bulk-soil-associated taxa, broad genus or family-specific trends were scarce. Nevertheless, one family, the Chitinophagaceae, consistently performed better when roots were present, even at both temperature regimes. This indicates that several members of the Chitinophagaceae might be root beneficiaries. Members of this family have been identified from root microbiomes before [59–61] and potentially protect plants against pathogens such as fungi, harboring enzymes such as chitinases that are involved in fungal cell wall degradation [62–64]. Chitinophagaceae may also decompose cellulose and could have benefited from the root turnover in the root ingrowth cores [65]. Interestingly, we detected higher exochitinase and exoglucanase (the latter being involved in cellulose degradation) activities in root ingrowth cores where Chitinophagaceae accounted for a substantial part of the bacterial community growth.

In this study, we demonstrate that more than 50 years of soil warming persistently increased microbial growth at the community level. While this has previously been shown and assumed to be driven by generally faster-growing taxa, we found this response, at least for bacteria, to be caused by a larger body of distinct active taxa, growing at rates indistinguishable from

ambient temperatures. This suggests an alternative mechanism behind the warming-induced increase in relative community growth which cannot rule out thermal acclimation at the level of individual bacterial populations. This pattern, i.e., shifts in the number, diversity, and identity of growing taxa, rather than shifts in their individual growth rates might be a central mechanism behind changes in bacterial activity due to environmental change. While there exists supporting evidence from a drought study in a montane grassland [29], future studies need to examine if this is generalizable across ecosystems and disturbances. If yes, this might add an additional layer of complexity to predicting the microbial warming response, especially in microbial-explicit models. Taxa becoming active under warmed conditions may be functionally different from those active at ambient temperatures including their interactions. If accelerated microbial activities are not driven by the same active community, only working at faster rates, but by a larger active community with a different composition, a more complex equation may be necessary to model the microbial warming response. Roots also played an important role in shaping bacterial activity, promoting higher growth rates of associated taxa at ambient temperatures, but not anymore after long-term warming. For putative root-associated taxa, indirect warming effects mediated by shifts in root-microbe interactions appeared to be even stronger than direct warming effects. The soil microbiome has often remained a black box regarding its response to climate change, complicating its incorporation into climate models. Our findings shed light on the range of microbial mechanisms underlying the warming response of the soil microbiome, opening this black box to improve our understanding of the fate of soil carbon in a warmer climate.

Materials and Methods

Study site, experimental set-up, and sample collection

We conducted our study in the frame of the ForHot natural warming experiment located in southern Iceland (64° 00′ 01′′ N, 21° 11′ 09′′ W) [66]. The ForHot experiment consists of naturally warmed grasslands where a soil temperature gradient established due to geothermal activity. Soil temperatures range from ambient conditions (mean annual soil temperature at 10 cm depth: 6.3 °C ± 0.3 °C; mean ± standard deviation) to + 20 °C of warming. The grassland sites differ in their warming history. Soils for this study were sampled from four neighboring fenced transects (fig. S1) located in a long-term warmed valley (LTW). The grassland at this site experienced sustained soil warming for > 50 years but probably since 1706 [66]. The distance between ambient and warmed (+ 6 °C) plots was 24.8 ± 7.2 m (mean ± standard deviation). Dominant grassland species were *Agrostis capillaris*, *Ranunculus acris,* and *Equisetum pratense* that established over Brown Andosols of approximately pH 5.7 [8]. The mean annual air temperature and mean annual precipitation recorded at the closest synoptic station were 5.2 °C and 1457 mm, respectively.

In October 2019, we installed stainless steel root-ingrowth (mesh size: 1 mm) and root-exclusion cores (mesh size: 30 µm) adjacent to each other along the four temperature gradients (Fig. 1 A). Soil was extracted and transferred into cores (cylindrical meshed compartment, length: 10 cm, diameter: 3.5 cm) in the field after the manual removal of roots and stones. Root-exclusion cores likely also prevented the entry of soil fauna > 30 µm, including predators such as larger nematodes and protists, while fungi had unhindered access to both core types. Cores were retracted after 10 months of in situ incubation at peak vegetation season in August 2020. Along with the pre-installed cores, fresh soil samples (undisturbed soil cores) were collected from the top 10 cm in an area adjacent to the permanently monitored warming plots where metal cores were installed (Fig. 1 A). These samples were taken to assess the warming effect on the soil microbiome without previous disturbance. For quantitative stable isotope probing, we focused on plots along the gradients that experienced on average + 6 °C (n = 4) of warming and their corresponding controls at ambient temperatures (n = 4). Overall, this resulted in 24 samples comprising material from

two warming levels and three core types (undisturbed, root ingrowth, root exclusion). Although warming intensities have been reported stable over time [66], they were subject to variation due to fluctuations in geothermal activity. During laboratory incubations, we maintained the previously confirmed temperature difference of + 6 °C [8] between ambient and selected warmed sites. Based on temperature measurements from control plots during field sampling, laboratory incubations were performed at 10.7 °C and 16.7 °C, respectively.

Total and microbial carbon and nitrogen pools

Four days after sampling and storage at 4 °C, soil was passed through a 2 mm sieve. Soil water content was determined gravimetrically by drying 2 g of fresh soil at 105 °C for 24 h. We analyzed microbial biomass carbon and microbial biomass nitrogen via the chloroform-fumigation extraction method (Vance, Brookes, and Jenkinson 1987). One soil sub-sample (2 g) was chloroform fumigated for 48 h prior to extraction in 15 ml 1 M KCl solution, whereas another sub-sample was extracted immediately. After KCl addition, samples were shaken for 30 minutes, filtered through ash-free filters, and stored at -20 °C. We analyzed both sub-subsets for extractable organic carbon (EOC) and extractable organic nitrogen (EON) on a TOC/N Analyzer (TOC- VCPH/CPNT-NM-1, Shimadzu, Japan). Microbial biomass carbon and nitrogen were then calculated as the difference between fumigated and non-fumigated sub-samples using an extraction coefficient of 0.45 [67]. Total carbon and nitrogen contents were determined from dried, weighed, and finely ground soil aliquots by EA-IRMS (EA 1110; CE Instruments, Milan, Italy), coupled to a Finnigan MAT Delta Plus IRMS (ThermoFisher Scientific, Waltham, MA, USA).

Potential extracellular enzyme activities

We measured the potential activities of four extracellular enzymes related to the degradation of cellulose, chitin, proteins, and organic phosphorus using a modified fluorometric method [68] (table S2). In short, 50 ml sodium acetate buffer (50 mM, pH 5.8) was added to 1 g of sieved soil and ultrasonicated at approximately 350 J. Fluorogenic methylumbelliferyl (MUF) substrates were used to measure enzymatic cleavage of all enzymes except for protease assays which required an aminomethylcoumarin (AMC) substrate. We prepared one standard

row and four analytical replicates for each sample in a black microtiter plate by combining 200 µl of mixed sample and 50 µl fluorogenic substrate. Plates were incubated in the dark at room temperature and fluorescence was measured after 10 minutes, 60 minutes, and 100 minutes at an excitation wavelength of 365 nm and an emission wavelength of 450 nm (Tecan Infinite M200 fluorimeter, Werfen, Austria). The increase in fluorescence over time was then used to calculate potential enzyme activities.

Quantitative stable isotope probing via ^{18}O water vapor equilibration (vapor-qSIP)

Prior to vapor-qSIP incubations, soil samples were kept at field temperatures for two days (10.7 °C and 16.7 °C) to allow microbial communities to acclimate after transportation and storage. Samples for qSIP were incubated with ^{18}O-enriched water and water at natural abundance using the ^{18}O water vapor equilibration method [69]. In vivo ^{18}O water vapor equilibration avoids changes in soil water content by letting labeled water redistribute into the soil pore space from a spatially separated source in a closed system. By using this method, we could maintain the original moisture of our soil samples while avoiding air-drying and rewetting, potentially masking in situ activities [69]. Soil samples were sieved to remove rocks, roots, and plant litter. They were weighed in 1.2 ml (~500 mg) cryovials before placing them into 27 ml glass headspace vials. We applied 500 µl of heavy water (97 atm %) to the bottom of each headspace vial, which was calculated using the initial soil water content and the target soil water enrichment of ~70 atom % ^{18}O . The volumetric water content was 34.9 ± 2.9 % (mean ± SD) in warmed and 40.1 ± 3.5 % in ambient soils. Headspace vials were closed air-tight with rubber septa after water application and incubated at ambient temperatures and at + 6 °C above (ambient = 10.7 °C, warmed= 16.7 °C) for five days. To monitor the ^{18}O enrichment of the soil water over time, we prepared an additional ^{18}O-calibration set-up for each temperature level using soil samples from one transect. These calibration samples were harvested after 3, 6, and 48 hours to collect the remains of liquid water at the bottom of the headspace vials. At the end of the 5-day incubation period, the same procedure was performed for all other ^{18}O labeled samples. Water samples were analyzed for their ^{18}O enrichment through equilibration of ^{18}O in H_2O with CO_2 by a Gasbench II headspace sampler connected to a Delta V Advantage isotope ratio mass spectrometer (Thermo Fisher). These served as a proxy for ^{18}O enrichment of soil water over time. We used them to calculate the

average ^{18}O enrichment over the course of incubation by fitting a negative exponential function and determining its integral according to Canarini *et al.* 2020. Our samples approached the target enrichment (70 atom % ^{18}O) after 48 hours (fig. S12) but did not fully reach it. Hence, the average soil water enrichment over the five-day incubations was 32 - 37 atom% per sample.

After incubation, soil aliquots were flash-frozen and stored at -80 °C. Following manufacturer's instructions, we isolated DNA from soils using the FastDNA™ SPIN Kit for Soil (MO Biomedicals). DNA concentrations were quantified fluorometrically using the PicoGreen Assay (Quant-iTTM PicoGreen dsDNA Reagent, Life Technologies) on a TECAN Infinite 200 PRO plate reader. To determine atom percent excess ^{18}O (APE ^{18}O) of our DNA extracts, we analyzed their ^{18}O isotopic composition on a thermochemical elemental analyzer (TC/EA ThermoFisher) coupled via a Conflo III open split system (ThermoFisher) to an Isotope Ratio Mass Spectrometer (IRMS, Delta V Advantage, ThermoFisher). DNA extracts were separated based on their density to detect underlying patterns in ^{18}O isotope incorporation by ultracentrifugation in a cesium chloride density gradient [28]. We loaded 2 µg DNA into a 4.7 mL OptiSeal ultracentrifuge tube (Beckman Coulter) with ~4 ml saturated CsCl solution and gradient buffer (100 mM Tris, 100 mM KCl, 1 mM EDTA). Two replicates from the root-exclusion core experiment incubated at elevated temperatures showed lower DNA yields. Hence, only 750 ng of DNA could be loaded into the ultracentrifuge tubes. For comparability reasons and downstream calculations, this was considered by multiplying DNA and 16S rRNA gene copies by a correction factor of 2.67. DNA Samples were spun in a Beckman Optima ultracentrifuge using a Beckman VTi 90 rotor (50,000 rpm at 20°C) for 72 h. We manually collected 24 fractions of 250 µl after puncturing the tubes with a cannula (Braun Sterican, 0.9 x 25 mm) while mineral oil served as a displacement medium. During fractionation, tubes were secured with a three-prong clamp attached to a retort stand. We measured the density of each fraction with a Krüss DR301-95 digital refractometer. DNA was purified from the CsCl solution by glycogen-aided isopropanol precipitation, resuspended in 50 µl nuclease-free water, and quantified by PicoGreen fluorescence (see above).

Sequencing was performed (15-16 fractions per sample) at the Joint Microbiome Facility of the Medical University of Vienna and the University of Vienna (JMF project ID: JMF-2107-05). Fractions were selected based on DNA content excluding those without detectable DNA. A

two-step barcoding approach was used to generate amplicon libraries of archaeal and bacterial communities using Illumina MiSeq (V3 Kit) in the 2 x 300 bp configuration [70]. Primer sequences (515F–806R) and PCR amplification protocols (30 cycles) were used as specified by the Earth Microbiome Project [71] standard protocols (https://earthmicrobiome.org/protocols-and-standards/16s/). We used the following cycling conditions: initial denaturation at 94°C for 4 min, 7 cycles of 94°C for 30 s, 52°C for 30 s, 72°C for 60 s, and final elongation at 72°C for 7 min [70]. Amplicon pools were extracted from the raw sequencing data using the FASTQ workflow in BaseSpace (Illumina) with default parameters. Demultiplexing was performed with the python package demultiplex (Laros JFJ, github.com/jfjlaros/demultiplex) allowing one mismatch for barcodes and two mismatches for linkers and primers [70]. Amplicon sequence variants (ASVs) were inferred using the DADA2 R package [72] applying the recommended workflow. FASTQ reads 1 and 2 were trimmed at 220 nt and 150 nt with allowed expected errors of 2 and 2, respectively. ASV sequences were subsequently classified using DADA2 and the SILVA database SSU Ref NR 99 release 138.1 [73, 74] using a confidence threshold of 0.5. Datasets were deposited in the NCBI Sequence Read Archive under BioProject accession number PRJNA1013122.

We measured the concentration of total 16S rRNA gene copies per fraction on the Bio-Rad QX200 digital droplet PCR (ddPCR) system using the same primers used for sequencing but without adapters. Individual PCR reactions comprised the following components: 11 µl 1× EvaGreen Droplet Generation Mix (Bio-Rad), 0.2 µl forward primer (10 µM), 0.2 µl reverse primer (10 µM), 8.6 µl nuclease-free water, and 2µl diluted DNA template. Prior to ddPCR quantification, DNA samples were diluted to 0.05 ng/µl as 0.1 ng of total DNA per reaction was found optimal for the separation of negative and positive droplets. The following cycling conditions were used for ddPCR: 95°C for 5 min, 5 cycles of 95°C for 30 s, 57°C for 2.5 min (-1 °C each step), followed by 35 cycles of 95 °C for 30 s, 52 °C for 2.5 min, followed by 4 °C for 5 min, and 90 °C for 5 min. Droplets were stored at 4 °C for a least one hour before reading. We used QuantaSoft software (Bio-Rad) to calculate 16S rRNA gene copies.

Microbial community growth

We used the ^{18}O enrichment of our DNA samples before ultracentrifugation together with the estimates of microbial biomass carbon (C_{mic}) and the DNA content to calculate microbial community growth – including other microorganisms such as fungi - as described before [8, 20, 75]. In short, we determined DNA production ($DNA_{produced}$) using the difference in ^{18}O abundance between labeled and natural abundance samples using a factor of 31.21 (proportional mass of O (%) in an average DNA molecule). Microbial community growth (G, expressed as µg carbon per hour per gram of dry soil) was then calculated by multiplying DNA production with the quotient of microbial biomass carbon and DNA content ($G = DNA_{produced} * (C_{mic}$ / Total DNA). We determined microbial community growth per unit of microbial biomass (Gm, relative community growth or mass-specific growth, expressed as µg carbon per hour per gram of microbial biomass carbon) using: $Gm = G / C_{mic}$.

qSIP and statistical analyses

All analyses were performed in R 4.1.1 [76]. Amplicon sequencing data was manipulated using the phyloseq package [77]. We removed ASVs without taxonomic assignment at the phylum level or classified eukaryotes, mitochondria, or chloroplasts (2553 ASVs). In addition, we removed contaminant ASVs identified by decontam 1.6.0 [78] using the prevalence method and a threshold setting of 0.01. Negative controls from DNA extraction and dilution steps served as input data (number of negative controls = 6). Only samples with > 2000 reads were retained for further analyses. Post-filtering, we yielded a feature table with 19,092 ASVs and 10,139,236 reads.

We determined weighted average densities (WADs) at the sample level, as explained in Hungate et al. 2015. Previous reports suggest that variations in CsCl gradients between independent ultracentrifugation runs affect WAD estimates [54, 79]. Thus, we used direct IRMS measurements of the ^{18}O composition of our unfractionated DNA to calibrate WADs as described in Papp et al. (2018) [80]. The calibration was based on a previously described [28] relationship between density and $APE^{18}O$ of DNA: Expected WAD = 0.0644* $APE^{18}O$ of DNA + 1.6946. The intercept represents the density of *E. coli* DNA at natural abundance. Since density measurements can vary considerably between labs, we replaced this term with the

density estimates of our unlabeled control samples. A correction factor was determined by subtracting the measured WADs from the expected WADs and then applied to the measured WADs. One sample pair (control, labeled) from the root-ingrowth treatment at ambient temperatures was spun in a slightly less concentrated CsCl gradient, resulting in overall lower WADs. To account for this, we calculated the mean offset in WAD from the control samples of the remaining replicates of the same treatment and added it to the density estimates.

Taxon-specific ^{18}O enrichment (APE ^{18}O), a proxy for microbial growth, was determined based on the relationships between ^{18}O incorporation, DNA density, GC-content, and DNA molecular weight as described in Hungate *et al.* 2015. We used publicly available code to perform qSIP calculations (https://bitbucket.org/QuantitativeSIP/qsip_repo, https://github.com/brams-tone/qsip, https://doi.org/10.5281/zenodo.8109566 [81]). A presence-absence filtering step was applied prior to qSIP analysis to exclude infrequent taxa [14]. Taxa had to occur in at least four fractions and two replicates per treatment, yielding 7601 ASVs and accounting for 85% of all sequence reads. We calculated taxon-specific APE ^{18}O values, first, at the treatment level by bootstrap resampling of replicates and, second, at the replicate level without bootstrap resampling. Bootstrap testing allowed us to estimate whether taxon-specific density shifts via ^{18}O incorporation were consistent across replicates, resulting in a single enrichment value (bootstrap mean or median) for each taxon [28]. To also harness growth variations between replicates, we merged both approaches by first identifying consistently growing taxa at the treatment level using bootstrap resampling and then determining their individual growth rates at the replicate level. Hence, we considered a taxon to be actively growing if its bootstrapped and non-bootstrapped APE ^{18}O values were > 0. Taxon-level relative growth rates per day (RGR) were calculated as follows assuming linear growth: RGR = AFE $^{18}O_{taxon}$ / (Average AFE $^{18}O_{soil\ water}$ * days of incubation) [48, 82]. For this, APE ^{18}O percent values were converted into decimals also called ^{18}O atom fraction excess (AFE ^{18}O), and commonly used in qSIP studies.

Absolute abundances (16S rRNA gene copies per ASV per g of dry soil) were calculated for each ASV individually by multiplying their sequencing-inferred relative abundances by the total amount of 16S rRNA gene copies of each fraction before summing over all fractions of a sample. To determine the size, or percentage, of the actively growing community, we summed the absolute abundances of all growing taxa and divided it by the sum of the

absolute abundances of all taxa. Prior to summing the absolute abundances of the growing taxa, we multiplied them by their AFE ^{18}O values. By doing so, we aimed to estimate how many 16S rRNA gene copies were labeled within the population of a growing taxon (= size of growing subpopulation). We accounted for this because qSIP targets populations and not cells and it is possible that only a subfraction of a taxon's population was growing. By multiplying the absolute abundance of a growing taxon by its AFE ^{18}O, we assumed that the enrichment of a taxon represents its abundance of fully labeled 16S rRNA gene copies. Although this is a conservative approach since there are probably also partially labeled 16S rRNA gene copies, it avoids overestimating the size of the growing community.

Since microbial community growth estimates (G, G_m), as described above, inherently included other microorganisms such as fungi, we additionally calculated total and relative growth rates of the bacterial community. Total bacterial growth, expressed as the amount of produced 16S rRNA gene copies per gram of dry soil per day, was determined by summing the total growth across all growing taxa per day ($\sum RGR_{ASV}$ * 16S rRNA gene copies per gram dry soil $_{ASV}$) [49]. Relative bacterial community growth was then calculated by dividing total growth by the size of the total bacterial community (16S rRNA gene copies per gram of dry soil).

We compared the effects of long-term warming on carbon and nitrogen pools (total and microbial), 16S rRNA gene copies, soil moisture, and extracellular enzymes activities using two-way ANOVA (factors: Warming $_{ambient/\ +6°C}$, Core $_{undisturbed/\ root\ ingrowth/\ root\ exclusion}$) or two-sided Student's t-tests when testing for overarching effects. When parametric testing was performed, we examined if normality (Shapiro–Wilk test) and homoscedasticity (Levene's test) requirements were fulfilled and applied log transformation if necessary. To focus on the impact of root presence on extracellular enzyme activities we also used two-way ANOVA but excluded the undisturbed cores.

To assess community shifts of the total and active community (subset based on growth), we computed Euclidean distances based on ASV absolute abundances followed by two-way PERMANOVA tests with the "adonis" function [83]. Absolute abundances were summed over all fractions per sample (only labeled) and, according to a new quantitative sequencing framework [84], centered-log transformed (clr) before performing a principal component analysis (PCA).

We compared RGRs, ASV richness, and active population sizes across treatments using two-way ANOVA (factors: Warming $_{\text{ambient/ +6°C}}$, Core $_{\text{undisturbed/ root ingrowth/ root exclusion}}$) followed by Tukey post hoc tests. To avoid pseudo-replication (multiple taxon-specific growth estimates per sample), we calculated mean relative growth rates for each sample before testing. For pairwise comparisons of RGRs of taxa shared between warming levels, we employed two-sided Student's t-tests. In addition, we used three-way ANOVA, (factors: Warming $_{\text{ambient/ +6°C}}$, Core $_{\text{root ingrowth/ root exclusion}}$, Experiment $_{\text{undisturbed cores, in situ cores}}$) to compare mean RGRs of taxa that were active in either distinct or multiple treatments (exclusive/ shared) to infer if taxa associated with warming or root presence show different response levels.

We calculated how the number of growing taxa within major phyla and families shifted with long-term warming in the undisturbed cores as an indicator of their taxonomic response. We tested for significant shifts using separate nonparametric Kruskal–Wallis rank sum tests and corrected for multiple comparisons using false detection rate. Shifts in the number of growing taxa were visualized across families and phyla using relative changes between ambient and warmed conditions (0 = no change, 1 = increase by 100 %). Relative changes were calculated using the following equation: (Growing ASV richness $_{\text{Warmed}}$ /Mean growing ASV richness $_{\text{Ambient}}$) -1.

Although some taxa might be growing faster than others, their contribution to the overall community-level growth will also depend on their abundance. Therefore, we estimated proportional ^{18}O-assimilation, or proportion of growth, for each growing ASV by re-calculating their relative abundances (sum of relative abundances of growing taxa = 1) and multiplying them by their relative growth rate (RGR). These weighted enrichment values were then divided by their sum, producing a proportional ^{18}O-assimilation value ranging between 0 - 1. We ranked ASVs that were growing in at least two replicates based on their proportional ^{18}O-assimilation to identify the top 15 ^{18}O assimilating taxa per sample, the top 15 ^{18}O assimilating families per treatment, and how many taxa accounted for 50% of the total community's growth. We visualized changes in proportional ^{18}O-assimilation with heatmaps using functions from the ampvis2 package [85]. To test for significant differences in proportional ^{18}O-assimilation between warming levels or root in-growth and root exclusion cores at the family level, we used pairwise Wilcoxon signed-rank tests using false detection rate correction for multiple comparisons.

References

1. Cavicchioli R, Ripple WJ, Timmis KN, Azam F, Bakken LR, Baylis M, et al. Scientists' warning to humanity: microorganisms and climate change. *Nature Reviews Microbiology* 2019; **17**: 569–586.

2. Hutchins DA, Jansson JK, Remais J V, Rich VI, Singh BK, Trivedi P. Climate change microbiology — problems and perspectives. *Nature Reviews Microbiology* 2019; **17**: 391–396.

3. Wieder WR, Bonan GB, Allison SD. Global soil carbon projections are improved by modelling microbial processes. *Nature Climate Change* 2013; **3**: 909–912.

4. Raich JW, Potter CS. Global patterns of carbon dioxide emissions from soils. *Global Biogeochemical Cycles* 1995; **9**: 23–36.

5. Crowther TW, Thomas SM, Maynard DS, Baldrian P, Covey K, Frey SD, et al. Biotic interactions mediate soil microbial feedbacks to climate change. *Proceedings of the National Academy of Sciences* 2015; **112**: 7033–7038.

6. Karhu K, Auffret MD, Dungait JAJ, Hopkins DW, Prosser JI, Singh BK, et al. Temperature sensitivity of soil respiration rates enhanced by microbial community response. *Nature* 2014; **513**: 81–84.

7. Bradford MA, McCulley RL, Crowther TW, Oldfield EE, Wood SA, Fierer N. Cross-biome patterns in soil microbial respiration predictable from evolutionary theory on thermal adaptation. *Nature Ecology & Evolution* 2019; **3**: 223–231.

8. Walker TWN, Kaiser C, Strasser F, Herbold CW, Leblans NIW, Woebken D, et al. Microbial temperature sensitivity and biomass change explain soil carbon loss with warming. *Nature Climate Change* 2018; **8**: 885–889

9. Domeignoz-Horta LA, Pold G, Erb H, Sebag D, Verrecchia E, Northen T, et al. Substrate availability and not thermal-acclimation controls microbial temperature sensitivity response to long term warming. *Global Change Biology* 2022; **29**: 1574-1590.

10. Jansson JK, Hofmockel KS. Soil microbiomes and climate change. *Nature Reviews Microbiology* 2020; **18**: 35–46

11. Naylor D, Sadler N, Bhattacharjee A, Graham EB, Anderton CR, McClure R, et al. Soil Microbiomes Under Climate Change and Implications for Carbon Cycling. *Annual Review of Environment and Resources* 2020; **45**: 29–59.

12. Classen AT, Sundqvist MK, Henning JA, Newman GS, Moore JAM, Cregger MA, et al. Direct and indirect effects of climate change on soil microbial and soil microbial-plant interactions: What lies ahead? *Ecosphere* 2015; **6**: art130.

13. Trivedi P, Batista BD, Bazany KE, Singh BK. Plant–microbiome interactions under a changing world: responses, consequences and perspectives. *New Phytologist* 2022; **234**: 1951–1959.

14. Stone BW, Li J, Koch BJ, Blazewicz SJ, Dijkstra P, Hayer M, et al. Nutrients cause consolidation of soil carbon flux to small proportion of bacterial community. *Nature Communications* 2021; **12**: 1–9.

15. Allison SD, Wallenstein MD, Bradford MA. Soil-carbon response to warming dependent on microbial physiology. *Nature Geoscience* 2010; **3**: 336-340.

16. Neill C, Gignoux J. Soil organic matter decomposition driven by microbial growth: A simple model for a complex network of interactions. *Soil Biology and Biochemistry* 2006; **38**: 803–811.

17. Blagodatskaya E, Kuzyakov Y. Active microorganisms in soil: Critical review of estimation criteria and approaches. *Soil Biology and Biochemistry* 2013; **67**: 192–211.

18. Jansson JK, Hofmockel KS. The soil microbiome—from metagenomics to metaphenomics. *Current Opinion in Microbiology* 2018; **43**: 162–168.

19. Dijkstra P, Martinez A, Thomas SC, Seymour CO, Wu W, Dippold MA, et al. On maintenance and metabolisms in soil microbial communities. *Plant and Soil* 2022; **476**: 385-396.

20. Simon E, Canarini A, Martin V, Séneca J, Böckle T, Reinthaler D, et al. Microbial growth and carbon use efficiency show seasonal responses in a multifactorial climate change experiment. *Communications Biology* 2020; **3**: 1–10.

21. Liu XJA, Pold G, Domeignoz-Horta LA, Geyer KM, Caris H, Nicolson H, et al. Soil aggregate-mediated microbial responses to long-term warming. *Soil Biology and Biochemistry* 2021; **152**: 108055.

22. Bradford MA, Davies CA, Frey SD, Maddox TR, Melillo JM, Mohan JE, et al. Thermal adaptation of soil microbial respiration to elevated temperature. *Ecology Letters* 2008; **11**: 1316–1327.

23. Romero-Olivares AL, Allison SD, Treseder KK. Soil microbes and their response to experimental warming over time: A meta-analysis of field studies. *Soil Biology and Biochemistry* 2017; **107**: 32–40.

24. Fanin N, Mooshammer M, Sauvadet M, Meng C, Alvarez G, Bernard L, et al. Soil enzymes in response to climate warming: Mechanisms and feedbacks. *Functional Ecology* 2022; **24**: 1378–1395.

25. Söllinger A, Séneca J, Borg Dahl M, Motleleng LL, Prommer J, Verbruggen E, et al. Down-regulation of the bacterial protein biosynthesis machinery in response to weeks, years, and decades of soil warming. *Science Advances* 2022; **8**: eabm3230.

26. Marañón-Jiménez S, Soong JL, Leblans NIW, Sigurdsson BD, Peñuelas J, Richter A, et al. Geothermally warmed soils reveal persistent increases in the respiratory costs of soil microbes contributing to substantial C losses. *Biogeochemistry* 2018; **138**: 245–260.

27. Fierer N, Bradford MA, Jackson RB. Toward an ecological classification of soil bacteria. *Ecology* 2007; **88**: 1354–1364.

28. Hungate BA, Mau RL, Schwartz E, Gregory Caporaso J, Dijkstra P, van Gestel N, et al. Quantitative microbial ecology through stable isotope probing. *Applied and Environmental Microbiology* 2015; **81**: 7570–7581.

29. Metze D, Schnecker J, Canarini A, Fuchslueger L, Koch BJ, Stone BWG, et al. Microbial growth under drought is confined to distinct taxa and modified by future climate conditions. *Nature communications* 2023; **14**: 5895.

30. Fan K, Holland-Moritz H, Walsh C, Guo X, Wang D, Bai Y, et al. Identification of the rhizosphere microbes that actively consume plant-derived carbon. *Soil Biology and Biochemistry* 2022; **166**: 108577.

31. López JL, Fourie A, Poppeliers SWM, Pappas N, Sánchez-Gil JJ, de Jonge R, et al. Growth rate is a dominant factor predicting the rhizosphere effect. *The ISME Journal* 2023; **17**: 1396–1405.

32. Bardgett RD, Manning P, Morriën E, De Vries FT. Hierarchical responses of plant–soil interactions to climate change: consequences for the global carbon cycle. *Journal of Ecology* 2013; **101**: 334–343.

33. Pugnaire FI, Morillo JA, Peñuelas J, Reich PB, Bardgett RD, Gaxiola A, et al. Climate change effects on plant-soil feedbacks and consequences for biodiversity and functioning of terrestrial ecosystems. *Science Advances* 2023; **5**: eaaz1834.

34. Bardgett RD, Freeman C, Ostle NJ. Microbial contributions to climate change through carbon cycle feedbacks. *The ISME Journal* 2008; **2**: 805–814.

35. Malhotra A, Brice DJ, Childs J, Graham JD, Hobbie EA, Vander Stel H, et al. Peatland warming strongly increases fine-root growth. *Proceedings of the National Academy of Sciences* 2020; **117**: 17627–17634.

36. Kwatcho Kengdo S, Peršoh D, Schindlbacher A, Heinzle J, Tian Y, Wanek W, et al. Long-term soil warming alters fine root dynamics and morphology, and their ectomycorrhizal fungal community in a temperate forest soil. *Global Change Biology* 2022; **28**: 3441–3458.

37. Fang C, Verbrigghe N, Sigurdsson BD, Ostonen I, Leblans NIW, Marañón-Jiménez S, et al. Decadal soil warming decreased vascular plant above and belowground production in a subarctic grassland by inducing nitrogen limitation. *New Phytologist* 2023; **240**: 565–576.

38. Bhattarai B, Sigurdsson BD, Sigurdsson P, Leblans N, Janssens I, Meynzer W, et al. Soil warming duration and magnitude affect dynamics of fine roots and rhizomes and associated C and N pools in subarctic grasslands. *Annals of Botany* 2023; **132:** 269-279.

39. Wang C, Morrissey EM, Mau RL, Hayer M, Piñeiro J, Mack MC, et al. The temperature sensitivity of soil: microbial biodiversity, growth, and carbon mineralization. *The ISME Journal* 2021; **15**: 2738–2747.

40. Malik AA, Puissant J, Goodall T, Allison SD, Griffiths RI. Soil microbial communities with greater investment in resource acquisition have lower growth yield. *Soil Biology and Biochemistry* 2019; **132**: 36–39.

41. Malik AA, Martiny JBH, Brodie EL, Martiny AC, Treseder KK, Allison SD. Defining trait-based microbial strategies with consequences for soil carbon cycling under climate change. *ISME Journal* 2020; **14**: 1–9.

42. Sheik CS, Beasley WH, Elshahed MS, Zhou X, Luo Y, Krumholz LR. Effect of warming and drought on grassland microbial communities. *The ISME journal* 2011; **5**: 1692–1700.

43. Rocca JD, Simonin M, Blaszczak JR, Ernakovich JG, Gibbons SM, Midani FS, et al. The microbiome stress project: toward a global meta-analysis of environmental stressors and their effects on microbial communities. *Frontiers in Microbiology* 2019; **9**: 3272.

44. Carrell AA, Kolton M, Glass JB, Pelletier DA, Warren MJ, Kostka JE, et al. Experimental warming alters the community composition, diversity, and N2 fixation activity of peat moss (Sphagnum fallax) microbiomes. *Global Change Biology* 2019; **25**: 2993–3004.

45. Propster JR, Schwartz E, Hayer M, Miller S, Monsaint-Queeney V, Koch BJ, et al. Distinct Growth Responses of Tundra Soil Bacteria to Short-Term and Long-Term Warming. *Applied and Environmental Microbiology* 2023; **89:** e01543-22.

46. Rijkers R, Dekker M, Aerts R, Weedon JT. Maximum summer temperatures predict the temperature adaptation of Arctic soil bacterial communities. *Biogeosciences* 2023; **20**: 767–780.

47. Tilman D. Some Thoughts on Resource Competition and Diversity in Plant Communities BT - Mediterranean-Type Ecosystems. In: Kruger FJ, Mitchell DT, Jarvis JUM (eds).1983. Springer Berlin Heidelberg, Berlin, Heidelberg, pp 322–336.

48. Purcell AM, Hayer M, Koch BJ, Mau RL, Blazewicz SJ, Dijkstra P, et al. Decreased growth of wild soil microbes after 15 years of transplant-induced warming in a montane meadow. *Global Change Biology* 2021; **28**: 128–139.

49. Purcell AM, Dijkstra P, Hungate BA, McMillen K, Schwartz E, van Gestel N. Rapid growth rate responses of terrestrial bacteria to field warming on the Antarctic Peninsula. *The ISME Journal* 2023; **17**: 2290-2302

50. Zhou L, Zhou X, He Y, Fu Y, Du Z, Lu M, et al. Global systematic review with meta-analysis shows that warming effects on terrestrial plant biomass allocation are influenced by precipitation and mycorrhizal association. *Nature Communications* 2022; **13**: 4914.

51. Liu M, Wen J-H, Chen Y-M, Xu W-J, Wang Q, Ma Z-L. Warming increases soil carbon input in a Sibiraea angustata-dominated alpine shrub ecosystem. *Journal of Plant Ecology* 2022; **15**: 335–346.

52. Hopkins FM, Filley TR, Gleixner G, Lange M, Top SM, Trumbore SE. Increased belowground carbon inputs and warming promote loss of soil organic carbon through complementary microbial responses. *Soil Biology and Biochemistry* 2014; **76**: 57–69.

53. Qiu Y, Guo L, Xu X, Zhang L, Zhang K, Chen M, et al. Warming and elevated ozone induce tradeoffs between fine roots and mycorrhizal fungi and stimulate organic carbon decomposition. *Science Advances* 2021; **7**: 1–10.

54. Morrissey EM, Mau RL, Hayer M, Liu X-JA, Schwartz E, Dijkstra P, et al. Evolutionary history constrains microbial traits across environmental variation. *Nature Ecology & Evolution* 2019; **3**: 1064–1069.

55. Roller BRK, Schmidt TM. The physiology and ecological implications of efficient growth. *The ISME Journal* 2015; **9**: 1481–1487.

56. Song C, Schmidt R, de Jager V, Krzyzanowska D, Jongedijk E, Cankar K, et al. Exploring the genomic traits of fungus-feeding bacterial genus Collimonas. *BMC Genomics* 2015; **16**: 1103.

57. Takahashi Y. Genus Kitasatospora, taxonomic features and diversity of secondary metabolites. *The Journal of Antibiotics* 2017; **70**: 506–513.

58. Malik A, Kim YR, Kim SB. Genome Mining of the Genus Streptacidiphilus for Biosynthetic and Biodegradation Potential. *Genes* 2020; **11**: 1166.

59. Pérez-Jaramillo JE, Carrión VJ, Bosse M, Ferrão LF V, de Hollander M, Garcia AAF, et al. Linking rhizosphere microbiome composition of wild and domesticated Phaseolus vulgaris to genotypic and root phenotypic traits. *The ISME Journal* 2017; **11**: 2244–2257.

60. Znój A, Gawor J, Gromadka R, Chwedorzewska KJ, Grzesiak J. Root-Associated Bacteria Community Characteristics of Antarctic Plants: Deschampsia antarctica and Colobanthus quitensis—a Comparison. *Microbial Ecology* 2022; **84**: 808–820.

61. Pérez-Jaramillo JE, Carrión VJ, de Hollander M, Raaijmakers JM. The wild side of plant microbiomes. *Microbiome* 2018; **6**: 143.

62. Chuntao Y, H. HS, L. SK, Olga M, Dmitri M, Amit D, et al. Role of Bacterial Communities in the Natural Suppression of Rhizoctonia solani Bare Patch Disease of Wheat (Triticum aestivum L.). *Applied and Environmental Microbiology* 2013; **79**: 7428–7438.

63. Chapelle E, Mendes R, Bakker PAHM, Raaijmakers JM. Fungal invasion of the rhizosphere microbiome. *The ISME Journal* 2016; **10**: 265–268.

64. Carrión VJ, Perez-Jaramillo J, Cordovez V, Tracanna V, de Hollander M, Ruiz-Buck D, et al. Pathogen-induced activation of disease-suppressive functions in the endophytic root microbiome. *Science* 2019; **366**: 606–612.

65. Dang C, Walkup JG V, Hungate BA, Franklin RB, Schwartz E, Morrissey EM. Phylogenetic organization in the assimilation of chemically distinct substrates by soil bacteria. *Environmental Microbiology* 2021; **24**: 357-369.

66. Sigurdsson BD, Leblans NIW, Dauwe S, Gudmundsdóttir E, Gundersen P, Gunnarsdóttir GE, et al. Geothermal ecosystems as natural climate change experiments: The ForHot research site in Iceland as a case study. *Icelandic Agricultural Sciences* 2016; **29**: 53–71.

67. Vance ED, Brookes PC, Jenkinson DS. An extraction method for measuring soil microbial biomass C. *Soil Biology and Biochemistry* 1987; **19**: 703–707.

68. Kaiser C, Koranda M, Kitzler B, Fuchslueger L, Schnecker J, Schweiger P, et al. Belowground carbon allocation by trees drives seasonal patterns of extracellular enzyme activities by altering microbial community composition in a beech forest soil. *New Phytologist* 2010; **187**: 843–858.

69. Canarini A, Wanek W, Watzka M, Sandén T, Spiegel H, Šantrůček J, et al. Quantifying microbial growth and carbon use efficiency in dry soil environments via ^{18}O water vapor equilibration. *Global Change Biology* 2020; **26**: 5333–5341.

70. Pjevac P, Hausmann B, Schwarz J, Kohl G, Herbold CW, Loy A, et al. An Economical and Flexible Dual Barcoding, Two-Step PCR Approach for Highly Multiplexed Amplicon Sequencing. *Frontiers in Microbiology* 2021; **12**: 669776.

71. Gilbert JA, Jansson JK, Knight R. The Earth Microbiome project: successes and aspirations. *BMC Biology* 2014; **12**: 69.

72. Callahan BJ, McMurdie PJ, Rosen MJ, Han AW, Johnson AJA, Holmes SP. DADA2: High-resolution sample inference from Illumina amplicon data. *Nature Methods* 2016; **13**: 581.

73. Quast C, Pruesse E, Yilmaz P, Gerken J, Schweer T, Yarza P, et al. The SILVA ribosomal RNA gene database project: improved data processing and web-based tools. *Nucleic Acids Research* 2013; **41**: D590–D596.

74. McLaren MR, Callahan BJ. Silva 138.1 prokaryotic SSU taxonomic training data formatted for DADA2. 2021.

75. Spohn M, Klaus K, Wanek W, Richter A. Microbial carbon use efficiency and biomass turnover times depending on soil depth – Implications for carbon cycling. *Soil Biology and Biochemistry* 2016; **96**: 74–81.

76. R Core Team. R: A language and environment for statistical computing. http://www.R-project.org/. *R Foundation for Statistical Computing, Vienna, Austria*.

77. McMurdie PJ, Holmes S. phyloseq: An R Package for Reproducible Interactive Analysis and Graphics of Microbiome Census Data. *PLoS One* 2013; **8**: e61217.

78. Davis NM, Proctor DM, Holmes SP, Relman DA, Callahan BJ. Simple statistical identification and removal of contaminant sequences in marker-gene and metagenomics data. *Microbiome* 2018; **6**: 226.

79. Morrissey EM, Mau RL, Schwartz E, McHugh TA, Dijkstra P, Koch BJ, et al. Bacterial carbon use plasticity, phylogenetic diversity and the priming of soil organic matter. *The ISME Journal* 2017; **11**: 1890–1899.

80. Papp K, Hungate BA, Schwartz E. Glucose triggers strong taxon-specific responses in microbial growth and activity: insights from DNA and RNA qSIP. *Ecology* 2020; **101**: e02887.

81. Metze D, Schnecker J, Canarini A, Fuchslueger L, Koch BJ, Stone BW, et al. R code and data (Metze et al., 2023 Nature Communications). 2023. Zenodo. https://zenodo.org/records/8109566.

82. Li J, Mau RL, Dijkstra P, Koch BJ, Schwartz E, Liu X-JA, et al. Predictive genomic traits for bacterial growth in culture versus actual growth in soil. *The ISME Journal* 2019; **13**: 2162–2172.

83. Oksanen J, Blanchet FG, Friendly M, Kindt R, Legendre P, McGlinn D, et al. Vegan: Community Ecology Package. R Package Version. 2.5-6. *http://CRANR-project.org/package=vegan* 2019.

84. Barlow JT, Bogatyrev SR, Ismagilov RF. A quantitative sequencing framework for absolute abundance measurements of mucosal and lumenal microbial communities. *Nature Communications* 2020; **11**: 2590.

85. Andersen KS, Kirkegaard RH, Karst SM, Albertsen M. ampvis2: an R package to analyse and visualise 16S rRNA amplicon data. *bioRxiv* 2018; 299537.

Acknowledgments

Acknowledgments: We thank Jasmin Schwarz and Gudrun Kohl for 16S rRNA gene amplification and sequencing. We also thank Joana Senéca Silva for handling the submission of the sequencing data to the NCBI Short-Read Archive and Leila Hadziabdic for optimizing the conditions for 16S rRNA gene amplification using ddPCR. Furthermore, we thank Stephanie Eichorst for her support with the ultracentrifuge and Páll Sigurðsson for his help during sampling. We also thank Amir Hamedpour and Svarmi for the permission to use their drone footage.

Funding: D. Metze, C. Le Noir de Carlan, and B. Bhattarai were financially supported by FutureArctic, a European Union's Horizon 2020 research and innovation program under the Marie Skłodowska-Curie Actions (grant no. 813114).

Author contributions: DM, AR, CK, EV, and IO conceived the study, and BDS, IJ, and AR established the field site. DM, CLNDC, and BB carried out fieldwork. DM, JS, and CLNDC performed the lab experiments. DM performed data analyses. BH processed the raw amplicon sequencing data. DM and AR drafted the manuscript. All co-authors contributed to the revision of the manuscript.

Competing interests: The authors declare that they have no competing interests.

Data and materials availability: All code and data used to produce the analyses and figures of this study are openly available in the Zenodo database under accession code 10115521 [http://doi.org/10.5281/zenodo.10115521.]. DNA sequence data generated in the frame of this study have been deposited in the NCBI Short-Read Archive under the BioProject accession number PRJNA1013122 [https://www.ncbi.nlm.nih.gov/bioproject/?term= PRJNA1013122].

Supplementary Material

Table S1: Soil parameters, potential extracellular enzyme activities, ^{18}O enrichment of DNA, and total 16S rRNA gene copies across core types and warming levels (means ± SD)

	Ambient					
	Undisturbed Ambient		**Roots Ambient**		**No roots Ambient**	
	Mean ± SD (n=4)		Mean ± SD (n=4)		Mean ± SD (n=4)	
DOC (mgC/g dry soil)	0,03	0,01	0,03	0,01	0,03	0,02
TDN (mgN/g dry soil)	0	0	0,01	0	0,01	0,01
Cmic (mgC/g dry soil)	0,37	0,12	0,47	0,1	0,54	0,16
Nmic (mgN/g dry soil)	0,04	0,01	0,07	0,02	0,09	0,02
Exoglucanase (nmol/ h / g dry soil/ mg Cmic)	460,73	133,14	362,21	179,12	201,08	98,47
Exochitinase (nmol/ h / g dry soil/ mg Cmic)	1518,44	408,81	574,87	165,16	432,44	238,04
Phosphatase (nmol/ h / g dry soil/ mg Cmic)	7306,6	1727,18	3931,25	703,59	3202,74	1318,93
Protease (nmol/ h / g dry soil/ mg Cmic)	108,83	47,63	93,43	55,07	90,13	16,87
Total N (mgN/g dry soil)	0,29	0,03	0,37	0,08	0,34	0,03
Total C (mgC/g dry soil)	3,07	0,47	3,7	0,64	3,67	0,27
Soil water content (% /g fresh soil)	38,02	2,63	41,75	2,35	43,37	2,79
APE ^{18}O DNA	0,02241	0,00922	0,02509	0,01692	0,02186	0,00917
16S gene copies (copies/ g dry soil)	4,53E+09	7,16E+08	4,29E+09	2,33E+09	4,60E+09	1,39E+09
	Warmed					
	Undisturbed +6°C		**Roots +6°C**		**No roots +6°C**	
	Mean ± SD (n=4)		Mean ± SD (n=4)		Mean ± SD (n=4)	
DOC (mgC/g dry soil)	0,01	0	0,02	0,02	0,03	0,02
TDN (mgN/g dry soil)	0	0	0,01	0,01	0,01	0,01
Cmic (mgC/g dry soil)	0,5	0,31	0,41	0,15	0,41	0,11
Nmic (mgN/g dry soil)	0,06	0,04	0,08	0,02	0,08	0,02
Exoglucanase (nmol/ h / g dry soil/ mg Cmic)	426,85	247,97	668,14	186,95	443,93	297,5
Exochitinase (nmol/ h / g dry soil/ mg Cmic)	1277,39	1164,43	1214,27	127,06	879,63	312,78
Phosphatase (nmol/ h / g dry soil/ mg Cmic)	7527,75	5991,95	6386,58	1797	5021,04	4328,72
Protease (nmol/ h / g dry soil/ mg Cmic)	91,4	50,43	155,17	65,19	105,94	52,85
Total N (mgN/g dry soil)	0,26	0,07	0,27	0,05	0,29	0,08
Total C (mgC/g dry soil)	2,78	1,26	2,86	0,5	2,96	0,92
Soil water content (% /g fresh soil)	35,59	5,72	35,39	1,87	38,04	2,09
APE ^{18}O DNA	0,03129	0,00862	0,03747	0,02531	0,03897	0,02030
16S gene copies (copies/ g dry soil)	5,46E+09	1,49E+09	4,91E+09	2,68E+09	4,49E+09	2,27E+09

DOC: Dissolved organic carbon; TDN: Total dissolved nitrogen; Cmic: Microbial biomass carbon; Nmic: Microbial biomass nitrogen.

Table S2: List of measured extracellular enzymes including associated functions and used substrates.

Enzyme	Enzyme function	Substrate
Exoglucanase (cellobiosidase)	Release of cellobioside from cellulose	4-Methylumbelliferyl β-Dcellobioside
Exochitinase (N-acetyl-βglucosaminidase)	Chitin decgradation	4-Methylumbelliferyl N-acetyl-β-Dglucosaminide
LeucineAminopeptidase (Protease)	Protein and peptide degradation	L-Leucine-7-amido-4-methylcoumarin
Acid Phosphatase	Releases inorganic P from organic phosphorus	4-Methylumbelliferyl phosphate

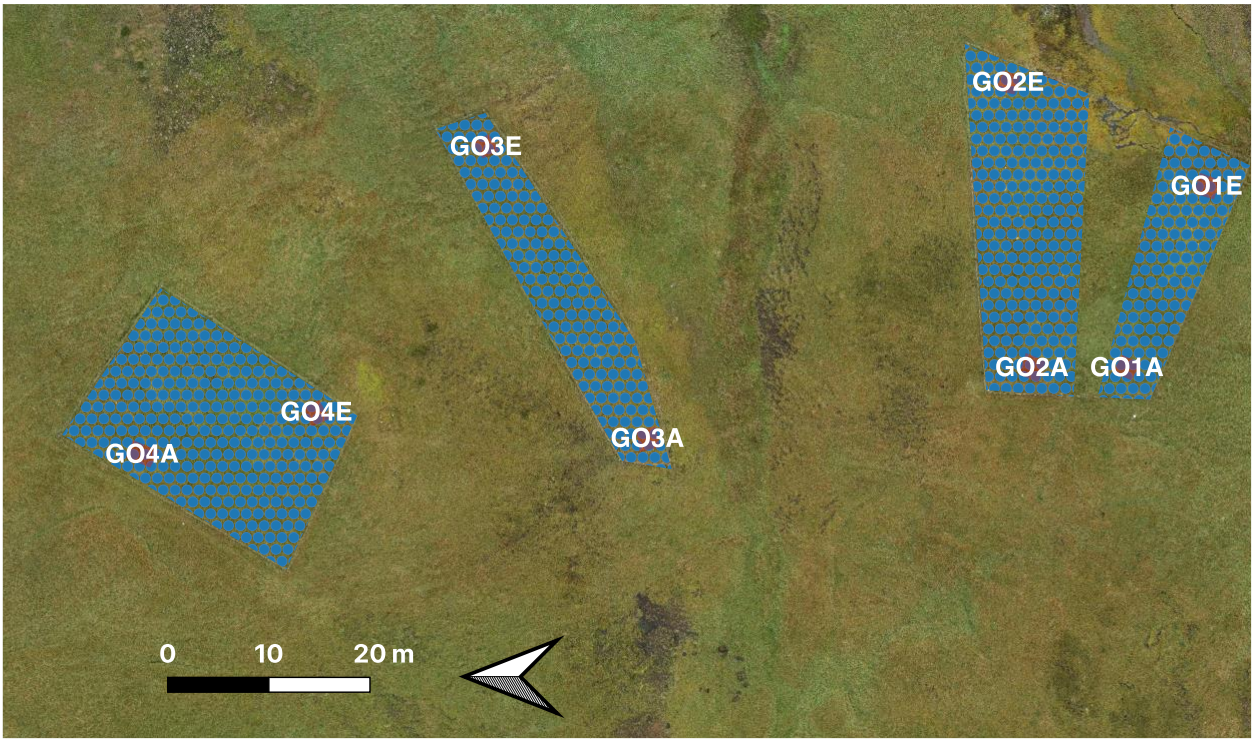

Figure S1: **Aerial image of the long-term warmed field site**. Four replicated grasslands (GO1-4 = biological replicates) were geothermally warmed for > 50 years and located in the Grændalur valley close to Hveragerði, Iceland. The average distance between warmed (E = + °6C) and ambient plots (A) was 24.8 ± 7.2 m (mean ± standard deviation, min = 17.8, max= 33). The arrow indicates the direction of the north. The drone image was provided by Amir Hamedpour (Svarmi, Agricultural University of Iceland) and included with his permission.

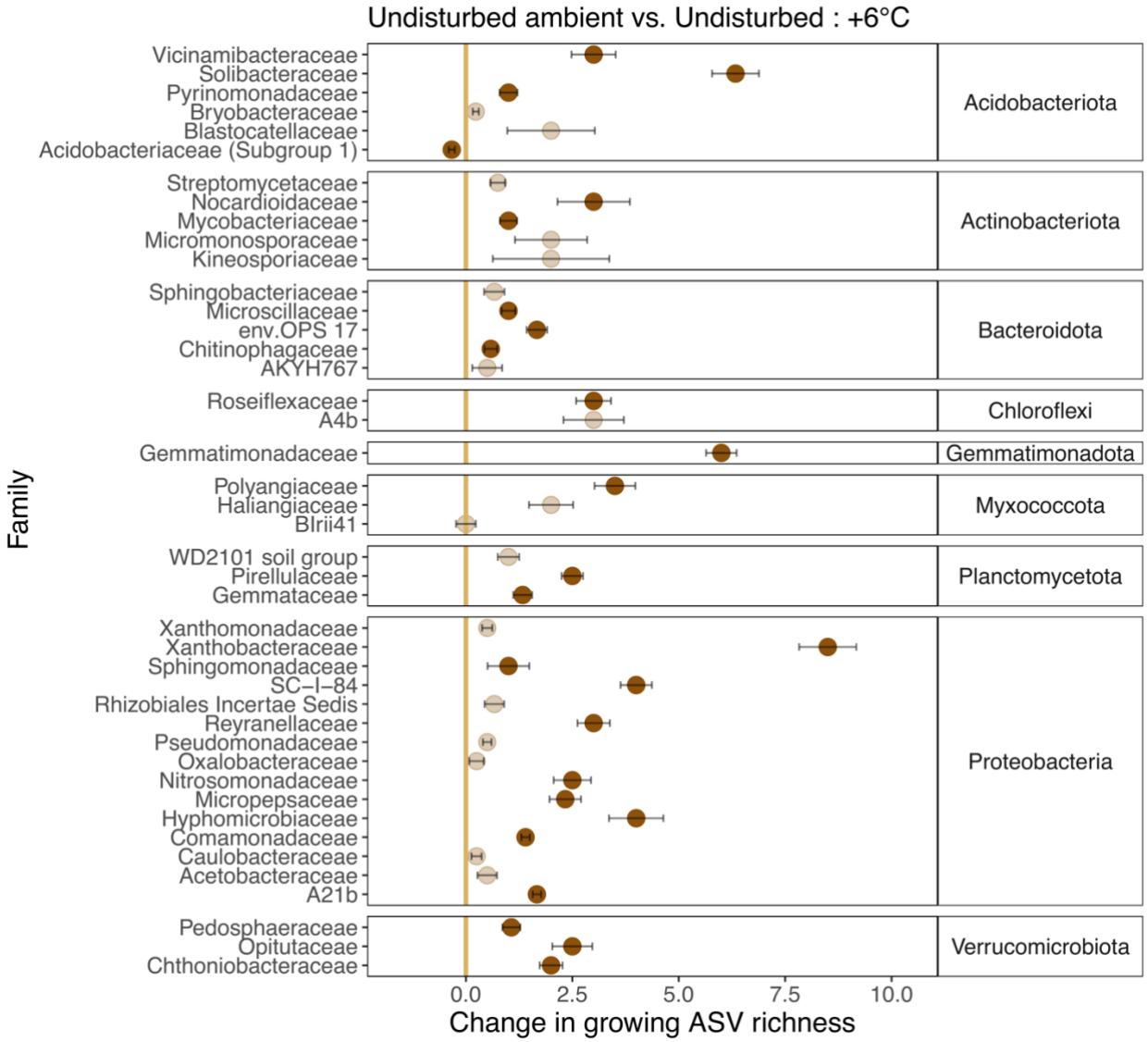

Figure S2: **Family-level changes in the number of growing taxa in undisturbed cores in response to long-term warming**. Points represent relative changes (0 = no change, 1 = increase by 100 %) in the number of growing taxa per family including standard errors. Bold colored points denote significant shifts (Kruskal-Wallis test and false detection rate (fdr) correction for multiple comparisons, n= 4 biological replicates) and transparent points non-significant ones. The vertical line depicts the mean of the reference treatment (Undistributed core at ambient conditions) used to calculate relative changes.

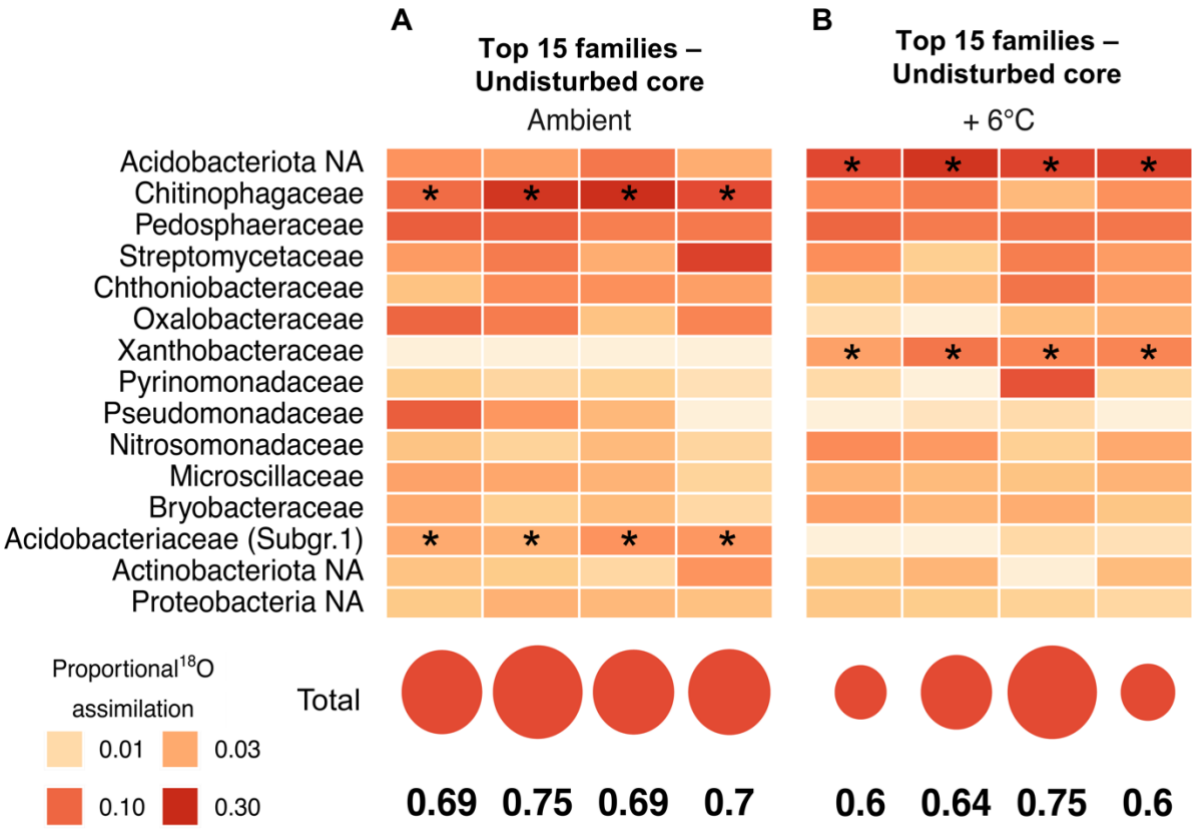

Figure S3: Proportional ^{18}O assimilation of the top 15 families in undisturbed cores. Heatmap showing the top 15 families based on their proportional ^{18}O assimilation in undisturbed cores at ambient (A) and long-term warmed conditions (B). Individual boxes represent replicates per treatment (n= 4 biological replicates). Proportional ^{18}O assimilation ranges from 0 - 1 and estimates how much a single taxon contributes to the total community's growth. It was calculated using re-computed relative abundances of only growing taxa (sum: relative abundances growing taxa = 1) and their relative growth rates (RGR). Proportional ^{18}O assimilation was then agglomerated at the family level and visualized for the top 15 families. Hence, proportional ^{18}O assimilation can be considered as the proportion of bacterial growth a family was responsible for. If family identity could not be assigned (NA), phylum names were provided. Bubbles below each replicate box show the cumulative growth summarized over all displayed families. Asterisks represent significant differences between ambient or warmed conditions based on Wilcoxon rank tests using false detection rate (fdr) correction for multiple comparisons (n= 4).

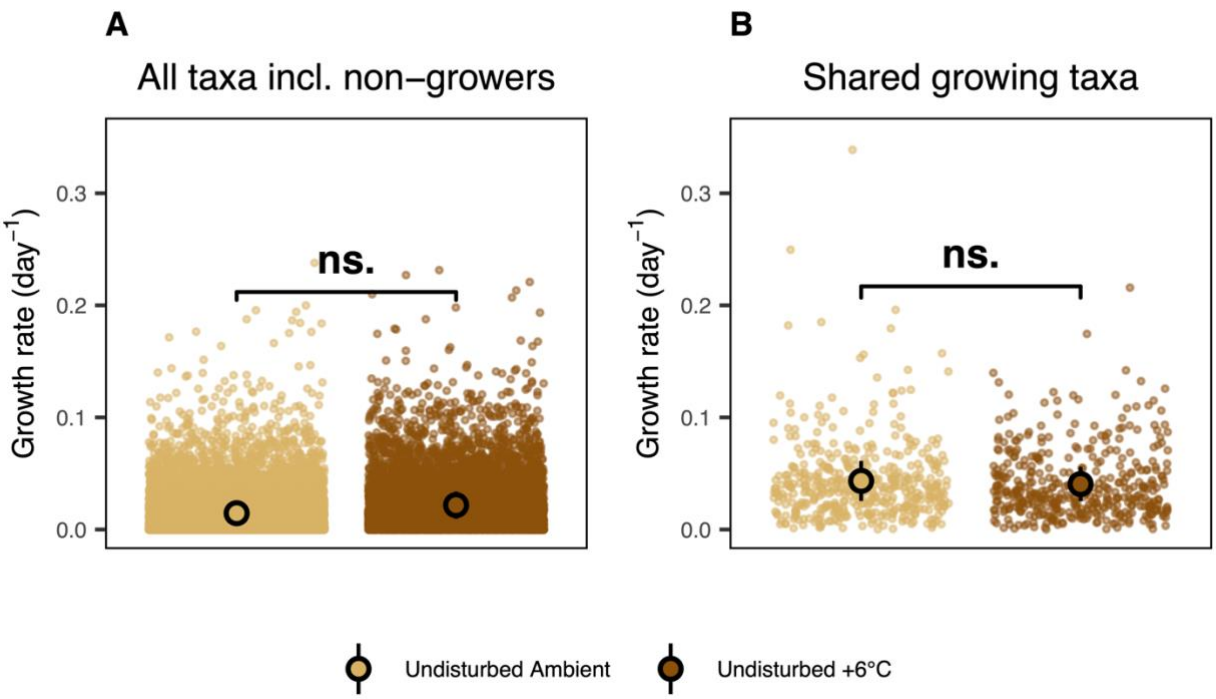

Figure S4: Mean taxon-specific growth rates in undisturbed cores did not change with long-term warming when accounting for inactive taxa or focusing taxa growing at both temperature levels. (A) Mean taxon-specific growth rates including active (APE $^{18}O > 0$) and inactive taxa (APE $^{18}O < 0$) that passed prevalence filtering. (B) Mean taxon-level growth rates of taxa growing at ambient as well as warmed conditions (shared taxa). Statistics (n=4 biological replicates) were inferred from two-way ANOVA (factors: Warming $_{ambient/\ +6°C}$, Core $_{undisturbed/\ root\ ingrowth/\ root\ exclusion}$) followed by Tukey post hoc tests (A) or two-sided Student's t-test (B). Points represent means and error bars standard errors. Small points represent taxon-specific growth rates.

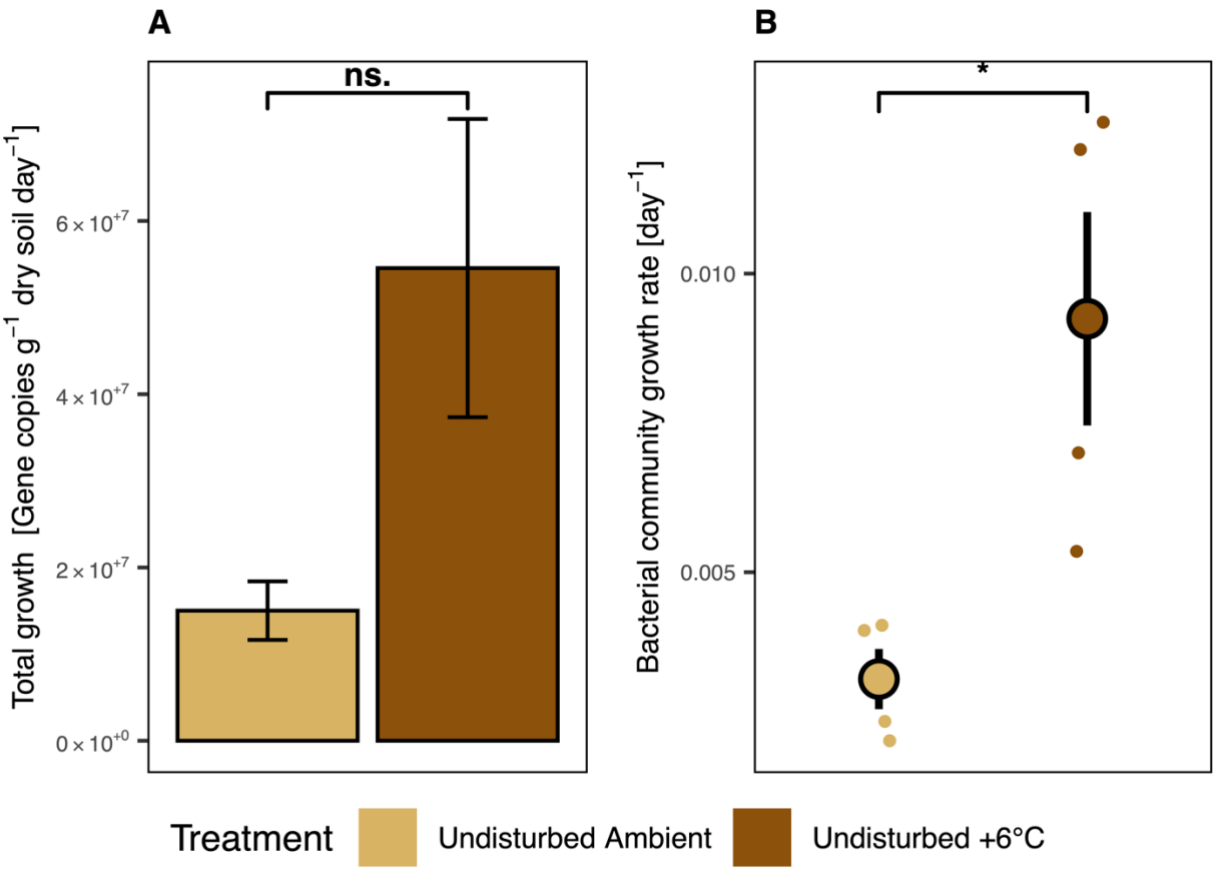

Figure S5: Total and relative bacterial growth increased with long-term warming. (A) Total bacterial growth, expressed as the amount of produced 16S rRNA gene copies per gram of dry soil per day summed across all growing taxa (Relative growth rate $(RGR)_{ASV}$ * 16S rRNA gene copies per g dry soil $_{ASV}$). (B) Relative growth rates of the growing bacterial community (bacterial mass-specific growth), calculated by dividing total bacterial growth (16S rRNA gene copies g $^{-1}$ dry soil day $^{-1}$) by total bacterial community size [16S rRNA gene copies g $^{-1}$ dry soil]). Bars and large points represent means including standard errors (error bars). Small points represent individual samples. Statistics (n=4 biological replicates) were inferred from two-way ANOVA (factors: Warming $_{ambient/\ +6°C}$, Core $_{undisturbed/\ root\ ingrowth/\ root\ exclusion}$) followed by Tukey post hoc tests.

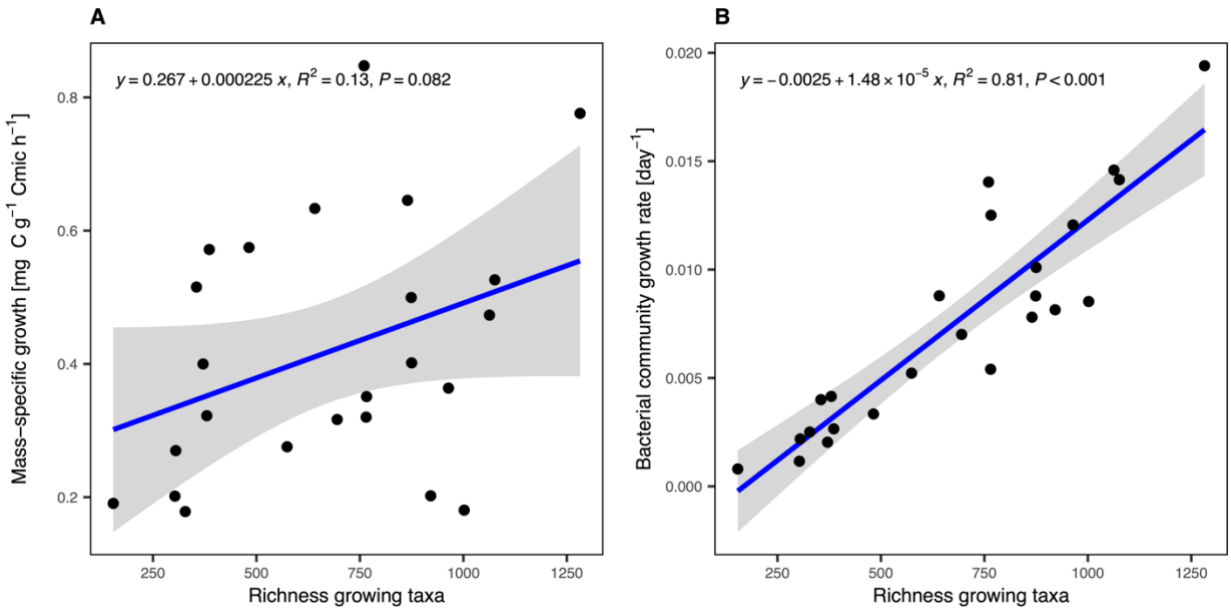

Figure S6: Total microbial and bacterial community growth increases with the number of growing taxa. Comparison of relative community growth (mass-specific) of the total microbial (A, based on DNA content and ^{18}O enrichment of DNA, also including fungi) and only the bacterial community (B) with the richness of growing taxa across all samples (n = 24). The trend line shows the best fit from a linear regression including its equation and statistic results.

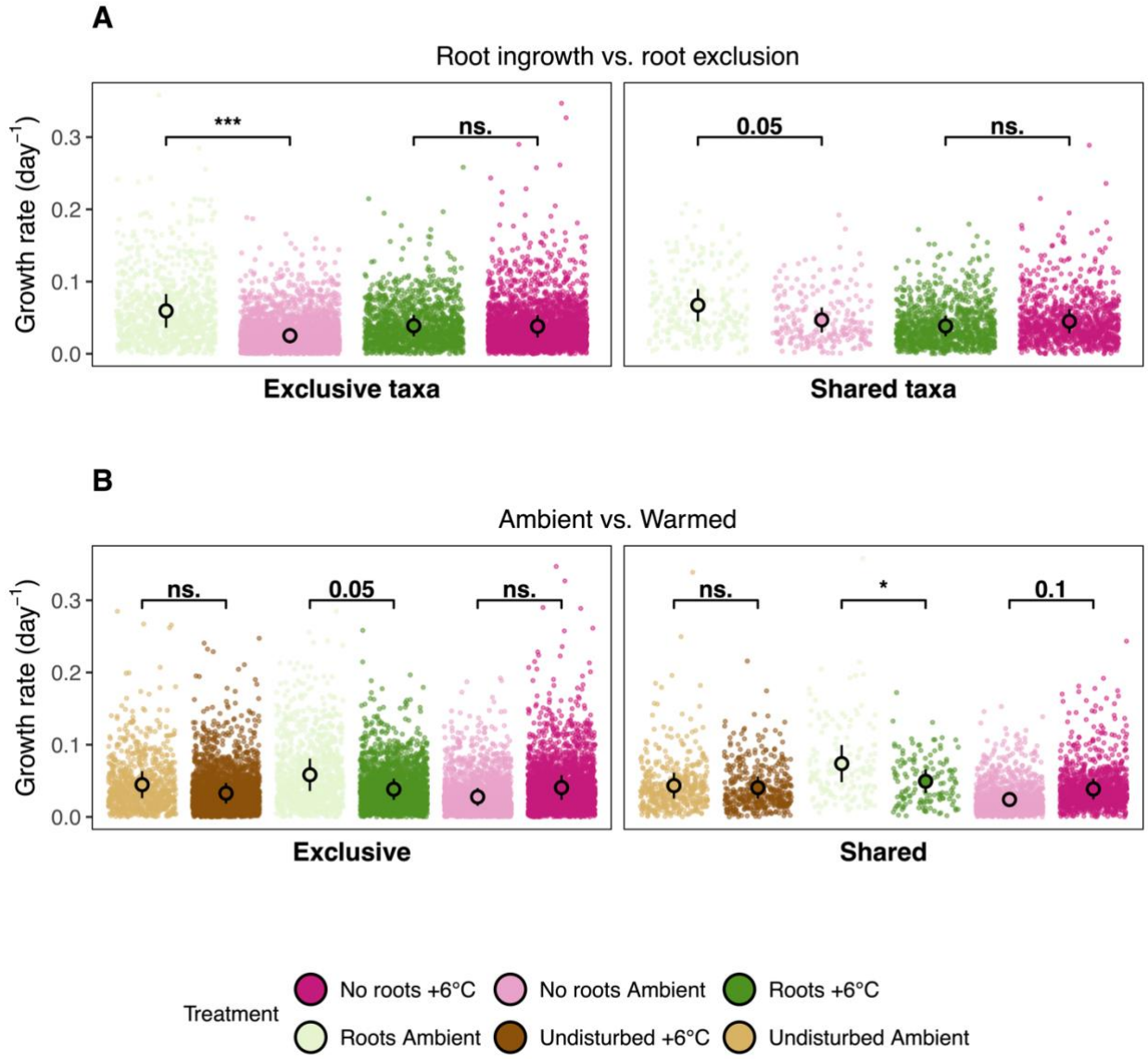

Figure S7: Comparison of mean growth rates of taxa shared between treatment pairs or exclusively active in either one of them. (A) Mean taxon-specific growth rates of taxa exclusively growing in the presence or absence of roots (left panel) and of taxa growing in the presence of both (right panel), determined for ambient and warmed temperatures, respectively. Asterisks reflect statistics (n=4 biological replicates) inferred by three-way ANOVA, (factors: Warming $_{\text{ambient/ +6°C}}$, Core $_{\text{root ingrowth/ root exclusion}}$, Experiment $_{\text{undisturbed cores, in situ cores}}$) followed by Tukey post hoc tests. (B) Mean taxon-specific growth rates of taxa exclusively growing at either ambient or warmed temperatures (left panel) and of taxa growing at both temperature regimes (right panel), determined for each core type, respectively. Asterisks reflect statistics (n=4 biological replicates) inferred by three-way ANOVA, (factors: Warming $_{\text{ambient/ +6°C}}$, Core $_{\text{root ingrowth/ root exclusion}}$, Experiment $_{\text{undisturbed cores, in situ cores}}$) followed by Tukey post hoc tests. Points represent means and error bars standard errors.

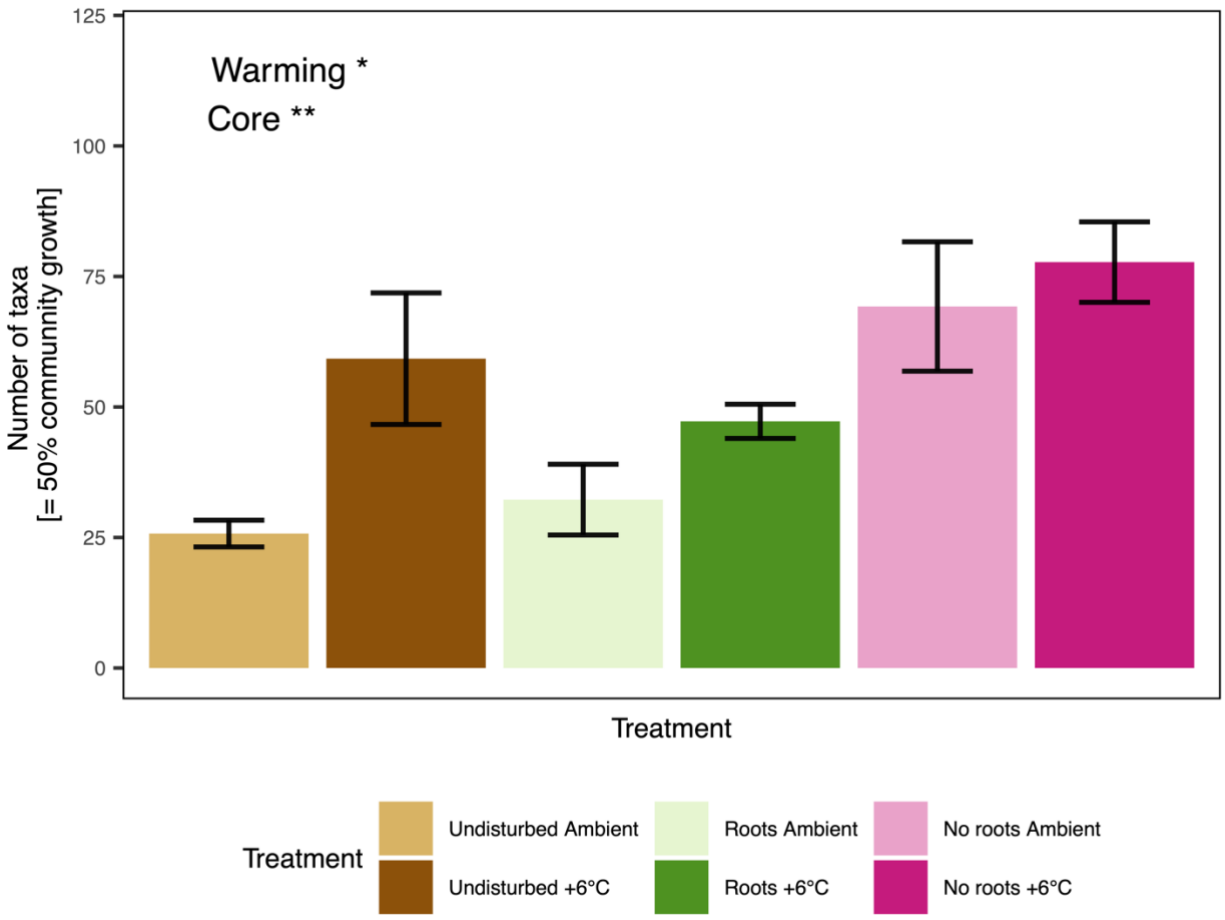

Figure S8: Number of taxa responsible for 50% of the community's growth. Taxa were ranked according to their proportional ^{18}O assimilation in descending order until cumulative growth reached 50%. Bars represent means and error bars standard errors (n= 4 biological replicates). Statistics are derived from two-way ANOVA (Warming: F= 7.4, p= 0.01; Core: F= 9.69, p= 0.001; factors: Warming $_{\text{ambient/ +6°C}}$, Core $_{\text{undisturbed/ root ingrowth/ root exclusion}}$).

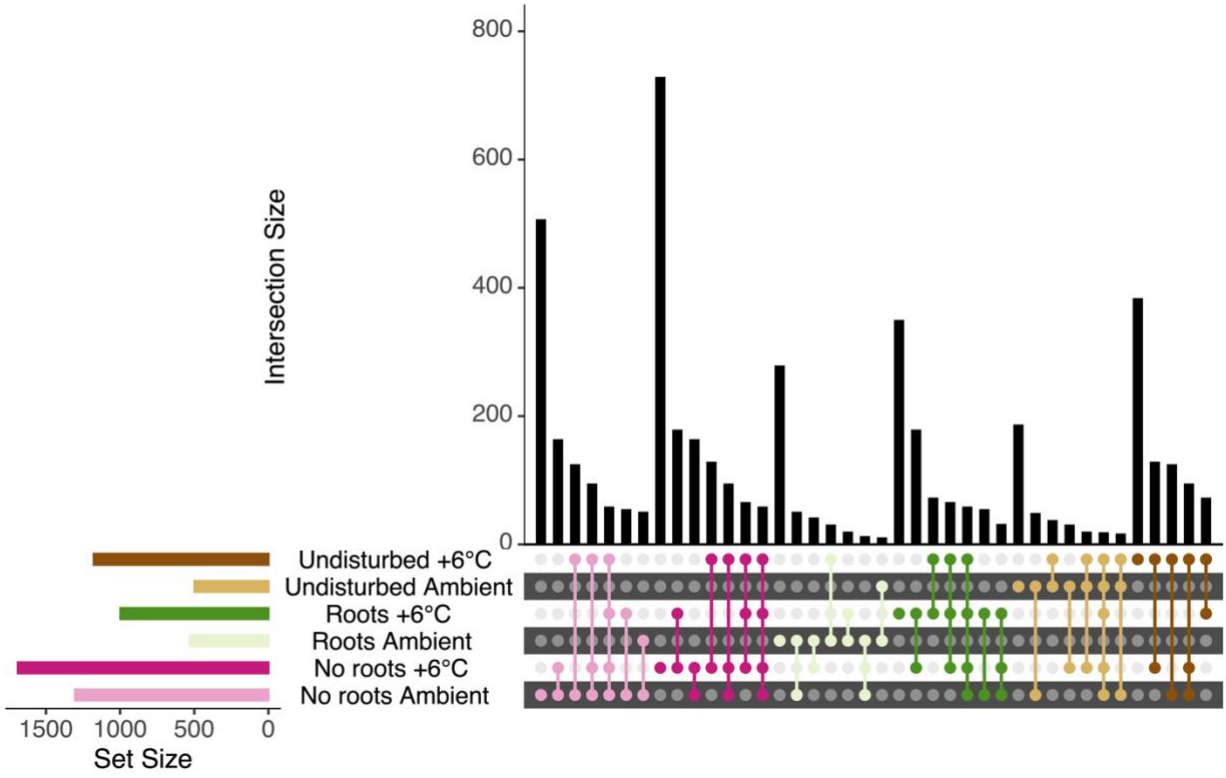

Figure S9: Upset plot showing the number of shared and unique taxa among soil core types and warming levels. Each vertical line represents a unique combination of treatments, and the size of the bar indicates the number of shared taxa for each subset of treatments. The bars the left indicate the total number of taxa per treatment. The plot shows that a significant portion of the growing taxa across treatments consists of unique taxa.

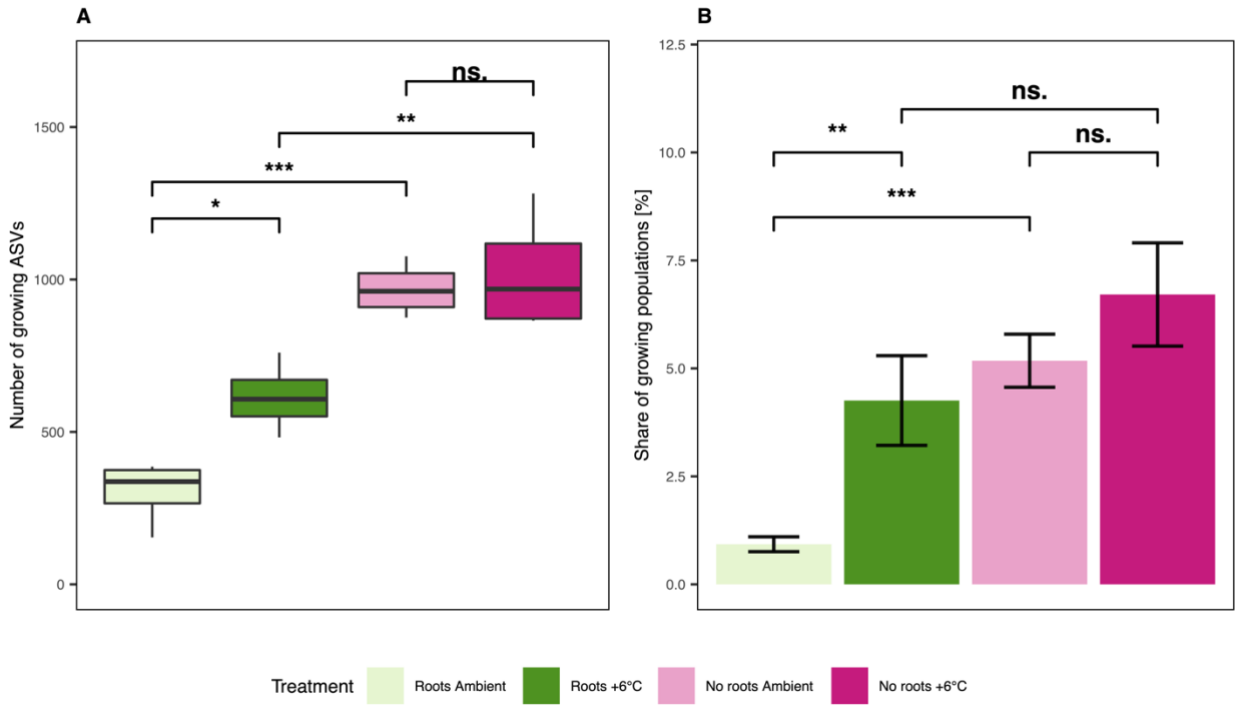

Figure S10: Diversity and relative size of growing communities of root ingrowth and exclusion cores. (A) The number of unique growing amplicon sequence variants (ASVs) The median is represented by the center line of the box, while the upper and lower quartiles are indicated by the box limits. The whiskers represent 1.5 times the interquartile range; any outliers are shown as separate points. (B) The proportion of growing taxa of the total community expressed as the percentage of 16S rRNA gene copies. Bars represent means and error bars standard errors. Asterisks reflect statistics (n=4 biological replicates) inferred by two-way ANOVA (Table 2, factors: Warming $_{\text{ambient/ +6°C}}$, Core $_{\text{undisturbed/ root ingrowth/ root exclusion}}$) followed by Tukey post hoc tests.


A
Top taxa 25 – Root ingrowth cores
Ambient
Warmed
Roots
No roots
Roots
No roots
Alkanindiges ASV 499
Alkanindiges ASV 500
Actinobacteriota NA NA ASV 12
Alkanibacter ASV 503
Marmoricola ASV 510
Elusimicrobiota NA NA ASV 99
Kitasatospora ASV 5
Puia ASV 203
Puia ASV 62
Cytophaga ASV 546
Cytophaga ASV 555
Microscillaceae NA ASV 245
Bryobacter ASV 771
Pseudomonas ASV 2264
Bradyrhizobium ASV 1055
Bryobacter ASV 1010
Pseudomonas ASV 1
BIrii41 NA ASV 23
Microscillaceae NA ASV 2713
Xanthobacteraceae NA ASV 994
Chitinophagaceae NA ASV 2719
Microscillaceae NA ASV 1589
RB41 ASV 2731
Candidatus Udaeobacter ASV 1279
Collimonas ASV 2
0.18 0.2 0.16 0.31 0.07 0.05 0.16 0.09 0.18 0.16 0.24 0.21 0.07 0.08 0.19 0.22
Proportional 18O assimilation
0.01
0.03
0.10
0.30
B
Top taxa 25 – Root exclusion cores
Ambient
Warmed
Roots
No roots
Roots
No roots
Alkanibacter ASV 503
Acidobacteriota NA NA ASV 989
Micropepsaceae NA ASV 992
Xanthobacteraceae NA ASV 994
env.OPS 17 NA ASV 995
Actinobacteriota NA NA ASV 12
env.OPS 17 NA ASV 1003
Bryobacter ASV 1004
Bryobacter ASV 1010
Acidobacteriota NA NA ASV 1012
Alkanindiges ASV 499
BIrii41 NA ASV 23
Bradyrhizobium ASV 1055
Alkanindiges ASV 500
Collimonas ASV 2
Microscillaceae NA ASV 1589
Kitasatospora ASV 5
Pseudomonas ASV 1
env.OPS 17 NA ASV 1940
Cytophaga ASV 546
Pseudomonas ASV 2264
AKYH767 NA ASV 2073
Chitinophagaceae NA ASV 2719
Microscillaceae NA ASV 2713
Cytophaga ASV 555
0.15 0.01 0.08 0.29 0.12 0.15 0.3 0.28 0.17 0.1 0.21 0.19 0.09 0.09 0.26 0.26

Figure S11: The dominance of certain taxa is affected by whether roots or no roots are present. Heatmap showing taxa (amplicon sequence variants, ASVs) with the highest proportional ^{18}O assimilation across root ingrowth (ambient & warmed, A) and root exclusion cores (ambient & warmed, B) conditions, visualized across individual samples (boxes, n=4). Proportional ^{18}O assimilation is calculated using re-computed relative abundances of only growing taxa (sum: relative abundances $_{growing\ taxa}$ = 1) and their relative growth rates (RGR). Proportional ^{18}O assimilation can be considered as the proportion of bacterial growth an ASV is responsible for. ASVs were ranked based on their proportional ^{18}O assimilation per replicate. After retaining the top 15 ASVs across all replicates per treatment (total $_{root\ ingrowth}$: 94 ASVs, total $_{root\ exclusion}$: 80 ASVs), we visualized the top 25 ASVs using heatmaps. Bubbles below each replicate show the cumulative growth summarized over all displayed ASVs. ASVs were only considered if they were growing in at least two samples per treatment. If genus or family identity could not be assigned (NA), phylum names were provided.

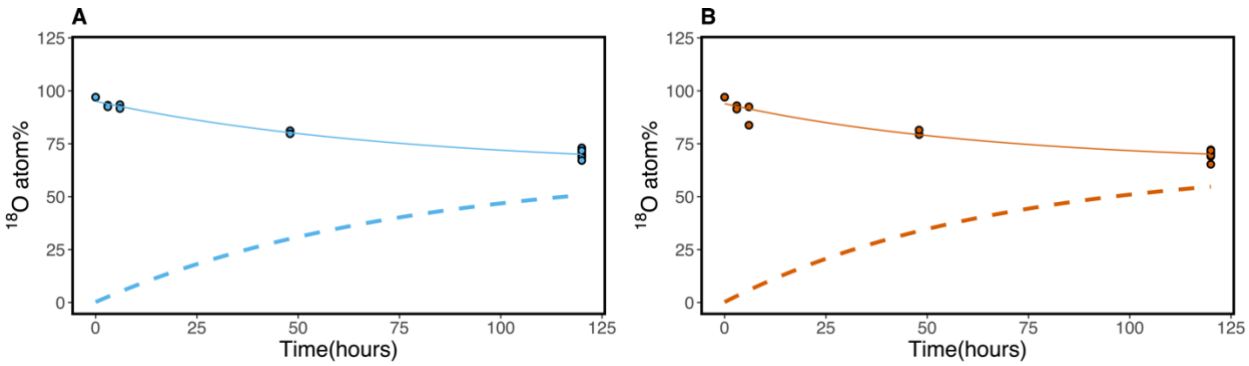

Figure S12: Development of ^{18}O soil water enrichment over the incubation period of five days at ambient temperatures (A, 10.7 °C) and + 6 °C of warming (B). Soil water enrichment (dashed line) was predicted using a negative exponential model based on the decrease of the measured isotopic label (points, solid line) of the added ^{18}O-water.

Chapter IV

Summary and Synthesis

Summary and Synthesis

Soil microorganisms are the drivers of all biogeochemical processes in soil [1]. Through their activities, they control whether soil organic carbon is sequestered or lost to the atmosphere as CO_2 or CH_4. Despite their crucial role in the climate system, many aspects of the microbial response to drought, warming, and elevated atmospheric CO_2 remain elusive. Open questions include whether different global change factors act in an additive or interactive way in their impact on the soil microbiome. Or how the soil microbiome is shaped by the plant's response to climate change. We also lack an understanding of which part of the soil microbiome is active and growing under different environmental conditions. This includes the growth of individual members of the microbial community as well as their response to the altered conditions in a future climate. This knowledge gap is particularly large for drought-affected soils. In contrast to community-aggregated measurements, taxon-specific data may help us develop a better understanding of the mechanisms behind shifts in microbe-driven processes due to climate change and ultimately improve our ability to predict and manipulate them.

In the frame of this thesis, I aimed to address these questions and knowledge gaps by investigating the growth response of individual populations of bacteria and archaea (hereafter: bacteria) under drought, warming, and elevated atmospheric CO_2. This comprised the development of vapor-qSIP, a non-invasive method to measure in situ taxon-specific growth, and its application to two field climate change experiments located in grasslands in Austria (Chapter 2) and Iceland (Chapter 3).

In Chapter 2, I studied how a severe summer drought (six weeks) affected taxon-specific bacterial growth rates and the composition of the active bacterial community in a current and potential future climate. To this end, I took advantage of the ClimGrass experiment [2–6], located in a montane grassland in Central Austria. It represents a type of managed grassland of agricultural relevance that is typical to wide areas of alpine countries in Europe. ClimGrass is one of the few existing multifactorial climate change experiments where drought is simulated in combination with potential future climate conditions (+ 3 °C, + 300 ppm CO_2). In this study, we were, for the first time, able to measure taxon-specific bacterial growth in dry soils without increasing soil moisture by combining qSIP [7] with the ^{18}O water vapor equilibration method [8] (vapor-qSIP). Drought caused the majority (> 90 %) of bacterial taxa active in control soils to stop growing, reducing the percentage of active taxa in the total

community from 35 % to 4 %. Few bacterial taxa persisted in drought-affected soils but at reduced growth rates. Other taxa increased in abundance and showed strong signs of drought tolerance. The bacterial growth in drought-affected soils was dominated by specific groups of the phylum Actinobacteriota. A single member of the genus *Streptomyces* accounted for 2 – 38 % of the community growth under drought conditions. Six years of pre-exposure to future climate conditions altered the drought response of the growing bacterial community. More taxa persisted in drought-affected soils and the size of the active community (9 %) was more than twice as large as compared to drought simulations in a current climate. Future climate conditions might have pre-conditioned the soil microbiome to drought via more frequent drops in soil moisture in previous years as a consequence of the warming treatment [9] or may have increased plant belowground carbon allocation, at least until the beginning of the drought simulation [10, 11]. Elevated atmospheric CO_2 may have also positively affected the microbial drought response via reduced plant water uptake due to lower stomatal conductance [12]. In our study, pre-exposure to future climate conditions seemed to have improved the drought tolerance of the bacterial community with implications for soil functioning and soil-carbon cycling. This highlights the importance of capturing interactive climate change effects on the soil microbiome to improve predictions of future soil-climate feedbacks.

The main aim of Chapter 3 was to elucidate the bacterial growth response to long-term warming and how it is impacted by indirect warming effects mediated by root-microbe interactions. The research conducted in this chapter was undertaken at the ForHot experiment [13–24] in Southern Iceland where a natural soil temperature gradient developed due to geothermal activity. The studied (Sub)Arctic grassland has experienced sustained soil warming for at least 50 years but probably since 1706 [13]. Consistent with a previous study [17], long-term warming increased the relative growth of the entire microbial community. So far, this has been interpreted as a constant acceleration of microbial activities without signs of thermal acclimation [16]. Focusing on the bacterial community, we observed, in contrast, that the increase in community growth was not associated with generally higher taxon-specific growth rates but a larger number of actively growing taxa. The composition of the total and active bacterial community was significantly different in long-term warmed soils and the community growth was dominated by different taxa. Although many additional taxa

started growing at elevated temperatures (+ 6°C), their growth rates were indistinguishable from the growth rates of taxa active at ambient temperatures. In this study, we also examined shifts in root-microbe interactions with the aid of in situ installed root ingrowth (1 mm mesh) and root exclusion (30 µm mesh) cores that were harvested after 10 months during peak vegetation season. Root presence promoted higher bacterial growth rates at ambient temperatures whereas this effect was lost with long-term warming. The growth rates of putative root-associated taxa even decreased with warming, possibly due to lower belowground carbon allocation indicated by a previously reported reduction in fine root biomass and fine root production in long-term warmed soils [19, 23]. Putative bulk soil-associated taxa seemed to be limited less by substrate availability but more by temperature. Overall, negative warming effects on plant roots may have reduced the carbon supply to root-associated bacteria, restricting the extra energy needed for accelerated growth at elevated temperatures. This underlines the impact of indirect effects on the warming response of soil bacteria but also that their magnitude may differ between taxa with different life history strategies.

In this thesis, I have developed a novel approach (vapor-qSIP) to estimate taxon-specific growth under near in-situ conditions. In chapters 2 and 3, I applied this method to elucidate interactive or indirect climate change effects on the soil microbiome. The population-resolved approach and focus on active bacteria also allowed me to gain new insights into microbial dynamics beyond community-aggregated measurements. Several commonalities were observed between the two studies. Although the conclusions drawn should be treated with caution due to the limited number of experiments and until support from additional studies is available, I present five learnings about the soil microbiome based on the results of this thesis.

1. The composition of the active microbial community reacts more sensitively to environmental change than that of the total microbial community. Effects of future climate conditions and root presence as well as their interaction with drought and warming were only visible when examining the growing subsection of the total community. Shifts in the total community could only be observed in response to warming and drought. Hence, monitoring only the total community composition, as done in most microbiome studies, may lead to

underestimations of climate change effects. This advocates the use of activity-based community composition approaches in future climate change studies.

2. The growth response of individual taxa across different conditions indicates their life history traits. A soil microorganism may only grow when it possesses the traits necessary to thrive in a current environment and becomes inactive when conditions are no longer favorable. Comparatively few taxa were still growing in drought-affected soil, such as members of the genera *Streptomyces*, *Oryzihumus*, *Rhodococcus*, and *Marmoricola*. This suggested that they possess traits that enable drought tolerance, albeit not revealing the nature of these traits. Similarly, members of the Chitinophagaceae performed better in the presence of roots which may indicate that they either live in association with roots or profit indirectly from them. Hence, tracing the growth response of individual taxa across various conditions can narrow the gap between taxonomy and function, especially with a future integration of qSIP with metagenomics [25–27] and metatranscriptomics.

3. The realized growth niche of many microbial taxa is narrow. Many bacterial taxa were only growing in a single climate change treatment although they were often part of the total community in other treatments. For instance, out of 3,553 ASVs that showed growth in at least two replicates, more than two-thirds were exclusively active in only one treatment of the experiment in Austria. A similar pattern, yet less pronounced, was observed in the long-term warmed soils in the (Sub)Arctic. Although most of these taxa were probably rare, this observation suggests that a different subset of bacteria becomes more competitive and starts growing when environmental conditions change. If different taxa become active under different conditions based on their set of traits, mediating soil processes, our findings support that microbial diversity plays an important role for the maintenance of soil functioning with environmental change.

4. The percentage of active bacteria in soil is higher than predicted by the paradigm of largely inactive soil microorganisms. We found that either 4 – 45 % or 1 - 7 % (using a more conservative analysis approach) of the bacterial community was actively growing. This contrasts the existing paradigm in soil microbiology that only 0.5 to a maximum of 2 % of the microbial biomass is active [28]. Here, the share of 16S rRNA gene copies belonging to growing taxa was used to determine the size of the growing community. The use of DNA as a bacterial biomass proxy is debatable, albeit there exists current support for it [29]. Together with

recent data [30–32], this points to a different understanding of microbial activity in soils and the distribution of active soil microbes.

5. Population-resolved data improves the understanding of microbial community dynamics. Drought has been shown to reduce microbial activities such as growth [8] and respiration [33–35] whereas warming has been observed to increase them [17]. An obvious interpretation of these results may be that the same soil microorganisms grow either better or worse when exposed to warming or drought, i.e., they divide faster or slower. However, the actual population dynamics behind these community-aggregated measurements remained a black box, even if combined with analyses of the total community composition. Taxon-specific growth data from our experiments suggests that shifts in microbial processes seem to be associated with changes in the number and identity of growing taxa, manifesting through a fluctuating size of the active community. For instance, long-term warming did not accelerate the average growth rates of bacterial populations but the number of growing taxa and, consequently, total bacterial community growth. Depending on the environment, distinct active communities formed, and microbial growth was dominated by different taxa. Although several taxa persisted in drought-affected soils and showed lower growth rates, many others have become inactive and gave rise to different, probably more competitive, taxa rather than adjusting their growth. This expands our mechanistic understanding of the phenotypic response of the soil microbiome to climate change and the variety of individual reactions behind it.

In summary, I was able to demonstrate which bacteria and archaea might still be growing in future soils that will be increasingly affected by warming, drought, and higher CO_2 concentrations with the ongoing climatic change. This may help us to better predict associated changes in microbial processes and manipulate soil microbiomes to mitigate negative climate change effects.

References

1. Falkowski PG, Fenchel T, Delong EF. The Microbial Engines That Drive Earth's Biogeochemical Cycles. *Science* 2008; **320**: 1034–1039.

2. Simon E, Canarini A, Martin V, Séneca J, Böckle T, Reinthaler D, et al. Microbial growth and carbon use efficiency show seasonal responses in a multifactorial climate change experiment. *Communications biology* 2020; **3**: 1–10.

3. Meeran K, Ingrisch J, Reinthaler D, Canarini A, Müller L, Pötsch EM, et al. Warming and elevated CO2 intensify drought and recovery responses of grassland carbon allocation to soil respiration. *Global Change Biology* 2021; **27**: 3230–3243.

4. Séneca J, Pjevac P, Canarini A, Herbold CW, Zioutis C, Dietrich M, et al. Composition and activity of nitrifier communities in soil are unresponsive to elevated temperature and CO2, but strongly affected by drought. *ISME Journal* 2020; **14**: 3038–3053.

5. Piepho H-P, Herndl M, Pötsch EM, Bahn M. Designing an experiment with quantitative treatment factors to study the effects of climate change. *Journal of Agronomy and Crop Science* 2017; **203**: 584–592.

6. Maxwell TL, Canarini A, Bogdanovic I, Böckle T, Martin V, Noll L, et al. Contrasting drivers of belowground nitrogen cycling in a montane grassland exposed to a multifactorial global change experiment with elevated CO2, warming, and drought. *Global Change Biology* 2022; **28**: 2425–2441.

7. Hungate BA, Mau RL, Schwartz E, Gregory Caporaso J, Dijkstra P, van Gestel N, et al. Quantitative microbial ecology through stable isotope probing. *Applied and Environmental Microbiology* 2015; **81**: 7570–7581.

8. Canarini A, Wanek W, Watzka M, Sandén T, Spiegel H, Šantrůček J, et al. Quantifying microbial growth and carbon use efficiency in dry soil environments via ^{18}O water vapor equilibration. *Global Change Biology* 2020; **26**: 5333–5341.

9. Reinthaler D, Harris E, Pötsch EM, Herndl M, Richter A, Wachter H, et al. Responses of grassland soil CO2 production and fluxes to drought are shifted in a warmer climate under elevated CO2. *Soil Biology and Biochemistry* 2021; **163**: 108436.

10. Preece C, Peñuelas J. Rhizodeposition under drought and consequences for soil communities and ecosystem resilience. *Plant and Soil* 2016; **409**: 1–17.

11. de Vries FT, Williams A, Stringer F, Willcocks R, McEwing R, Langridge H, et al. Changes in root-exudate-induced respiration reveal a novel mechanism through which drought affects ecosystem carbon cycling. *New Phytologist* 2019; **224**: 132–145.

12. Leakey ADB, Bernacchi CJ, Dohleman FG, Ort DR, Long SP. Will photosynthesis of maize (Zea mays) in the US Corn Belt increase in future [CO2] rich atmospheres? An analysis of diurnal courses of CO2 uptake under free-air concentration enrichment (FACE). *Global Change Biology* 2004; **10**: 951–962.

13. Sigurdsson BD, Leblans NIW, Dauwe S, Gudmundsdóttir E, Gundersen P, Gunnarsdóttir GE, et al. Geothermal ecosystems as natural climate change experiments: The ForHot research site in Iceland as a case study. *Icelandic Agricultural Sciences* 2016; **29**: 53–71.

14. Walker TWN, Janssens IA, Weedon JT, Sigurdsson BD, Richter A, Peñuelas J, et al. A systemic overreaction to years versus decades of warming in a subarctic grassland ecosystem. *Nature Ecology & Evolution* 2020; **4**: 101–108.

15. Söllinger A, Séneca J, Borg Dahl M, Motleleng LL, Prommer J, Verbruggen E, et al. Down-regulation of the bacterial protein biosynthesis machinery in response to weeks, years, and decades of soil warming. *Science Advances* 2022; **8**: eabm3230.

16. Poeplau C, Kätterer T, Leblans NIW, Sigurdsson BD. Sensitivity of soil carbon fractions and their specific stabilization mechanisms to extreme soil warming in a subarctic grassland. *Global Change Biology* 2017; **23**: 1316–1327.

17. Walker TWN, Kaiser C, Strasser F, Herbold CW, Leblans NIW, Woebken D, et al. Microbial temperature sensitivity and biomass change explain soil carbon loss with warming. *Nature Climate Change* 2018; **8**: 885–889

18. Marañón-Jiménez S, Peñuelas J, Richter A, Sigurdsson BD, Fuchslueger L, Leblans NIW, et al. Coupled carbon and nitrogen losses in response to seven years of chronic warming in subarctic soils. *Soil Biology and Biochemistry* 2019; **134**: 152–161.

19. Fang C, Verbrigghe N, Sigurdsson BD, Ostonen I, Leblans NIW, Marañón-Jiménez S, et al. Decadal soil warming decreased vascular plant above and belowground production in a subarctic grassland by inducing nitrogen limitation. *New Phytologist* 2023; **240**: 565–576.

20. Marañón-Jiménez S, Soong JL, Leblans NIW, Sigurdsson BD, Peñuelas J, Richter A, et al. Geothermally warmed soils reveal persistent increases in the respiratory costs of soil microbes contributing to substantial C losses. *Biogeochemistry* 2018; **138**: 245–260.

21. Verbrigghe N, Leblans NIW, Sigurdsson BD, Vicca S, Fang C, Fuchslueger L, et al. Soil carbon loss in warmed subarctic grasslands is rapid and restricted to topsoil. *Biogeosciences* 2022; **19**: 3381–3393.

22. Radujkovic D, Verbruggen E, Sigurdsson BD, Leblans NIW, Janssens IA, Vicca S, et al. Prolonged exposure does not increase soil microbial community compositional response to warming along geothermal gradients. *FEMS Microbiology Ecology* 2018; **94**.

23. Bhattarai B, Sigurdsson BD, Sigurdsson P, Leblans N, Janssens I, Meynzer W, et al. Soil warming duration and magnitude affect dynamics of fine roots and rhizomes and associated C and N pools in subarctic grasslands. *Annals of Botany* 2023; **132**: 269–279.

24. Séneca J, Söllinger A, Herbold CW, Pjevac P, Prommer J, Verbruggen E, et al. Increased microbial expression of organic nitrogen cycling genes in long-term warmed grassland soils. *ISME Communications* 2021; **1**: 69.

25. Alex G, Ella S, Olivier Z, J. KB, M. FM, A. KJ, et al. Quantitative Stable-Isotope Probing (qSIP) with Metagenomics Links Microbial Physiology and Activity to Soil Moisture in Mediterranean-Climate Grassland Ecosystems. *mSystems* 2022; **7**: e00417-22.

26. Starr EP, Shi S, Blazewicz SJ, Koch BJ, Probst AJ, Hungate BA, et al. Stable-Isotope-Informed, Genome-Resolved Metagenomics Uncovers Potential Cross-Kingdom Interactions in Rhizosphere Soil. *mSphere* 2021; **6**: e00085-21.

27. Sieradzki ET, Morando M, Fuhrman JA. Metagenomics and Quantitative Stable Isotope Probing Offer Insights into Metabolism of Polycyclic Aromatic Hydrocarbon Degraders in Chronically Polluted Seawater. *mSystems* 2021; **6**: e00245-21.

28. Blagodatskaya E, Kuzyakov Y. Active microorganisms in soil: Critical review of estimation criteria and approaches. *Soil Biology and Biochemistry* 2013; **67**: 192–211.

29. Čapek P, Choma M, Kaštovská E, Tahovská K, Glanville HC, Šantrůčková H. Revisiting soil microbial biomass: Considering changes in composition with growth rate. *Soil Biology and Biochemistry* 2023; **184**: 109103.

30. Couradeau E, Sasse J, Goudeau D, Nath N, Hazen TC, Bowen BP, et al. Probing the active fraction of soil microbiomes using BONCAT-FACS. *Nature Communications* 2019; **10**: 1–10.

31. Foley MM, Blazewicz SJ, McFarlane KJ, Greenlon A, Hayer M, Kimbrel JA, et al. Active populations and growth of soil microorganisms are framed by mean annual precipitation in three California annual grasslands. *Soil Biology and Biochemistry* 2023; **177**: 108886.

32. Papp K, Mau RL, Hayer M, Koch BJ, Hungate BA, Schwartz E. Quantitative stable isotope probing with H218O reveals that most bacterial taxa in soil synthesize new ribosomal RNA. *The ISME Journal* 2018; **12**: 3043–3045.

33. Zhou G, Zhou X, Liu R, Du Z, Zhou L, Li S, et al. Soil fungi and fine root biomass mediate drought-induced reductions in soil respiration. *Functional Ecology* 2020; **34**: 2634–2643.

34. Ingrisch J, Karlowsky S, Hasibeder R, Gleixner G, Bahn M. Drought and recovery effects on belowground respiration dynamics and the partitioning of recent carbon in managed and abandoned grassland. *Global Change Biology* 2020; **26**: 4366–4378.

35. Kang E, Li Y, Zhang X, Yan Z, Zhang W, Zhang K, et al. Extreme drought decreases soil heterotrophic respiration but not methane flux by modifying the abundance of soil microbial functional groups in alpine peatland. *CATENA* 2022; **212**: 106043.